The Role of Kindlin-2 in the Progression of Renal Fibrosis

Budour H. Jan

Doctoral Thesis UPF/2017

Directors

Dr. Julio Pascual Santos   **Dr. Marta Riera Oliva**

Tutor

Dr. Jose Lloreta

Department of Biomedicine

University of Pompeu Fabra in Barcelona

upf. Universitat
Pompeu Fabra
Barcelona

INDEX

ACKNOWLEDGEMENTS

ACKNOWLEDGEMENT

In Allah´s will I believe and from my faith in Allah I get my strength, patience and well to be. To be human, to learn, to explore, to accept, to acknowledge. I have the greatest thank for Allah blessings, for being able to achieve this point in my life.

This thesis is also result of the vision of the entity of my country; Kingdom of Saudi Arabia, the vision of expanding knowledge in us as future leaders. I thank my supervisors in La Agregaduria Cultural de la Embajada del Reino de Arabia Saudi for the support throughout my whole scholarship period here in Barcelona.

Whoever is not thankful to the people, then he is not thankful to Allah, and this thesis is burnish with careful guidance and support of my thesis directors. To Dr. Julio Pascual thank you for mentoring and encouraging throughout the course of my thesis and trusting in me. To Dr Marta Riera thank you for your day-to-day help and gaudiness to expand my qualifications and scientific background, thank you for reaching out and giving positivity at hardest times.

Dr. Javier, thank you for your patience, thank you for helping me and encouraging me.

Pepa, I would never forget the time you accompanied me to the hospital and told me I´m not here as a Dr, i´m here as your friend! Thank you for being you, thank you for your inputs and suggestions.

Thanks to all the great friends and wonderful colleagues for unlimited support and kindness. I believe I have a home in the heart of each one of you all. Those papers will not be enough at all to express what I feel or what I want to say. You have all surrounded me all the time, kept reminding me to smile and to be strong, always telling me that YOU CAN DO IT!! During this period of my life here in Barcelona I have lived

Acknowledgements

wonderful moments and made unforgettable memories with each one of you all. It is really not possible to write down how I feel for each one of you!!!! But I know you all realise how big I feel for each of you…I will miss everyone who have I´ve shared each moment of this journey with, thank you friends from around the world, besties in different continents, people who always salute me and smile in PRBB corridors. Thank you to the people who became best friends and family, thank you all for everything, laughing and crying with me, hiking the Montserrat, screaming in Portaventura, walking Barcelona streets, the bike rides, travelling around, cooking, talking, dancing, the Corsega fun night, the gestures of visiting me …. Thank you all because I know I will smile when I will remember you and the memories we´ve shared!

My family…I´m who I´m because you love me, care much to make my hopes and dreams possible, live with me while we are miles away from each other. Because you are my family I know what is being strong, happy, confident and satisfied. You are my Serotonin!!! I LOVE YOU!

FUNDING

FUNDING

ABBREVIATIONS

ABBREVIATIONS

α-SMA	α Smooth Muscle Actin
ADH	Antidiuretic Hormone
AKI	Acute Kindey Injury
ATN	Acute Tubular Necrosis
ATP	Adenosine Triphosphates
BIRI	Bilateral Ischemia Reperfusion Injury
BUN	Blood Urea Nitrogen
CAN	Chronic Allograft Nephropathy
CKD	Chronic Kidney Disease
COL-1	Collagen Type 1
COL-4	Collagen Type 4
CTGF	Connective Tissue Growth Factor
DCT	Distal Convoluted Tubules
dNTPs	deoxynucleoside triphosphatase
ECM	Extracellular Matrix
EMT II	Epithelial Mesenchymal Transition Type II
ESRD	End Stage Renal Disease
ET-1	Endothelin-1
FBS	Fetal Bovine Serum
FN-1	Fibronectin-1
FSP-1	Fibroblast Specific Protein-1
GBM	Glomerular Basement Membrane
GFR	Glomerular Filtration Rate
H&E	Hematoxylin & Eosin
HIF	Hypoxia Inducible Factor
HKC	Human Kidney Cells
I/R	Ischemia/Reperfusion
IF/TA	Intersitital Fibrosis/Tubular Atrophy

Abbreviations

IGFBP	Insulin Like Growth Factor Binding Protein
IHC	Immunohistochemistry
IL-18	Interleukin-18
IL-6	Interleukin-6
ILK	Integrin Linked Kinase
Insr	Insulin Growth Factor Receptor
IPC	Ischemic Preconditioning
IRI	Ischemia Reperfusion Injury
kDa	Kilo Dalton
KDIGO	Kidney Disease Improving Global Outcomes
KIM-1	Kidney Injury Molecule-1
LAP	Latency Associated Peptide
L-FABP	Liver type fatty acid binding protein
LTBP	Latent TGF-ß-binding Protein
µg	micrograms
µl	Microliters
µM	Micromolar
mg	Milligrams
ml	Milliliter
mM	Millimolar
MTAL	Medullary Thick Ascending Limp
MTC	Mouse Tubular Cells
NGAL	Neutrophil Gelatinase Associated Protein
nM	Nanomolar
NMWL	Nominal Molecular Weight Limit
OD	Optical Density
PAGE	Polyacrylamide Gel Electrophoresis
PCT	Proximal Convoluted Tubules
PDVF	Polyvinylidene Fluoride Membrane
PHDs	Prolyl-Hydroxilaes

PST	Proximal Straight Tubule
PT	Proximal Tubule
ROS	Reactive Oxygen Species
RT-PCR	Real Time Polymerase Chain Reaction
sCr	Serum Creatinine
TAL	Thick Ascending Limb
TEC	Tubular Epithelial Cell
TGF-ß	Transforming Growth Factor-ß
TIF	Tubulointerstitial Fibrosis
TIMP	Tissue Inhibitor of Metalloproteinases
TβRI	TGFβ receptor I
TβRII	TGFβ receptor II
UIRI	Unilateral Ischemia Reperfusion Injury
UUO	Unilateral Ureteral Obstruction
VEGF	Vascular Endothelial Growth Factor

SUMMARY

SUMMARY

Chronic kidney disease (CKD) is usually characterized by histological lesions of glomerulosclerosis and tubulointerstitial fibrosis (TIF). The progressive TIF is mediated by multiple mediators such as growth factors, metabolic toxins and stress molecules. One of the key mediators of this process is TGF-β1 that induces cellular responses in a wide variety of cell types. In renal tubular cells TGF-β1 activation requires the binding of Kindlin-2 to the TGF- β1 receptor.

The expression of Kindlin-2 was assessed in three different situations and correlated with the progression of the renal fibrotic process.

After 48 hours, 7 days and 45 days of ischemic lesion, mouse cortical tissue expressed Kindlin-2 in similar level through the progression of the fibrotic process.

In human biopsies presenting histological characteristic of acute tubular necrosis (ATN), Kindlin-2 was also increased and showed high expression in tubules. Smooth muscle cells from arteries showed decreased expression as compared to the biopsies without ATN characteristics.

Kindlin-2 is demonstrated to be activated in a very early time after injury and will likely to keep the progression of the fibrotic lesion of the kidney.

RESUMEN

RESUMEN

La enfermedad renal crónica (ERC) se caracteriza habitualmente por lesiones histológicas relacionadas con la glomeruloesclerosis y la fibrosis tubulointersticial (FTI). La progresión de la FTI se induce por múltiples mecanismos moleculares como factores de transcripción, toxinas metabólicas y moléculas de estrés. Uno de los mediadores clave en esta progresión es TGF-β1 que induce respuestas en gran variedad de tipos celulares. En las células tubulares renales, la activación del TGF-β1 requiere la unión de Kindlin-2 al receptor de TGF-β1.

La expresión de Kindlin-2 se testó en tres condiciones de lesión distintas y se encontró su correlación con la progresión del proceso fibrótico renal.

Después de 48 horas, 7 días y 45 días tras una lesión isquémica, el tejido renal de ratón expresó Kindlin-2 de una forma similar durante la evolución del proceso fibrótico.

En las biopsias humanas con características compatibles con la necrosis tubular aguda (NTA), Kindlin-2 se detectó en varias zonas del tejido renal. Se describió una alta expresión en túbulos y en células de músculo liso de las arterias se encontró disminuido. Este perfil fue opuesto en las biopsias sin características histológicas de NTA.

Kindlin-2 está activado en los procesos más inmediatos en la lesión y se mantiene a lo largo de la progresión, asumiendo un papel necesario en este proceso.

INTRODUCTION

1.   INTRODUCTION

1.1.   THE RENAL SYSTEM

The renal system is primarily responsible for removing all catabolic final products and waste substances, end products of cellular metabolism. This system consists of the kidneys, producing and secreting urine, the ureters carrying urine to the bladder and the urethra which will excrete urine out from the body (1).
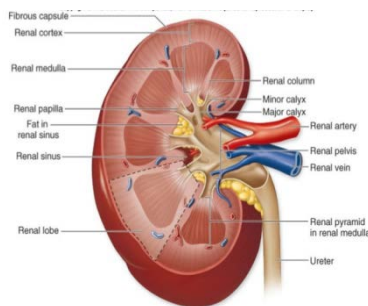
Figure 1: Scheme of cut surface of bisected kidney. Each kidney is bean shaped, with a concave hilum where the ureter and the renal artery and veins enter *(from McGraw-Hill).*

1.2.   THE KIDNEY FUNCTIONS

The kidneys have three main groups of functions; endocrine functions, excretory and homeostatic (1).

The kidneys are essential organs in the urinary system that filter waste products from the blood and also have homeostatic functions as the regulation of electrolytes, maintenance of acid-base balance and blood pressure regulation by maintaining salt and water balance. They serve as natural filter of the blood, and remove wastes which are diverted to the urinary bladder. In urine production, the kidneys excrete wastes such as urea and ammonia, and they are responsible also for the reabsorption of

water, glucose, and amino acids. They also produce hormones including calcitriol; the active form of vitamin D, erythropoietin, and renin enzyme.

In response to hypoxia in the renal circulation, erythropoietin is released, stimulating erythropoiesis in the bone morrow. Calcitriol promotes calcium intestinal absorption and phosphate renal absorption. Renin enzyme is part of renin-angiotensin-aldosterone system and it is involved in the regulation of aldosterone levels and blood pressure.

The kidney accomplishes these homeostatic functions both independently and in concert with other organs, particularly those of the endocrine system. Various endocrine hormones coordinate the endocrine functions, including renin, angiotensin II, aldosterone, antidiuretic hormone (ADH), and atrial natriuretic peptide (1).

1.3. ANATOMY OF THE KIDNEY

Kidneys are bean-shaped paired retroperitoneal structures normally located between the transverse processes of T12-L3 vertebrae. In humans, the left kidney is usually more superior in position than the right kidney with weight ranging from 115-175g in adult. Kidneys are directly covered by a fibrous capsule composed of dense, irregular connective tissue that helps to hold their shape and protect them. The adrenal gland lies on the superior aspect of each kidney. Renal pelvis is located at the hilum on the medial surface of each kidney. This compartment is formed from the major and minor calyxes in the kidney, renal artery and vein, and nerve plexus.

Two distinct regions can be identified on the cut surface of a bisected kidney; a pale outer region which is **the cortex**, and a darker inner

region which is **the medulla**. The renal medulla is the inner part of the kidney and split up into 10 to 18 conical subdivisions known as renal pyramids. The cortex is the outer part of the kidney between the renal capsule and the renal medulla, and it forms a cap over the base of each renal pyramid and extends downward between the individual pyramids to form renal columns of Bertin. The cortex contains the renal corpuscle and the renal tubules except for parts of the loop of Henle which descend into the renal medulla. It also contains blood vessels and cortical collecting ducts (1).

Kidney blood supply is via the left and right renal arteries, which branch directly from the abdominal aorta. The kidneys receive approximately 20% of the cardiac output. Each renal artery branches into segmental arteries that run through the boundary of the cortex and medulla. Each arcuate artery supplies several interlobular arteries that feed into the afferent arterioles that supply the glomeruli.

1.3.1. The Nephron

Nephrons are the functional unit of the kidney. The kidney is structurally composed of about 1.3 million nephrons enveloped in conjunctive tissues. Each nephron consists of: the renal corpuscle or glomerulus, the juxtaglomerular apparatus, the proximal tubule, the loop of Henle, the distal tubule. The glomerulus is a high-pressure capillary formed by afferent and efferent arterioles. The large solutes are filtered out from the blood in the renal corpuscle, while water and small solutes are delivered to the renal tubule (1–4).

The functional anatomy of a nephron
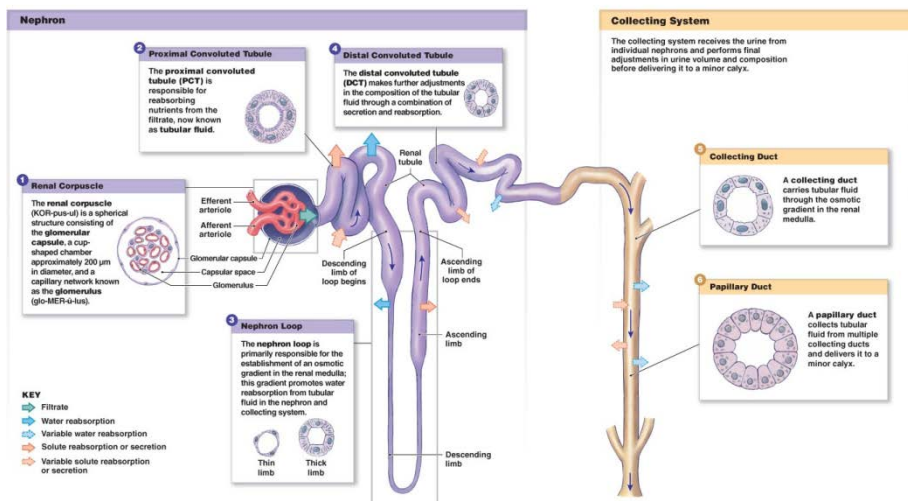
Figure 2: Nephron structure scheme *(Pearson Education).*

1.3.1.1.   Glomerulus or renal corpuscle

The renal corpuscle is composed of a tuft capillary network, called glomerulus, and is surrounded by cup-like sac called Bowman´s capsule. The glomerulus receives blood supply from the afferent arteriole, and the glomerular blood pressure filters out water and solutes from the blood into Bowman´s capsule. The filtered blood passes into the narrow efferent arteriole and moves into the vasa recta which are collecting tubes intertwined with the convoluted tubules through the interstitial space, and which the reabsorbed substances enter. The filtration barrier between the blood and the urinary space is composed of fenestrated endothelium, the peripheral glomerular basement membrane, and the slit pores between the foot processes of the visceral epithelial cells (1,5–7).

Between the glomerular capillaries lies modified cells; called mesangial cells with contractile capacity providing structural support and regulates blood flow of the glomerular capillaries. Podocytes are uniquely shaped

cells with extending finger-like arms called pedicles covering the glomerulus capillaries. Podocytes forms a crucial component of the glomerular filtration barrier, and cooperate with mesangial cells to support the structure and function of the glomerulus. The juxtaglomerular apparatus is located in the vascular region of the glomerulus and is responsible for regulating blood pressure via renin-angiotensin-aldosterone system (1,8,9).

1.3.1.2. The cortex

All glomeruli and both the proximal convoluted tubules (PCTs) and distal convoluted tubules (DCTs) are located in the cortex.

The renal tubules are divided into several segments classified according to the function into; the proximal tubule, the loop of Henle or Intermediate tubule, distal tubule and collecting ducts.

The proximal tubule (PT) begins at the urinary pole in the glomerulus. The most characteristic of the proximal tubule is the brush border, which cover the luminal surface of the epithelial cells in this segment of the nephron. It greatly increases the luminal surface area and facilitates its absorption function.

The proximal tubule consists of the initial portion; proximal convoluted tubule (PCT) (or pars convolute) which is a direct continuation of the parietal epithelium of Bowman´s capsule, and proximal straight tubule (PST) (or pars recta); which is located in the medullary ray. Furthermore, three morphological segments are identified in the proximal tubules which are S1, S2 and S3. The length of brush border in the three segments varies, being tall at the S1 segments and shorter at the S3, although this variation differ also between species (1,10,11).

The descending loop of Henle consists of simple cuboidal epithelium similar to the PCT. The descending and thin ascending portion consists of simple squamous epithelium.

Distal Convoluted Tubule (DCT) is formed by simple cuboidal epithelium, shorter than PCT. The cells in DCT are less active than in PCT with less microvilli on the apical surface.

1.3.1.3. The medulla

This is the inner part of the kidney containing the renal pyramids and renal papillae. The base of the pyramids consists of medullary rays of Ferrein which extend into the cortex, which are formed by the collecting ducts and the straight segments of the proximal and distal tubules of the cortex. The medulla can be divided into inner and outer zones, the outer zone is further subdivided into inner and outer stripe. The inner medulla contains descending and ascending thin limbs and collecting ducts and the outer stripe of the outer medulla contains the terminal segments of the pars recta of the proximal tubule, thick ascending limbs and collecting ducts. Thus, the pyramids consist mainly of tubules or papillae that transport urine from the cortical outer part of the kidney to the calyces in which urine collects before passing through the ureter to the bladder (1).

1.4. GENERAL PATHOLOGY OF THE KIDNEY

Renal failure is described as a decrease in glomerular filtration rate (GFR) and an increase of albuminuria associated with abnormal fluid levels in the body, altered acid levels, abnormal levels of potassium and phosphate. Non-effective control of decreased GFR and increased creatinine or urea during kidney disease leads to renal insufficiency requiring dialysis or kidney transplant. Multiple acute reasons could

cause nephropathy such as deposition of IgA antibodies in the glomerulus, administration of analgesics, toxicity of chemotherapy agent (1,12). Furthermore, several conditions as hypertension, diabetes, increased body mass index, smoking and history of established cardiovascular disease are associated consistently with kidney disease (13,14). There are two forms of kidney failure; acute Kidney injury (AKI) or chronic kidney disease (CKD). Although both syndromes have distinguished characteristics, yet studies are suggesting that the two syndromes are closely interconnected, sharing common risk factors, and in both, the disease stage is determined by measuring serum creatinine concentration or GFR (15,16). When AKI occurs without preexisting kidney disease, CKD may still develop. On the other hand, the presence of CKD is important risk factor for the development of AKI. Both acute and chronic diseases are associated with increased risk of death and may lead to cardiovascular disease, progressive decrease in kidney function End Stage Kidney Disease (ESRD) (17,18).

AKI is rapid progressive loss of kidney function and increase in serum creatinine concentration and often accompanied by decreased urine output, could lead to long term chronic kidney disease. AKI is reversible if treated; it could be developed as a result of damage to the kidney tissue or impairment of oxygen and blood flow to the kidneys (19).

CKD is defined as an alteration in kidney structure and function with variable clinical presentation depending on the cause, severity and rate of progression of the disease. Kidney Disease, Improving Global Outcomes (KDOQI) clinical practice guidelines have established two criteria defining CKD:

1. Kidney damage for more than 3 months with or without decreased glomerular filtration rate (GFR), manifested by pathological abnormalities; histological abnormalities, and patient

history with kidney transplantation or detection of kidney damage markers.

2. GFR < 60 mL/min/1.73m^2 for more than 3 months, with or without kidney damage (20,21)

1.5. ACUTE KIDNEY INJURY

1.5.1. Definition, Clinical Diagnosis, Epidemiology and Progression

AKI is broad clinical syndrome of various causes that affects the kidney structure and function. The main major causes are classified in three categories:

1. **Pre-renal** is the most frequent cause of AKI as 55% of them results by renal hypoperfusion and is reversible once the cause has been eliminated. Several diseases can cause pre-renal AKI as heart failure, fluid and blood loss and sepsis. Usually, the tissue is not structurally damaged.

2. **Intra-renal** with 45 % of AKI patients are rising from intra-renal AKI caused by a process within the kidney. Some of the major causes of intra-renal AKI are acute glomerulonephritis, acute tubulointerstitial nephritis, acute vasculopathy and acute tubular necrosis. Around 60% of intra-renal AKI is due to tubular damage where cells display phenotypic changes including epithelial cells flattening, loss of brush borders, nuclear loss, apoptosis and necrosis.

3. **Post-renal** which counts 5% of AKI and is induced by any disease that is associated with urinary tract obstruction such as; hematoma within renal pelvis, tumors of the ureter or abdominal

malignancies that is compromising the urinary flow, and diseases of bladder and prostate (22).

AKI requires an accurate understanding of the epidemiology with the use of standardized definitions and descriptions which will aid in having true incidence of AKI worldwide (23–25). AKI is recognized as an important risk factor for loss kidney function, leading to poor life quality, disability and high long term cost (26). Studies have showed that AKI is a global problem and is associated with high mortality rates especially in developing countries which have limited resource for patient care and controlling the progression of kidney failure leading to the importance of early detection of AKI during the reversible stages preventing its progression to kidney failure acquiring dialysis or transplant (19).

Acute kidney injury AKI is characterized by rapid decrease in kidney function as reflected by a significant increase in serum creatinine. In addition, urine output is reduced in 70% of patients (22). The definition of the syndrome is periodically refined. According to the latest KDIGO guidelines (19), AKI is defined as any of the following:

−   Increased serum creatinine, greater than 0.3 mg/dl within 48hrs

−   Or a 1.5-fold serum creatinine increase within 7 days

−   Or a reduction in urine output to less than 0.5 ml/kg/day for at least 6 hours

AKI occurs in about 13.3 million people per year, with around 85% from developing countries population. Epidemiology of AKI in developing countries differs from that in the developed countries. In latter, the highest percentage of patients is rising in elderly patients while in developing countries it is a disease of young and children. Although not

linked directly to death, yet it is thought that AKI contribute to around 1.7 million deaths every year. Furthermore, in several epidemiological studies the increasing severity of AKI is associated with higher risk of death in patients in both hospitalized and community settings (23,26).

AKI is a clinical syndrome with multiple entities implying renal damage and/or impairment of renal function. It is not associated with any specific symptoms and its diagnosis is largely based on laboratory measurements estimating renal function. Due to the high risk of AKI and its impact in the increasing mortality and morbidity, it is important to identify the syndrome at early stages before the loss of kidney function and structure and also to prevent its exacerbation. Moreover, the pathophysiology of AKI is highly complex and involves multiple cellular systems. Global efforts are focusing to develop a management system which aid to prevent, diagnose, and treat AKI as preventable and treatable disease (26). Several markers have been used yet it should be noted that not all are suitable for detecting early kidney damage and preventing the kidney disease. While serum creatinine (sCr) is known as an indicator for renal function, yet it is not suitable for detecting the early stages of kidney injury, because its concentration begins to rise late in AKI, where 60% of kidney function is lost, and it also varies with muscle mass, age, sex, medication and hydration status; such variabilities changes even normal levels of sCr. Furthermore, the elevated sCr does not differentiate the nature, type and timing of renal insult, and most importantly this marker is useless once dialysis is started as dialysis clears the serum creatinine. Thus, improved evaluating method for the GFR and a direct marker of renal injury is highly required (15,16,19,22,27,28). The severity and duration of AKI affects outcomes such as dialysis requirements, renal functional recovery and survival. Recently multiple biomarkers especially in cell cycle arrest biomarkers are rising with acceptance aiding in

understanding the mechanism of AKI, diagnostic and the possible therapeutic approaches (26).

1.5.2. Pathophysiology of AKI

The pathophysiology of AKI is highly complex and involves multiple cellular systems that affect the different cells and structural compartment of the kidney (19,29). Renal ischemia/reperfusion (I/R) is the leading cause of AKI which results from a generalized or localized impairment of oxygen and nutrients delivery to, and waste products removal from, kidney cells. The impairment of local tissue oxygen supply with the demand and accumulation of waste products of metabolism injure the tubular epithelial cells and cause death if severe by apoptosis and necrosis (30). Although that ischemia/reperfusion leads to AKI, it has been merged that short episodes of nonlethal ischemia are protective to the kidney; which is referred to as ischemic preconditioning (IPC). Such protection include upregulation of cell survival pathways and downregulation of apoptotic pathways (31–34).

Tubular damage is initiated with reducing ATP cell production and thus affecting cellular homeostasis accompanied with several molecular events: loss of cytoplasmic calcium load, certain proteins and cell membrane embedded phospholipids are degraded, apoptosis is induced, accumulation of reactive oxygen species (ROS). In addition, ischemia destabilizes cell to cell contact areas and cause to loss cell polarity, decreasing sodium and water reabsorption from tubular lumen, aggravating the cellular damage. Meanwhile epithelial cell is flattened, losing brush border and nuclear loss. Finally, epithelial cell detaches from basement membrane and accumulate within the tubular lumen. This accumulation inhibits the tubular flow and promotes filtrate backflow into the interstitial space. Altogether events are reducing the glomerular filtration rate (15,22,35). Ischemia leads to rapid loss of cytoskeletal

integrity and cell polarity, shedding the proximal tubule brush border; losing the cell polarity, mislocalization of adhesion molecules and other membrane proteins. Cytokines induce disruption of cell-matrix adhesion and disruption of cell-cell interactions at adherent and tight junctions. Severe injury increases the permeability between the filtrate and peritubular interstitium, which results in back leak of glomerular filtrate from the tubular lumen to the interstitium. The cells detach from the basement membrane and with combination of the existing fibronectin forming casts obstructing the tubule and increasing intra-tubular pressure (36).

Tubular epithelial cell death is a cause of tubular dysfunction that activates the tubular glomerular feedback mechanism which reduce glomerular filtration to prevent water and electrolyte loss. The tubular cell death activates extant cells to proliferate and replace dead cells and to attract immune system cells to aid in repairing. Furthermore, the tubular cell activation involves the production of pro-inflammatory and vasoactive mediators such as; cytokines and ROS, which act to maintain filtration flow. Various forms of cell death have been reported to occur simultaneously to different relative and absolute extent depending on AKI type (ischemic, toxic, septic…etc.), the stage of injury and the level of repair. Each form of cell death produces specific functional and histological consequences. Necrotic debris and poured intracellular content attract immune system cells and increases the release of inflammatory cytokines and increased production of reactive oxygen species, which all in turn results in subsequent or further renal damage (27,29,35,36).

The medullary thick ascending limp (MTAL) of the distal tubule has close association with the proximal straight tubule in the outer spatial of the outer medullary. Cells of the distal nephrons found to be more resistant to hypoxia, ischemia and oxidative injury, and remain intact during ischemia reperfusion injury (IRI). The MTAL has greater capacity to convert into glycolytic metabolism under limited mitochondrial function during reduced oxygen presence, for that it has better adaptation to hypoxia during ischemia (36).
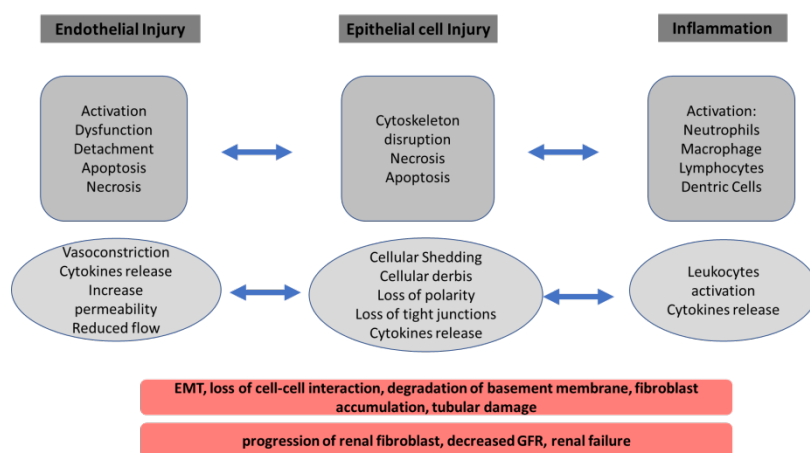
Figure 3: Schematic diagram of pathophysiology of acute kidney injury and the compartments associated with the injury

AKI activates large number of genes, among those genes are kidney injury molecule (KIM-1) and neutrophil gelatinase associated lipocalin (NGAL), which are the most highly upregulated in the proximal and distal tubules, and both are useful noninvasive biomarker of injury. KIM-1 is phosphatidylserine receptor that recognizes and directs apoptotic cells to lysosomes in proximal tubular cells, and mediated phagocytosis of necrotic cells and oxidized lipoproteins by renal proximal tubular cells; in addition, it plays an important role in limiting the immune response to

injury. NGAL is produced in distal nephron, filtered and reabsorbed by the normal proximal tubule; it is an iron transporting protein and found to inhibit apoptosis, enhances proliferation and provides significant functional and pathological protection in murine models or ischemic renal injury (IRI) (35,36).

Inflammatory process contributes to tissue damage in post ischemia AKI as well as for kidney repair/regeneration process by upregulating endothelial adhesion molecules. As a result, leukocytes adhere to the endothelium aggravating tissue ischemia by producing inflammatory mediators and ROS aggravating tubule cell damage. The tubular epithelium releases pro-inflammatory cytokines. Almost all types of immune cells are activated in AKI; however, results of different studies performed to analyze the role of each type of these cells were quite conflicting. Blocking neutrophils was successful in one, while many other studies showed non-protective effect. In a study by Klausner and co-authors, mean creatinine in the neutrophil depleted rat group was decreased in comparison to the control group (37). Hellberg and co-authors demonstrated that inulin clearance in neutrophil-depleted group was four-folded higher than in control animals (38). Paller and co-authors used anti-neutrophil serum but neutropenia did not protect against ischemic injury in rat ischemia model (39). In a study by Thronton and co-authors it was showed that neutrophils depletion did not demonstrate protection in bilateral renal ischemic model (40).

Macrophages infiltrate the post ischemic kidney and contribute to renal fibrosis in AKI, yet it was shown that they transdifferentiate into anti-inflammatory phenotype and promote renal repair post ischemia. Thus, post ischemic inflammation is essential in terms of aggravating tissue damage and mediating tissue repair in AKI (41,42).

Under normal circumstances, human proximal tubule cells divide at low rate. Cell proliferation balances the loss of tubular epithelial cells due to death or release from the basement membrane into the urine. This low rate of turnover changes after ischemic or toxic insult by replacement of the dead cells. The origin of the cells that replace the epithelial cells after injury has been in a debate, proposing the endogenous surviving epithelial cells, the bone marrow stromal cells or the intrarenal progenitor cells. It has been hypothesized earlier that the cells came from surviving proximal tubule cells, however studies suggested that bone marrow derived cells, including hematopoietic stem cells and mesenchymal stem cells, directly replace the lost epithelial cells. Moreover, studies have clarified that bone marrow derived cells do not directly replace the tubule epithelial cells that are lost with injury, but exert paracrine effects that facilitate the repair by reducing inflammation. Genetic fate-mapping techniques demonstrated that surviving tubular cells proliferate and this accounts for replenishment of the tubular epithelium after ischemia. When the kidney recovers after the loss of epithelial cells, the surviving cells differentiate, migrate along the basement membrane, proliferate to restore cell number, and then differentiate, restoring the functional integrity of the nephron (15,43,44).

However, epithelium repair after injury is more frequently maladaptive. Acute kidney injury can lead to incomplete tubular repair, persistent tubulointerstitial inflammation, fibroblasts proliferation and excessive deposition of extracellular matrix (ECM). Different factors could cause injury; one of them is long term hypoxia that contributes to post ischemic fibrosis. However, the nature of the molecular switch that determines renal tubular reparative or atrophic/fibrotic responses to injury in the pathogenesis of kidney fibrosis after AKI is still controversial.

Epithelial mesenchymal transition (EMT) has been thought to be one of the major pathways in fibrosis progression. However recent studies

suggest that the myofibroblasts are generated mainly from perivascular fibroblasts, or pericytes, but not due to EMT by tubular epithelial cells. Yet the epithelial cells generate pro-fibrogenic cytokines, including transforming growth factor (TGF-β1) and connective tissue growth factor (CTGF), which production is enhanced by cell cycle abnormalities as the surviving cells attempt to repair the epithelium. In severe or sustained kidney injury there is an arrest in cell cycle phase G2/M, which facilitates the generation of TGF-β1 and CTGF, inducing epigenetic changes in the resident fibroblast which results in prolonged fibroblast activation and fibrogenesis (36,44).

Within all factors associated to AKI, high salt intake has shown to be critical for the development of fibrosis in the kidney disease. Although high salt intake is linked to hypertension, evidences have showed that dietary high salt can lead to fibrosis even without hypertension (45,46). The kidney plays an important role in the regulation of Na+ and blood pressure by the Na/K-ATPase on the basolateral membrane of renal epithelial cells and plays critical role in renal salt handling. The Na/K-ATPase signaling is found to be involved in number of clinical disorders such as; cardiovascular disease, hypertension, renal disease, diabetes, salt imbalance, other metabolic and neurological disorders. In normal renal function, renal adaptation to dietary sodium intake involves downregulation of renal proximal tubules sodium reabsorption. Scr family kinases are non-receptor tyrosine kinases which are present in wide variety of cell types including kidney epithelial cells and play major role in signal transduction pathways regulation, implicated in the generation of ROS, development of tissue fibrosis, and growth and metastasis of cancer. Evidences have demonstrated that reduction in Na/K-ATPase cellular expression is sufficient to increase the Src

activity, where the elevation of Src activity plays major role in the pathogenesis of the involved diseases. (47). In addition, the alteration of signaling receptor function is seen also in ischemia/reperfusion injury and tissue fibrosis (48). Cardiotonic Steriods (CTS) are endogenous steroid hormones regulated by angiotensin II, adrenocorticotropic hormone, high salt intake, volume expansion, chronic renal failure and congestive heart failure. CTS bind and fix the Na/K-ATPase inhibiting the pumping cycle. It has been also documented that CTS have a role in regulating cell growth; by activating multiple protein/lipid kinases and stimulating differentiation and/or apoptosis, or hypertrophic/proliferative growth in cell specific manner, and also elevated levels of endogenous CTS have been found in CKD patients (47,48). Evidences have demonstrated that excessive dietary salt intake increases circulating endogenous CTS that are specific inhibitors and ligands of Na/K-ATPase, which directly inhibit renal tubular Na/K-ATPase leading to the inhibition of sodium reabsorption (48,49).

In the study performed by the group of Pletinck and co-authors it was shown that the high salt intake induces epithelial mesenchymal transition (EMT) and upregulates TGFβ-1, and possible leading to retroperitoneal fibrosis. The study performed in Wistar rats in two groups; normal salt and high salt (2% NaCl drinking water). Results demonstrated that dietary salt intake induced EMT and peritoneal fibrosis in correlation with upregulated TGFβ-1 in mRNA level only after 2 weeks of high salt intake (46). Yin W. and Sanders P. have previously demonstrated that high salt intake (8.0% NaCl diet) increased steady-state mRNA levels of TGFβ-1, β-2 and β-3 in rat kidneys compared to the group of low salt kidneys (3.0% NaCl). This high salt intake increased the urinary excretion of TGFβ-1 indicating that the kidney is the source of the excess excretion of this growth factor. TGFβ-1 was increased in both

glomeruli and tubules, but active form of TGFβ-1 was secreted in high amounts only from the glomeruli (50). Thus, evidences are indicating a role of high salt intake in the progression of kidney disease by inducing TGFβ-1 and marked EMT.

1.6.   TUBULAR INTERSTITIAL FIBROSIS AND RENAL FIBROSIS

Progressive TIF is the final common pathway of all kidney diseases leading to ESRD (51). Progressive inflammation or injury in the renal interstitium can either begin as a secondary event following glomerular or vascular injury or form within the tubulointerstitial compartment. Although most forms of progressive, noncystic renal disease are glomerular in origin, yet the intensity of the evolving injury of the tubulointerstitial compartment, rather than the extent of glomerular changes is what predicts the overall decline in renal function (Le Clef et al., 2016a).

Despite that the kidney accounts for only 2% of total body weight, it receives 20% of the cardiac input, facilitating the high rates of glomerular filtration needed for the regulation of the body´s fluid and electrolyte balance. Under physiological conditions, the glomerular filtration rate (GFR) is maintained stable despite the changes in arteriolar pressure. In the other hand the renal cortex which counts the majority of the glomeruli, receives most of the renal blood flow, while the medulla receives 10% only, which in result classifying the renal cortical cells as the most sensitive to ischemia. The tubular transport in the medullary thick ascending limb (TAL) and S3 segment of the proximal tubule demand high oxygen consumption, for that when blood supply is interrupted; the oxygen balance is maintained by reducing the GFR and solute transport to TAL. The outer medullary cells switch to anaerobic metabolism, allowing

better surviving and adoption to the hypoxic environment, while cells of the inner medulla and papillae normally relay on anaerobic glycolysis for ATP generations making them more resistible to ischemia. This protective mechanism is undermined by the production of reactive oxygen species (ROS) decreasing the medullary blood flow and increasing TAL activity (52–57). However, during reperfusion injury is increased, because of the increased demand for tubular transport which in result increases the oxygen consumption. The initial injury further initiates cascade of events leading to endothelial damage. An inflammatory response leads also to vascular congestion and reduce the ability to filtrate toxic radicals. However, the extent of the tissue injury, cellular dysfunction and/or death is relatively influenced by the degree of blood flow reduction and length of ischemic period (24,54,55,58).

In all forms of progressive experimental and human CKD, a pro-inflammatory infiltrate exists within the interstitial compartment. The extent of the infiltrate and associated areas of fibrosis correlates with progressive decline in renal function. In many studies of persistent glomerular nephritis, a significant correlation was found between the extent of the eosinophilic deposits in glomeruli and creatinine clearance, plasma creatinine concentration and the ability of the kidney to concentrate the urine. However, the correlation between these functions and the glomerular changes were less striking than those documented between the extent of tubular lesions and the alteration in renal function, suggesting that in chronic glomerulonephritis the structural damage in the tubules may have much more effect on the GFR than the structural injury in the glomeruli (1,59). Furthermore, while TIF can be caused by glomerular damage induced by different glomerular disorders; glomerulonephritis, diabetic nephropathy and hypertensive nephrosclerosis.

Introduction

The mechanism of how the tubulointerstitial disease affects the renal function is still to be studied and defined. Several mechanisms have been suggested yet not exclusive. Briefly, the tubular obstruction resulting from interstitial inflammation and fibrosis would impede the urine flow and increase intra-tubular pressure, eventually lowering the glomerular filtration. A second possible mechanism implicates the reduction in the volume of peritubular capillaries as the interstitial inflammation and fibrosis increase. In this case the tubulointerstitial compartment becomes relatively avascular, and ischemic. As a result of the increase of the vascular resistant in the post glomerular region, the hydrostatic pressure in the glomerular capillaries may also increase. The intra-glomerular hypertension that ensues initially as a compensatory adaptor to the impaired glomerular arteriolar outflow can cause progressive deterioration of renal function due the severe structural damage of the glomerulus (1).

Progressive TIF is mediated by multiple mediators including growth factors, metabolic toxins, and stress molecules. Among them TGFβ has been recognized as key mediator for the progression of TIF. The most striking feature of TIF is excessive deposition of ECM, and the presence of collagenous fibers; collagen type I, III and IV (60).

Fibroblasts have been found to originate from variety of sources, including EMT, bone marrow, resident fibroblasts, or myofibroblasts. Some evidences show that large number of fibroblasts is produced by epithelial mesenchymal transition type II (EMT-II) and that play a critical role in tubulointerstitial fibrosis. EMT process allows the polarized epithelial cells to undergo to multiple biochemical changes enabling to assume mesenchymal phenotype. Thus, by this process, the polarized epithelial cells which normally interact with the basement membrane through its basal surface lose the polarity and degrade the basement membrane to become mesenchymal cell phenotype. By this change the

cell shows enhanced migratory capacity and excessive production of ECM components. Several molecular processes are engaged in inducing EMT such as transcription factors, expression of cytoskeletal proteins, and production of ECM-degrading enzymes.

EMT occurs in three different biological settings, although all types are associated in the generation of mesenchymal phenotype, the mechanism of EMT induction and progression is different in each type. EMT-I (type 1) is associated with implantation, embryogenesis and organ development. This type is not associated with inflammation or fibrosis. EMT-II (type 2) is associated with tissue regeneration and fibrosis, depends on inflammation inducing injuries to initiate and process. During injury, EMT-II continues to process until the initiate injury or infections is eliminated or injury is repaired. EMT-II generates mesenchymal cells, myofibroblasts producing excessive amount of EMC rich in collagen. Thus, its continuation could damage the tissue leading to fibrosis. EMT-III (type 3) is involved in tumor growth and cancer progression; when cancer cell is converted to mesenchymal phenotype. EMT-III produces cells with invasiveness properties in cancer pathologies (61,62).

EMT-II induces the transformation of epithelial cell into myofibroblasts, losing their cell-cell adhesion and E-cadherin expression, degradation of the basement membrane and migration of cells, in association with the production of pro-fibrotic molecules. EMT-II is mediated by different signaling pathways, one of which is TGFβ/Smad signaling (61–64). Several studies indicate that tubular epithelial cells incubated with fibrogenic TGF-β undergo phenotypic conversion characterized by loss of epithelial proteins as E-cadherin. Furthermore, acquisition of new mesenchymal markers including α-smooth muscle actin (α-SMA), fibroblast specific protein-1 (FSP1), interstitial matrix components type I collagen and fibronectin is described. Alterations in protein expression are accompanied by fibroblast appearance and enhanced migration capacity.

Introduction

It is very challenging to demonstrate EMT in vivo, however in a study performed by Iwano and colleagues (65) it has been indicated that EMT in vivo is a source of interstitial, matrix producing fibroblasts. Using genetically tagged proximal tubular epithelial cells it was been showed that up to 35% of all FSP-1 positive fibroblasts within the interstitial space are originated from renal proximal tubules after UUO, providing significant evidence of the contribution of EMT in the pathogenesis of chronic kidney disease. Meanwhile clinical studies using human kidney biopsies also demonstrate the role of EMT in the pathogenesis of human CKD, as tubular expression of mesenchymal markers have been shown in various progressive kidney diseases. Furthermore, its expression is usually correlated with the decline renal function (66–70). The contribution extent of EMT to renal fibrosis in vivo still remains a matter of debate. The presence of several mesenchymal markers as E-Cadherin and cytokeratin is a defined feature of EMT. On the other hand fibroblast conversion is more difficult to define due to the lack of specific markers. Most of the commonly used mesenchymal markers as vimentin, α-SMA, FSP-1, collagen-1, fibronectin, Snail, and matrix metalloproteinases 2 and 9 are not specific fibroblasts markers; they are also present in inflammatory cells and endothelial cells. Even more, after injury the tubular epithelial and endothelial cells in vivo may not undergo complete EMT but partial EMT, where the cells change only one or two phenotypic markers. The contribution and role of EMT in renal fibrosis still needs more investigations (8,71–73).

EMT can be induced by wide variety of stimuli involving several cellular signaling pathways and mediators cooperating in different phases of the process, from initiating injury, repair and inflammatory response, and fibrogenesis. TGFβ/Smad signaling is one of the pathways that have important impact and role in controlling EMT and as a result the pathogenesis of renal fibrosis depending on the pathological

circumstances (74–76). However, EMT leads to the formation of fibroblast in extreme pathological conditions but the transition itself does not induce fibroblast formation under normal repairing physiological conditions. Thus, the number of epithelial cells undergo EMT is not necessary the exact number of fibroblast produced. Also, it should be considered that EMT is a dynamic reversible mechanism involving intermediate stages in which the epithelial cells have features of the origin phenotype as well as the emerging fibroblasts. In advanced stages the original phenotype can be lost suggesting that the timing for the tissue analysis in the studies involved is very important (8,60,72).

Studies have demonstrated that kidney fibrosis is associated with Snail-1 activation in both human samples and mouse models. Furthermore, the role of Snail-1 have been shown to directly associate with partial EMT process of renal epithelial cells in kidney fibrosis and that Snail-2 reactivation is required for development of renal fibrosis. Furthermore, the damaged cells undergoing partial EMT remain integrated in the tubules relaying fibrotic and inflammatory signal. Most importantly, Snail-1 inhibition once fibrosis is established can ameliorate the disease (77).

In renal allograft, TIF is associated with tubular atrophy; and it is called interstitial fibrosis/tubular atrophy (IF/TA). IF/TA lesion is induced by immune and non-immune injuries to the graft. In a study investigating the causes of kidney allograft loss, biopsies at different time-points after transplantation from time-0 to 5 years post-transplant showed that death with functioning grafts was the most common cause of graft loss, with an average of 37% cases of glomerular disease, an average of 30.7% of interstitial fibrosis/tubular atrophy (IF/TA), and 12% of acute rejection (78,79).

Introduction

Diseases occurring post-transplant are absolutely heterogeneous process with variable consequences mostly causing kidney transplant failure. Furthermore, no matter what the original insult occurring on the grafts is, the end result is fibrogenesis. Many factors can contribute to renal fibrosis including ischemia-reperfusion injury, hypertensive damage, and nephrotoxicity of immunosuppressant, recurrent graft infection and post renal obstruction. Although early kidney fibrosis following glomerular and or tubular insult may reflect beneficial would healing, yet in late stages of disease fibrosis is pathologic (68,80).

Different cell types are involved during the injury depending on the initiate of the injury; inflammatory cells are involved during rejection, tubular cells during acute tubular necrosis, endothelial cells during thrombotic microangiopathy or glomerular cells during de novo glomerular diseases. Inflammation is initiated as a defensive mechanism eliminating pathogens or damaged tissue, and depending on the extent, duration and therapeutic manipulation the inflammation might lead to progressive kidney injury. But this healing process of inflammation is not the case in transplant patients, as they may suffer rejection processes. However, the use of immunosuppression is associated with several side effects that finally lead to fibrosis. Meanwhile, glomerular injury is a point of no return where the glomeruli react with focal scar formation and glomerulosclerosis. Podocytes play major role determining glomerular injury progression and glomerulosclerosis due to the unique anatomical position and the no regenerative capability of those cells. Mesangial cells are direct effector cells responsible for the deposition of ECM and the development of glomerulosclerosis during injury, with high regenerative potential. In the other hand, although the tubular epithelial cells are highly differentiated, metabolically active and polarized cells which react to stress and possess high regenerative capacity, in severe or repetitive stress

the adaptive response of the injured tubular cells leads to fibrotic and progressive kidney disease (68,81).

Myofibroblasts have been described as key effector cells in interstitial fibrosis. While the origin of myofibroblasts is a controversial topic, yet it has been demonstrated the tubular epithelial cells play a role as well in the production of myofibroblasts and progression of fibrosis, involving EMT process. EMT has been described to be of high prevalence in renal allograft dysfunction contributing to matrix accumulation and renal function deterioration (81). Studies have demonstrated that some features of EMT are apparent in human allografts during early acute rejection episodes; it has been showed that EMT occurs early in significant proportion of kidney transplant recipients with stable function, where at least 10% of tubules are in a transition state in 41% of the patients. Furthermore, findings demonstrated that EMT features are present when the kidney should have recovered from preimplantation ischemia and before severe lesions of chronic allograft nephropathy (CAN) appears (81–83).

1.7. TGFβ SIGNALING PATHWAY

Transforming growth factor-β (TGF-β) signaling plays a central role in the development of acute and chronic kidney diseases through regulation of cell differentiation and proliferation, apoptosis, immune response and extracellular matrix remodeling. Studies have demonstrated its pro-fibrotic role in kidney disease, as the activation of TGFβ signaling pathway in the tubular epithelium is sufficient to cause tubular injury, apoptosis, necrosis, oxidative stress, regenerative cell proliferation and accumulation of interstitial inflammatory cells (84), also it is found upregulated in kidney disease and correlates with the degree of fibrosis of both patients and animal disease models (85–88). TGFβ have three

Introduction

isoforms (TGF-β1, 2 and 3) are multifunctional polypeptide growth factors involved in the regulation of cellular growth, differentiation, apoptosis and immune functions. Inhibiting cell proliferation is one of the major effects in addition to the regulation of the production and structure of the extracellular matrix components. Furthermore, TGF- β1 is the most abundant isoform which is also producible by all types of renal resident cells. TGF-β1 is released in association with latency associated peptide (LAP) as a latent form of TGF-β1, which binds to latent TGF-β-binding protein (LTBP) in the target tissue. Under the stimulation of multiple factors as reactive oxygen species (ROS), plasmin and acid; TGF-β1 is activated as being released from LAP and LTBP. The active TGF-β1 transduce its signal to the nucleus through the formation of heteromeric receptor complexes between specific TGF-β type I and TGF-β II receptors (TβRI and TβRII), where TβRI acts downstream TβRII and phosphorylates two serine residues at the extreme C-terminal end of receptor regulated Smads (R-Smads: Smad2 and 3) which play critical roles in TGFβ signaling. The two activated Smads bind to a common partner Smad (Smad4) forming a complex which translocate into the nucleus, where they act as transcriptional regulators of TGF-β1 targeted genes (89). Most cells secrete TGF-β1 in a large latent complex that associates with ECM and is unable to bind TGF-β1 signaling receptors (90–93). It has been demonstrated that in most studied cultured cell lines TGF-β is secreted in the large latent complex (90). TGF-β1 pro-fibrotic effect on kidney is possible through several mechanisms: 1) TGF-β1 directly induces the production of ECM including collagen 1 (COL1) and Fibronectin through Smad3 dependent or independent mechanism. 2) TGF-β1 suppresses the degradation of ECM by inhibiting matrix metalloproteinase (MMP) and inducing inhibitors of MMP such as tissue inhibitor of metalloproteinase (TIMP). 3) TGF-β1 plays critical roles in the transdifferentiating several types of cells including epithelial cells,

endothelial cells and pericytes, into myofibroblasts. 4) TGF-β1 acts directly on different types of renal resident cells, for example it promotes the proliferation of mesangial cells to increase the matrix production, induce the elimination of tubular epithelial cells and podocytes which may lead to deterioration of renal injury and induce the progression of severe renal fibrosis (86).

1.8.   KINDLIN-2

Kindlins are group of FERM domain containing adaptor proteins. FERM is a common domain found in several proteins mediates the linkage of the cytoskeleton to the plasma membrane. The domain often interacts with the cytoplasmic tail of transmembrane proteins, such as integrins. They also contain N terminal subdomains, and a PH subdomain which interacts with multiple phosphoinositides supporting focal adhesion targeting, integrin-mediated adhesion and fibronectin deposition. Its name comes from the four proteins which this domain was originally described: band 4.1 F, Ezrin, Radixin, Meosin. Kindlins have great capacity to regulate the function of integrin adhesion receptors. They are found to be highly concentrated at sites of cell-ECM adhesions, and are important integrin regulators which are regulated by two mechanisms: 1) Kindlins bind to the β-integrin cytoplasmic domains, cooperating with talin in activating integrins. 2) Kindlins also interact with other cell-ECM components such as migflin and integrin linked kinase (ILK) and so regulating cytoskeletal reorganization and strengthening cell-ECM adhesion (94). There are three Kindlins encoded by separate genes; Kindlin-1, Kindlin-2 and Kindlin-3. Furthermore, Kindlins are expressed in a tissue dependent manner perhaps determining the differences in integrin functions in each tissue; Kindlin-1 is expressed in epithelial cells which form a defensive barriers against

Introduction

external environment such as skin and colonic epithelium; Kindlin-2 have broad expression in all solid tissues of mesenchymal origin where Kindlin-2 localizes to integrin in the focal adhesion complexes controlling the organization, and Kindlin-3 is primarily expressed in hematopoietic cells where integrin and adherent cells require quick transit to active state (95). Depletion of Kindlin-1 or Kindlin-3 cause diseases attributed to disruption of extracellular matrix-integrin-actin networks (96,97). Meanwhile the depletion of Kindlin-2 is lethal as demonstrated in early mouse embryonic development and is also associated with severe cardiac dysfunction in zebrafish (96,98,99).

Kindlins have been found to regulate Wnt and TGFβ signaling, where Kindlin-1 binds and activates αvβ6-integrin which binds to RGD motif to the latency-associated peptide (LAP) that is associated with latent TGFβ-binding protein (LTBP), which further induces the release of TGFβ (Figure 4). The released TGFβ binds to the TGFβ receptor I and II (TβRI and TβRII) triggering Smad3 phosphorylation, which associates with Smad4 and induce the translocation into the nucleus and cofactors the transcription of TGFβ targeted genes (100).

Kindlin-2, an integrin binding scaffolding protein that is concentrated at the intracellular face of cell-ECM adhesions, interacts with β-integrins and contributes to outside-in as well as inside-out signaling. Kindlin-2 is broadly expressed in organs and tissues (96,101,102). A recent study showed that the loss of Kindlin-2 in podocytes increased their motility by altering the actin cytoskeletal organization, affecting the podocytes foot processes and lead to massive proteinuria and kidney failure. However, studies have showed that Kindlin-2 depletion on other cells reduced the cell motility rather than increasing the motility (103).
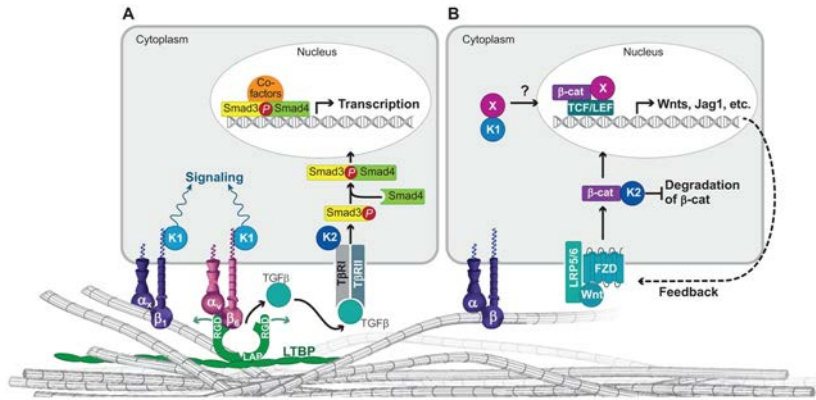
Figure 4: Kindlins regulate Wnt and TGFß signaling
(104)

Kindlin-2 physically interacts with both TGFβ receptor 1 (TβR1) and Smad3, promoting the activation of TGFβ/Smad signaling contributing to the pathogenesis of TIF, independently of integrins (87). Wei and colleagues have found that Kindlin-2 is highly expressed in human kidney TEC cells (HKCs) localized in cytosol of HKCs, while low levels of Kindlin-1 were detected (Figure 5) (87).
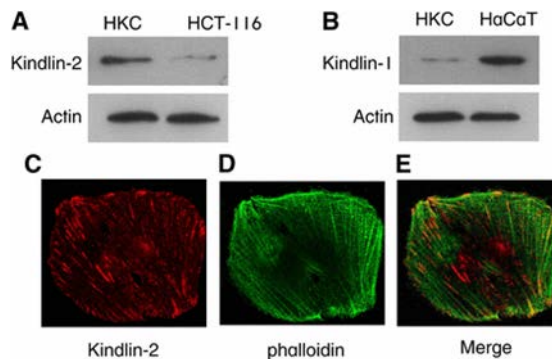

Figure 5: Detection of Kindlin-2 in HKCs and Immunofluorescence staining localizing Kindlin-2 in HKCs (102)

Furthermore, TGFβ-1 upregulates Kindlin-2 expression in time and dose dependent manner in cultured human kidney cells (HKCs). The

Introduction

interaction of endogenous Kindlin-2 with TβR-1 and Smad3 was detected in the absence of TGF-β1 and enhanced by TGF-β1 stimulation.
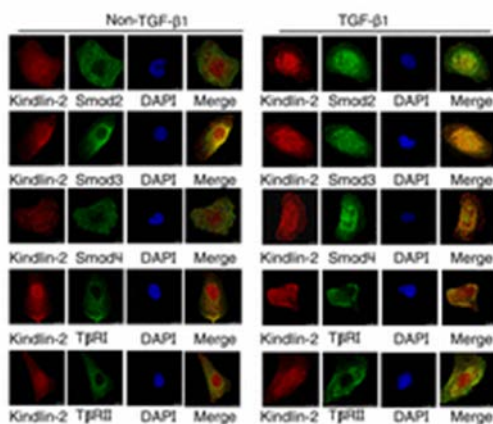

Figure 6: Transfection of HKCs with pFlag-Smad2, pFlag-Smad3, pFlag-Smad4, pHA-TβRI, or pHA-TβRII. Cells were treated with or without TGFβ1 (5ng/ml) for 30 minutes, 48hrs after transfection. Expression of Kindlin-2, Smad2, Smad3, Smad4, TβRI and TβRII analyzed by immunofluorescence staining (102)

In experimental animal models, Kindlin-2 is upregulated in unilateral ureteral obstructed mice accompanied by increased expression of TGFβ-1 and Smad-3, while knocking down Kindlin-2 decreased the renal expression of COL-1, α-SMA and Snail in both protein and mRNA levels, attenuating TIF. Furthermore, biopsies from TIF patients showed upregulation of Kindlin-2 in association with TGF-β1 overexpression. However, the localization of Kindlin-2 expression was not definitely described (87,102).

1.9.   MURINE MODELS OF RENAL FIBROSIS

1.9.1. Overview

Animal models help us to understand the multiple cellular changes involved in injury in order to find future therapeutic solutions. Among animal, mouse models are preferable for different reasons such as wide availability and easiness of manipulation by different approaches; surgically, genetically and therapeutically (105).

In renal injury studies representing AKI and interstitial inflammation several models are found, yet each has its own advantages and disadvantages. Unilateral Ureteral Obstruction (UUO) is the most commonly used model for renal fibrosis and TIF in CKD models. However, Ischemia reperfusion injury (IRI) mouse model is the most commonly used model to induce AKI, as it serves to study the molecular and cellular pathophysiology in this lesion and possibly to analyze renal regeneration (30).

1.9.2. Unilateral Ureteral Obstruction Model

UUO model serves as a model for both irreversible AKI and of the events taking place during CKD. It also allows studying the kidney response to urinary tract obstruction. The UUO causes AKI characterized by tubular cell injury, interstitial inflammation and fibrosis. The model is useful for the molecular mechanism studies of apoptosis, inflammation and fibrosis, key processes in kidney injury.

UUO surgery is performed by obstructing the ureter of the kidney, exposing the left ureter and suturing two knots; one proximal near the kidney and the other distal. Then the ureter can be cut between the knots. In this model the obstructed kidney will develop kidney injury and the contralateral non-obstructed kidney will recruit the loss or renal function as well as providing internal control tissue (106).

Introduction

1.9.3. Ischemia Reperfusion Injury Model

Renal ischemia reperfusion injury (IRI) is one of the most common used animal models for fundamental and therapeutic intervention studies in AKI. Despite the nephropathological relevance of ischemia, only few studies applied IRI to study long term progression of an acute ischemic insult. The IRI has different approaches of the renal dysfunction and histopathology. Cold ischemia is performed at 32°C of body temperature or by cooling the kidney to 4°C, this model is rarely used . On the other hand, warm ischemia is most frequently used and can be subdivided to bilateral (BIRI) or unilateral (UIRI), unilateral is usually performed in an attempt to reduce the results variability caused by differences between clamps efficiencies/pressure as well as the differences in renal responses to ischemia between right and left kidneys. The bilateral IR injury affects total renal mass and induces measurable increase in serum creatinine and blood urea nitrogen BUN; hallmarks of AKI in patients. The severity of the ischemic renal injury is very critical in this model; the kidneys recover near completely without chronic renal injury progression neither fibrosis when the renal injury is mild. However, animals are very likely to suffer acute renal failure and die within 48hrs when the injury is severe. The clumping time period is critical to determine the severity of the injury induced. It was indicated in most studies of BIRI that the kidney morphology returns to almost normal 2 weeks post the ischemic injury. Few studies reported limited number of damaged tubules with lymphocyte infiltration in the interstitium. In 4 weeks post BIRI, some glomerular atrophy, hypertrophy and interstitial scaring were noted. 16 days following the BIRI serum creatinine returned to sham levels and noted stable up to 49 days after BIRI, indicating non-long term functional affect (106–108).

In addition, unilateral IRI can be performed with or without right contralateral kidney nephrectomy. The unilateral IRI with contralateral nephrectomy is chosen in some studies for the low variability in the clamping pressure between two sides and also to the possibility to evaluate renal function without the effect of IRI. In UIRI with immediate contralateral nephrectomy during the surgery time the morphological and pathological changes are more likely to have the same pattern of the BIRI, as in both models the animals are considered to have ischemic kidneys after the surgery. In the other hand, UIRI model without contralateral nephrectomy have a healthy (non-ischemic) right kidney which reduced the risk of animal mortality caused by chronic kidney failure, which help to study the pathology insult of acute kidney injury induced in the model beyond the first days after the injury. In addition, this model allows longer ischemic time period making it valuable model to study the histopathology of renal acute ischemic injury progression to chronic kidney disease and for the induction of long-term tubulointerstitial fibrosis (106,107).

Many technical considerations during the surgery and recovery should be considered and controlled. Manipulation of body temperature and duration of ischemia induce variations in the long term affects, choice of anesthesia is also critical for example Barbiturates reduce blood flow to the kidney and decrease the blood pressure, in addition to reduce glomerular filtration rate and urine output. While dissociative anesthetics (Ketamine) have wider margin of safety, metabolized in liver and producing in active metabolites that are excreted by the kidney not affecting renal function (30,105).

HYPOTHESIS

2. HYPOTHESIS

Tubulointersitital fibrosis (TIF) is the final common pathway of all kidney diseases which lead to chronic renal failure. TIF may be caused by glomerular damage and tubulointerstitial damage, and also can occur in renal transplantation. Various mechanisms mediate TIF, with the implication of inflammatory molecules, growth factors, loss of tubular cell and fibroblasts accumulation. The most striking feature of TIF is excessive deposition of extracellular matrix (ECM) that is mainly produced by myofibroblasts.

Evidences show that TGF-β signaling mediates TIF, recognized as a key mediator which is sufficient to cause acute tubular injury and inflammation. TGF-β1 binds with TβRII receptor, activating TβR I receptor, phosphorylating Smad 2/3. The Smad 2/3 complex translocates to the nucleus, where it regulates target genes transcription, such as; Snail1, αSMA and Col1, thus promoting the pathogenesis of TIF.

Recently the role of Kindlin-2 in the progression of renal fibrosis have been described, by promoting the activation of TGFβ/Smad signaling and TIF pathogenesis. Furthermore, it was demonstrated that Kindlin-2 expression in HKCs was upregulated by TGF-β1 in HKCs, and its upregulated in UUO mice in association by increased TGF-β1 and Smad-3. Meanwhile knocking down Kindlin-2 expression have decreased the expression of targeted genes of the signaling pathway, such as; Snail, αSMA and Col-1 thus, attenuating TIF.

The pathophysiology of AKI and the progression of tubulointerstitial fibrosis to end stage renal disease is complex. An approaching therapeutic and protective detection system at cellular mechanism level is necessary to prevent injury progression to end stage of renal failure and loss of tissue.

Hypothesis

Recent findings involving role of Kindlin-2 activating TGFβ signaling is considered as key mediator leading to TIF. However, more knowledge is needed to implicate the protein in this process. The role of Kindlin-2 in the progression of renal fibrosis should be clarified in several renal injury processes.

OBJECTIVES

3. OBJECTIVES

The main aim of the thesis is to study the role of Kindlin-2 in the renal tubular lesion, to decipher the implication of this protein in the fibrotic process related to the TGF-β signaling. For this purpose, different injury settings have been used: Ischemia reperfusion injury in an experimental *in vivo* model, and hypoxic lesion in *in vitro* tubular cell culture.

1. To describe the expression of Kindlin-2 in a time-dependent manner after inducing a short period of ischemia in one renal pedicle.
2. To explore the effect of the induced injury by hypoxia in cultured renal tubular cells in expressing Kindlin-2.
3. To find the relationship of the Kindlin-2 expression in both *in vivo* and *in vitro* models with molecules and transcription factors related to fibrosis and TGFβ signaling.
4. To analyze the expression of Kindlin-2 in acute tubular necrosis human biopsies from kidney allograft transplants.

MATERIAL AND METHODS

4.   MATERIAL AND METHODS

4.1.   HYPOXIA/REOXYGENATION INJURY IN TUBULAR EPITHELIAL CELLS

An immortalized cell line of tubular epithelial cells from mice (MTC) were grown on 100Ø-mm Petri dishes in complete RPMI 1640 medium supplemented with 1% Penicillin/Streptomycin, 1% Glutamine and 10% inactive fetal bovine serum (FBS). Cells were incubated in normal incubators under normal conditions (20% O_2, 5% CO_2 at 37°C) until it reached around 80% of confluence. Cells were then serum-starved for 24 hours (RPMI supplemented with 1% P/S, 1% Glutamine) then incubated under hypoxic conditions (1% O_2, 5% CO_2 at 37°C) for 24/48 hours in complete RPMI medium. A control dish was maintained under normal conditions. After this period, some dishes were harvested at 0 time of reoxygenation and others were reoxygenated (20% O_2, 5% CO_2 at 37°C) in different time periods (15minutes-12hrs). Cells were harvested for RNA extraction and protein extraction. Culture medium was also collected. Furthermore, to test cells by immunofluorescence in each experiment, round sterile coverslips were placed in the same Petri dishes. At least five experiments for each condition were included.

4.2.   INDUCING ISCHEMIA REPERFUSION INJURY

Male C57BL/6J mice of 12 week-old, weighting 25-30g were obtained from PRBB animal facility, where all the experiments have been conducted. Mice were kept in cages with full access to chow and water, temperature were constantly maintained at 20-24°C, in controlled 12/12hours cycles of light/dark. All procedure was approved by the PRBB-Ethical Committee of Animal Experimentation.

The mice were subjected to 30 minutes of left kidney ischemia followed by different times of following up before the end of the study and tissue

collection. Animals were randomly included in different time periods of follow-up: 48hrs, 7 days and 45 days reperfusion. Each group was subdivided into normal drinking water group and high drinking water group (0.3%NaCl), (n=10 per group).

To start the procedure, animals were anesthetized by combined mixture of Ketamine and Medatomine, placed on heat pad. Hair was shaved from the surgical area and small left lateral opening was cut to expose the left kidney, visible detection of the renal vessels before starting. Occlusion was performed using metal clamps, dark kidney color should be observed to confirm ischemia on the kidney. Meanwhile kidney was placed in the anatomical position, monitoring the mouse vital status. After 30mins clamps were removed allowing blood to be flown back to the kidney and noting the reddish kidney color, place kidney into the right anatomical position and suture the opening using 6/0 silk sutures for the muscle and 4/0 silk sutures for the skin layer. Mice were injected with mixture of Atipemazol to reverse anesthesia and Buprenorfine for analgesia. Animals were monitored for complete recovery and followed-up according the schedule. At the end of the follow-up mice were weighted and Dolethal was injected (45mg/kg). After reaching the anesthetic plan, abdomen and thorax were opened to reach heart. Heart blood was collected and mice were reperfused using cold PBS1x (10ml). Then both right and left kidneys were collected, weighted and cut into two halves, one half for histological processing which been kept in 10% buffered formalin before paraffin processing and the other half for RNA/Protein extraction snap frozen in liquid nitrogen.

4.3.   HUMAN BIOPSIES

Protocol biopsies were used to analyze Kindlin-2 expression in human kidney. Two groups of patients were compared; the transplanted patients diagnosed histological characteristics compatible with Acute Tubular

Necrosis (ATN) and the transplanted patients without these tubular descriptions. Samples were cut in the microtome in 3μm sections on pretreated slides.

4.4. GENE EXPRESSION ANALYSIS

RNA Extraction

RNA was obtained from the frozen pellet of the harvested cells or from 50μgr of renal cortex using Tripure Isolation Reagent (Sigma). According to this protocol, pellet of cells was homogenized with 800μl of Tripure using a syringe. Then 160μl of Chloroform was added, the mixture was allowed to incubate 10 minutes at room temperature after vigorous shaking, followed by centrifugation at 12000g at 6°C for 15minutes to allow the three phases separation (transparent layer of RNA, interphase DNA, and lower red organic phase). The supernatant transparent layer was transferred to new eppendorfs tubes and 400μl of isopropanol was added. The mixture was shacked then allowed to incubate at room temperature for 10 minutes allowing RNA precipitation. Samples were then centrifuged at 12000g at 6°C for 10minutes. Supernatant was discarded and RNA pellet was washed by 1ml of 75% ethanol then centrifuged at 7500g at 6°C for 5minutes three times, and samples were air-dried for 30 minutes to eliminate the excess of ethanol. Finally, the RNA samples were re-suspended with 45μl RNase-free H_2O at 55°C and kept for 2 minutes before storing at -80ºC.

RNA Quantification and High Capacity cDNA Reverse Transcription

RNA quantity and purity was analyzed using Nanodrop spectrophotometer (ND-1000V3.3). The validity for reverse transcription

was evaluated by checking the ratio 260nm/280nm of each sample (range1.5-2).

First strand cDNA was synthesized from 2μg of RNA using High Capacity cDNA Reverse Transcription Kit (Applied Biosystems). For this purpose, appropriate RNA volumes and Nuclease-free water were mixed with 10μl of RT Master Mix 2x to obtain 20μl of final volume of reaction.

Reagent	Volume (μl/sample)
10x RT Buffer	2.0μl
25x dNTP mix (100mM)	0.8μl
10x RT Random Primers	2.0μl
MultiScribe Reverse Transcriptase	1.0μl
RNase Inhibitor	1.0μl
Nuclease-free H$_2$O	3.2μl

Table 1: Components of RT Master Mix 2x. RT Reverse Transcriptase, dNTP deoxyribose nucleoside triphosphate.

Retro-transcription was performed in a thermocycler (TProfessional Basic, Biomerta) by incubating for 10 minutes at 25°C, 120 minutes at 37°C and 5 minutes at 85°C.

Real time PCR

RT-PCR was performed using Roche SYBR Green master mix. The polymerase chain reaction (PCR) is a technique that amplifies DNA and generates thousands of millions of copies of a particular DNA sequence. The method relies on thermal cycling, repeated heating and cooling cycles for the reaction allowing different temperature-dependent reactions; DNA melting, primers annealing and enzymatic elongation of the new synthetized DNA strains. The cDNA generated is used as a template for replication, setting in motion a chain reaction where DNA template is exponentially amplified. In the real-time PCR (also known quantitative

PCR) the same methodology is used but a fluorophore is added to the amplification mix. Real-time PCR was performed using SYBRGreen Master Mix 2x (Roche), using the following reagents:

Reagent	Volume (µl/sample)	Final Concentration
SYBRGreen Master Mix 2x	5.0	1x
Forward primer (100µM)	0.025	0.25µm
Reverse primer (100µM)	0.025	0.25µm
RNase free H2O	2.95	-
cDNA sample (diluted)	2	-

Table 2: Reagents used for the real-time quantitative PCR reaction. Volume of each reagent employed per sample, as well as its final concentration, are specified

The reaction was carried out in Light Cycler 480 System (Roche) in 384-multiwell plates with final volume of 10µl. Real-time PCR settings were as following:

Step	Temperature	Ramp Rate	Time
Preincubation	95°C	4.8°C/s	5minutes
Amplification (45Cycles)			
I.	95°C	4.8°C/s	10seconds
II.	58°C	2.5°C/s	20seconds
III.	72°C	4.8°C/s	20seconds
Melting			
I.	95°C	4.8°C/s	5seconds
II.	58°C	2.5°C/s	1minute
III.	95°C	0.11°C/s	-
Cooling	4.0°C	2.5°C/s	10seconds

Table 3: Real-time PCR settings in the Light Cycler 480 System. After amplification cycles are completed, melting step is performed in order to assess that the PCR has produced single, specific products.

Material and Methods

Relative expressions of various genes were analyzed; Kindlin-2, Transforming Growth Factor (TGF-β1), Connective Tissue Growth Factor (CTGF), Collagen1a2, Collagen4a, Fibronectin-1 (FN1), Smooth Muscle Actin (αSMA) and β-Actin1.

Gene	Forward Primer	Reverse Primer	cDNA dilution
Kindlin-2	TTCGGCATCACACACTTCAT	GTCCATCCGAATCAACCTGT	1/30
TGF-β	TGAGTGGCTGTCTTTTGACG	AGCCCTGTATTCCGTCTCCT	1/30
CTGF	AAGACACATTTGGCCCAGAC	TAGAACAGGCGCTCCACTCT	1/30
COL-1	GCAGGTTCACCTACTCTGTCCT	CTTGCCCCATTCATTTGTCT	1/15
COL-4	TGTCCATGGCACCCATCTCT	CACAAACCGCACACCTGCTA	1/15
FN-1	GCCACCGGAGTCTTTACTACC	TCTCTGTCACCTCGGTGTTG	1/15
αSMA	ACTGGGACGACATGGAAAAG	AGTGTCGGATGCTCTTCAGG	1/10
ß-Actin1	GTCCACACCCGCCACCAGTTCG	GGAGCCGTTGTCGACGACCA	1/30

Table 4: Analyzed genes, primer sequences and cDNA dilution used for Real-time qPCR analysis.

Gene Expression Data Analysis

Data from real-time PCR were analyzed using Light Cycler 480 (Roche) software. For each qPCR reaction that took place in each of the multiwells plate, the threshold cycle (Ct value) was calculated using the (Abs Quant/2nd Derivative Max); only samples with standard deviation lower than 0.20 across replicates were considered for further analysis. The gene expression ratio of each target over the housekeeping gene was calculated using the delta-Cp equation.

Ultrafiltration of the Supernatant Medium:

The collected supernatant medium was concentrated using Amicon Ultra-2 Centrifugal Filter Devices (30K device – 30.000 NMWL). The device has the capability for 50-fold concentration in time periods from 10 to 60 minutes depending on the Nominal Molecular Weight Limit (NMWL).

The device can be centrifuged either in swinging bucket or fixed angle rotor. Efficient recovery of the concentrated sample is achieved by a convenient reverse spin after collecting the filtrate. The device is supplied with two tubes; filtrate collection tube and concentrate collection tube, in addition to filter device. The device was first fixed by inserting the ultra-filtration device into the filtrate collection tube, and then 900μl of the supernatant was added to the device and covered with the concentrate collection tube. Centrifugation was performed for 20 minutes at 4000xg using swinging bucket rotor as recommended in the kit. The filtrate collection tube was removed and the filtrate device with concentrate collection tube was inverted and centrifuged for 2 minutes at 1000xg to recover the concentrated solution. Finally, 10μl of the concentrated supernatant was used for protein expression analysis by western blot as performed for the total protein extracted from the harvested cells.

4.5.   WESTERN BLOT ANALYSIS

Western blot analysis technique was used to detect protein expression from the samples. Western blot is a technique where denatured proteins are separated in gel electrophoresis by molecular weight. Followed by transferring the separated proteins to absorbent membrane and incubated with antibodies specific to the proteins of interest; Kindlin-2 and TGFβ. The unbound antibody is washed off leaving only the bound antibody to the protein of interest, which is then detected by developing film. The thickness of the appearing bands corresponds to the amount of protein present.

Protein extraction

Proteins were extracted using HEPES buffer; containing 25mM HEPES at pH7.5, 25mM NaCl, 1% Triton, 10mM $MgCl_2$, 1mM EDTA pH8.5, 10%

Material and Methods

Glycerol, in addition to inhibitors; complete protease inhibitor cocktail, Pefablock, PFB protector and phosphatase cocktail inhibitor. Briefly, frozen pellets of harvested cells where homogenized with 200µl of buffer using 1ml syringe then allowed to incubate in ice for 30minutes. Samples were centrifuged at 16000xg for 10 minutes at 8°C and the proteins in the supernatant were transferred to new eppendorf tubes.

Protein Quantification

The obtained proteins were quantified using Pierce BCA Protein Assay Kit (Thermo Scientific). This assay is based on bicinchoninic acid (BCA) for the colorimetric detection and quantification of total proteins. It consists of the reduction of Cu2+ to Cu+1 by the presence of proteins in the samples and alkaline medium. A colorimetric reaction is carried out and a purple colored product is formed by the chelation of two molecules of BCA with one cuprous ion.

150µl of diluted protein extract (1/225 or 1/75) and BSA standard curve were loaded in 96-well plate. 150µl of working solution containing BCA and Cu2+ was prepared and added to all wells for 2-hour incubation at 37°C. Absorbance was measured by spectrophotometry at a wavelength of 562nm in TECAN Infinite 200 reader, and protein concentration in the samples were expressed in µg of protein /µl of sample after standard curve interpolation.

Protein expression

Western blot analysis of the protein extracts was performed by separating the proteins through polyacrylamide gel electrophoresis (PAGE) followed by transferring into polyvinylidene fluoride (PDVF) membrane (Millipore).

20µg of samples were diluted in 6x loading buffer which contain 0.21M Tris HCL (pH 6.8), 6% SDS, 34% Glycerol, 19% beta-meccaptoethanol and bromophenol blue. Heat shocked at 100°C was carried out for 10 minutes to denaturate samples were loaded onto SDS-PAGE gels, which are composed of:

1. Separating buffer 1.5M Tris-HCL at pH8.8, 2.5% sodium dodecyl sulphate (SDS), and final concentration of 7% of acrylamide-bisacrylamide.

2. Stacking buffer 0.5M Tris-HCL at pH6.8, 2.5% sodium dodecyl sulphate (SDS), and final concentration of 4% of acrylamide-bisacrylamide.

Acrylamide-bisacrylamide polymerization generates solid matrix, while SDS is protein denaturing detergent that destabilizes the protein structure and gives them global negative charge which allow protein migration under electric field.

Proteins were separated using electrophoresis system (BIO-RAD) containing running buffer (25mM TrisHCl, 192mM Glycine and 0.1%SDS), running on 80V for proteins in the stacking gel and 120V for separating gel. 8µl of Precision Plus Protein Dual Color Standard (BIO-RAD) was loaded in the first lane of the gel as a reference of the molecular weight.

PVDF membrane activation was carried out according to the manufacturer instructions by incubating in 100% methanol for 20seconds. The separated proteins were electro-transferred to the PVDF membrane using semi-dry Trans-blot Turbo blotting system (BIO-RAD) in a transfer buffer (25mM TrisHCl, 192mM Glycine pH 8.3 and 10% methanol). Nonspecific binding was blocked using blocking solution for 1hour at room temperature. The blocking solutions corresponding to each antibody manufacturer instructions were either BSA (5%) or skimmed milk (2.5% - 5%) diluted in TBS- Tween 0.1% (TBS-T 0.1%).

Material and Methods

The membranes were blotted with primary antibodies of our interest TGF-β and Kindlin-2 (Millipore, PVDF membrane) in overnight incubation at 4°C. After washing, the membranes were then incubated with secondary conjugated with horseradish peroxidase for 45 minutes at room temperature. Detection of proteins was performed by a chemiluminescent reaction (Clarity ECL Western Blotting Substrate, BIO-RAD), and the membranes were exposed to photographic films (x-Ray AGFA). The membranes were reblotted with β-Actin primary antibody for 1hour at room temperature then with conjugated secondary antibody for 1 hour at room temperature. After incubation period of each antibody membranes were washed in TBS-T 0.1% three times each for 5 mins. Following detection, films were scanned and bands were quantified by densitometry with ImageJ software (TGF-β molecular weight 65-45 kDa, Kindlin-2 72kDa, β-Actin 45 kDa).

4.6. IMMUNOFLUORESCENCE STAINING

Immunofluorescence is a technique based on the use of the specific antibodies to label a specific target antigen with a fluorescent dye. Cells were cultured under hypoxia/reoxygenation conditions as described previously for the time periods 24/48hrs of hypoxia followed by 15minutes and 3hours of reoxygenation in multi-well plates, on coverslips, which were then fixed in cold methanol (4°C). Fixing solution was aspired and cells were then washed with PBS 1x twice for 3 minutes each, before being incubated in the blocking solution which contained 2% BSA, 1% Tween-20, 1% goat serum in PBS 1x for 30 minutes at room temperature. Cells are then washed in PBS 1x twice for 2minutes each, stained with 1:500 dilution of Kindlin-2 antibody for one hour at room temperature. After two washes in PBS1x for 2 minutes, incubation of AlexaFluor-conjugated secondary antibody was performed for 45 minutes

at room temperature in dark. The coverslips were washed with PBS1x twice and mounted with Mowiol-Dabco 25% and DAPI 1:2000.

4.7. QUANTITATIVE COLORIMETRIC CREATININE ASSAY

Creatinine was measured using BioAssay Systems Creatinine Assay in serum to assess the kidney function. Using improved Jaffe method, the picrate forms red color complex with creatinine in the sample. The intensity of the color is measured at λ510nm and is directly proportional to the creatinine concentration in the sample. 30µl of different concentrated standards (1, 3 and 10 mg/dl) was added in 96-well plate, as well as 30µl of samples. Working reagent was added quickly to all wells which was prepared by mixing 100µl of reagent A with 100µl of reagent B for each sample, optical density was immediately read (OD0) and then after 5 minutes (OD5). The creatinine concentration of the sample was calculated following the equation: (OD5 sample – OD0 sample)/ (OD5 STD – OD0 STD) x (STD mg/dl).

4.8. HISTOLOGICAL STUDIES

Paraffin blocks were cut into 3µm-sections with rotary microtome (Leica). Sections were placed in water bath of 40ºC for stretching and collected on Superfrostdslides (Fisher Scientific). Slides were places in rack holder on heat platform for 1 hour to eliminate the excess of water and then placed overnight at room temperature. Slides were then stored at 4ºC.

Routine Staining (Hematoxylin & Eosin)

The hematoxylin & eosin (HE) is the most common routine staining. It was used in our study to evaluate the structural alterations observed in tubules and interstitium and structural differences between contralateral

non-ischemic kidneys vs. ischemic kidneys. Microscopic observation was performed using Olympus microscopy BX61. The staining protocol was carried out as following:

- Slides of 3µm of section of kidney were placed in oven at 60°C for 30 mins to discard the excess of paraffin (Dewaxing)
- Dewaxing by dipping twice in Xylol I & II for 15 mins each
- Rehydrated in sequence Ethanol concentrations 96, 70 and 50%, 5 mins each
- Washed in distilled water
- Stained in 30% Hematoxylin for 20seconds, then placed in distilled water before rinsing in tap water
- Dip 3 times in and out in Ammonia water 0.3% for blue staining, then washed in distilled water
- Rinse in 96% Ethanol for 5 mins
- Counterstain in Eosin for 20-30seconds
- Dehydrate in Absolute Ethanol I & II, dipping in and out 3 times in each
- Cleared in Xylol I & II, 5mins each
- Mounting the slides with DPX and cover them

Immunohistochemistry

Immunohistochemical staining for Kindlin-2 and α-SMA protein expression is performed in 3µm-kidney sections placed in Superfrost slides following the methods optimized for each analyzed protein.

As for the H&E staining, samples were initially dewaxed and hydrated.

- **Dewaxing**: Slides been placed at 65°C for 30 mins, then place in Xylol for 15 mins, twice. Place in absolute Ethanol for 10 mins, twice

- **Hydrating:** Passed in serial concentration of Ethanol each 1 min, gradually from 95%, 70% to 50%. Then place slides in distilled water.

For α-SMA staining:

1. **Boiling:** Using 250ml of Sodium Citrate Tribasic buffer, 10mM pH6 in microwave. Before boiling the slides, buffer is preheated (750W for 1:30mins). Samples are boiled in microwave (160W for 5 mins). Then allowed to cool down at room temperature to reach maximum 50°C before placing the slides in distilled water for 5 mins.

2. **Peroxidase blocking:** Slides were well dried, the tissues surrounding been marked using Dako Pen. 50 µl of 3% peroxidase blocking solution were added to each slide and allowed for 20 mins incubation in dark. Then, washed in TBS 0.1%Tween-20, 3 times, 3 mins each.

3. **Blocking of unspecific unions:** Slides were incubated in 1% BSA blocking solution for 30mins at room temperature, in dark humid box. Then washed in TBS-T 0.1%Tween-20 for 1 min.

4. **Blocking endogenous immunoglobulins:** Slides were incubated with 25µl of F(ab) anti-mouse diluted in PBS1x (1:10) in dark humid box (Jackson Immunoresearch). This mix of F(ab) monomeric secondary antibodies helps to reduce background when secondary antibody from the same species is used. After 1hr-incubation, samples were washed in TBS-Tween20 0.1% for 1 min.

5. **Primary Antibody:** 25µl of 1:800 anti-α-SMA primary antibody dilutions were used for 1 hour of incubation in humid dark box at RT.

Material and Methods

For Kindlin-2:

1. **Boiling:** Using 2L of Sodium Citrate tribasic, 10mM pH6. Samples were boiled in the pressure pot for 10 mins, and then allowed to cool down at room temperature to reach maximum 50°C before placing the slides in distilled water for 5mins.

2. **Peroxidase blocking:** Slides were well dried, the tissues surrounding been marked using Dako Pen. 50 µl of 3% peroxidase blocking solution have been added to each slide and allowed for 20 mins incubation in dark. Washed in TBS-Tween-20 0.1%, 3 times, 3 mins each

3. **Blocking of unspecific unions:** Slides were incubated in 1% BSA blocking solution for 30mins at room temperature, in dark humid box. Then washed in TBS-Tween-20 0.1% for 1 min.

4. **Primary Antibody:** 25µl of 1:500 Kindlin-2 primary antibody dilutions was used for each slide. Samples were kept in humid dark box during the overnight incubation at 4ºC.

For all the antibodies, next steps were followed:

- **Secondary Antibody:** The excess primary antibody were eliminated from slides by TBS-Tween-20 0.1% washings and 25µl of secondary dual antirabbit/mouse was added (Dako Mono Link) and allowed an incubation of 1 hr in humid dark box at RT before being washed in TBS-Tween-20 0.1%, 3 times each 3 mins.

- **Signal detection:** Using 30 µl of substrate-chromogen solution (50:1) which was prepared from the kit (Dako Mono Link). Solution was applied to each sample and allowed to react for 5 minutes. To stop the reaction samples were immediately placed in distilled water.

- **Hematoxylin Counterstaining:** the slides were dipped in hematoxylin for 30 seconds, placed in distilled water then placed in running tap water to wash out the excess of hematoxylin
- **Dehydration:** Slides placed in serial concentration of ethanol 50, 70, 95% for 1 min each. Twice in absolute Ethanol I and II for 1 min each and finally placed twice in Xylol I and II for 3mins
- **Mounting:** DPX was used to cover slides and left for air-drying

For each α-SMA-stained section or Kindlin-2-stained section, 10 microphotographs of the renal cortex were taken per kidney at 10x magnification. The α-SMA positive staining was quantified using ImageJ Software. The specific brown signal was digitally isolated and expressed as mean grey value (MGV). Quantitative analysis was performed by comparing the statistical mean values between contralateral non-ischemic kidney vs ischemic kidney in each study group.

4.8.1. STATISTICAL ANALYSES

Significant differences between groups were calculated by using the non-parametric Mann-Whitney U-test for two group comparisons (SPSS 18.0 for Windows). $P<0.05$ was considered statistically significant. Of mention that, although the majority of the studies variables followed a non-parametric distribution, we decided to present out data as mean±SEM for clarity.

RESULTS

5.   RESULTS

5.1.   *In-vivo* STUDIES

5.1.1. Serum Creatinine Levels

The ischemia/reperfusion injury alters the kidney function. This parameter was assessed in our model from blood collected at the end point of the study from each animal of the study group. For these comparisons, healthy animals without ischemia were used as control in order to compare the basal levels of sCrea with the levels in animals subjected to unilateral ischemia (Figure 7).

Although a trend of increase in serum creatinine levels were detected in our model as compared to control animals, yet it was seen that the contralateral non-ischemic kidney has the capability of maintaining the renal function. However, in long-term follow-up of 45 days, serum creatinine levels were significantly higher in the group of high-salt drinking water as compared to the normal water drinking group
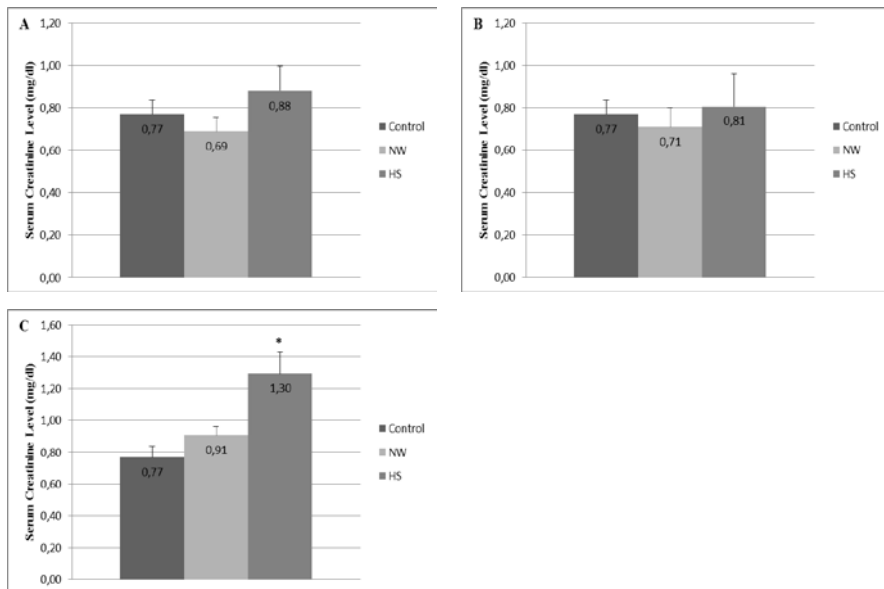
5.1.2. Renal Weight

Ratios of kidney weight to total body weight of the animals have been measured and analysis demonstrated that the ratio of kidney weight was significantly decreased in the ischemic kidney after 7 days of follow-up in high salt group when compared to the contralateral kidney. Furthermore, after 45 days post-ischemia the ratio of kidney weight was significantly decreased in ischemia kidney compared to the contralateral control kidney in both normal drinking water and high salt group, as shown in Figure 8.
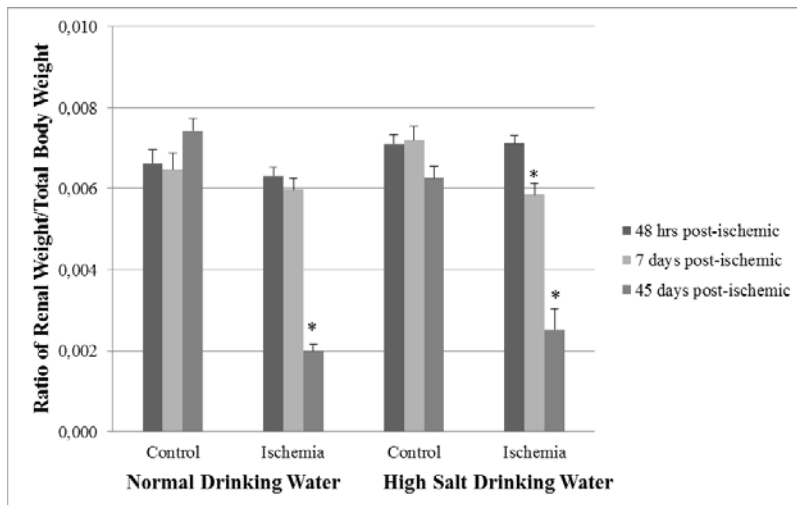
Figure 8: Ratio of Renal Weight/Total body weight. Ischemia significantly decreased some ratios of renal weight in ischemic

kidney when compared to the contralateral control kidney. Data are expressed as mean±SEM. *p≤0.05 ischemic vs. contralateral control kidney.

5.1.3. Histological Studies

5.1.3.1.　　　Hematoxylin-Eosin Staining

Microtome-sections of ischemic and non-ischemic kidneys were performed and stained using Hematoxylin-Eosin for histological examination. In all ischemic samples, we found morphological features compatible with acute tubular injury and acute tubular necrosis, consisting in focal detachment of tubular epithelial cells, loss of the epithelial apical brush border, tubular dilatation associated to flattening of the epithelium. We also found scatter hyaline tubular casts. These changes were focally identified in the renal cortex, alternating with more preserved areas. The extent of the morphological changes of acute tubular injury seemed to correlate with the follow-up periods. None of these tubular changes were identified in the contralateral non-ischemic kidney of each mouse. More severely dilated tubules associated with loss of individual tubular epithelial cells and loss of individual tubular nuclei was seen in the 45-day post-ischemic group (Figure 9).
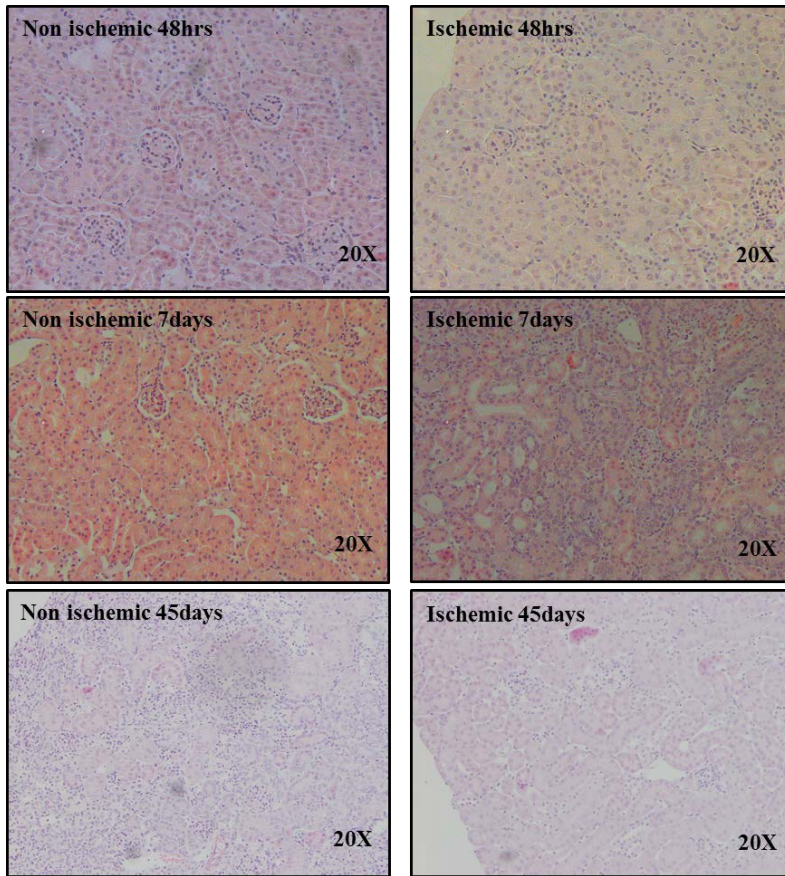
Figure 9: Hematoxylin & Eosin Stained Tissue (x10).
Representative microphotographs of hematoxylin eosin stained
sections of Ischemic and contralateral non-ischemic sections from
the following up periods 48hrs, 7days and 45days.

5.1.3.2. Kindlin-2 Immunostaining

Kindlin-2 expression was constantly identified in the tubular brush border
of the proximal convoluted tubules, in the basement membrane of the
Bowman´s capsule and in the cytoplasm of the cells composing the
juxtaglomerular glomerular apparatus in all of non-ischemic kidney

samples. Some of these staining were considered as non-specific such as of the brush border staining.

Within the ischemic kidneys, Kindlin-2 staining was similarly detected in the basement membrane of the Bowman´s capsule and in the cytoplasm of the cells composing the juxtaglomerular glomerular apparatus. In addition, Kindlin-2 staining was also detected focally in the cortical interstitium. Also, mild staining of the membranes of tubular epithelial cells and of tubular basement membranes of the tubules was identified. Finally, focal lineal cytoplasmic staining was detected in the epithelium of tubules without morphological alterations of acute tubular injury (Figure 10 to 12).
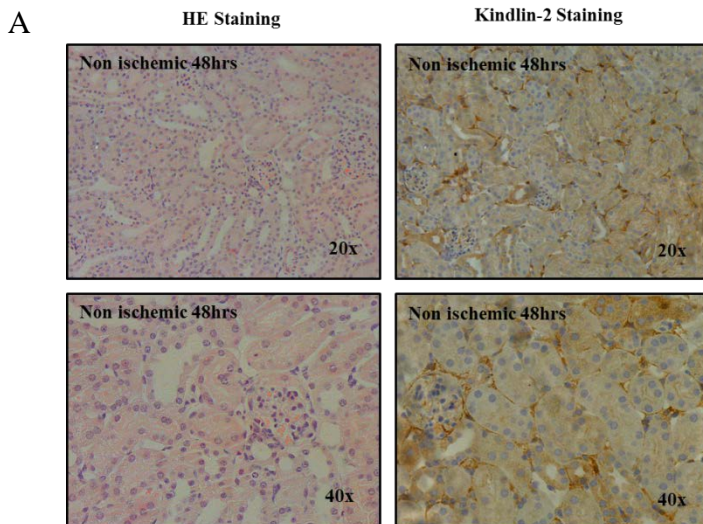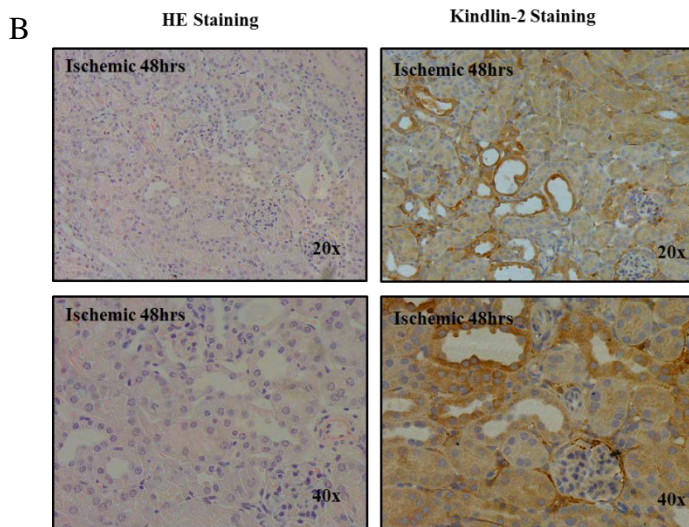
Figure 10: Kindlin-2 staining Ischemia/reperfusion influence on Kindlin-2 expression after 48-hrs post-ischemia. Representative microphotographs of stained cortical sections after 48hrs post-ischemia of both Kindlin-2 and HE. Group A represents non-ischemic contralateral tissue, B represents ischemic tissue.
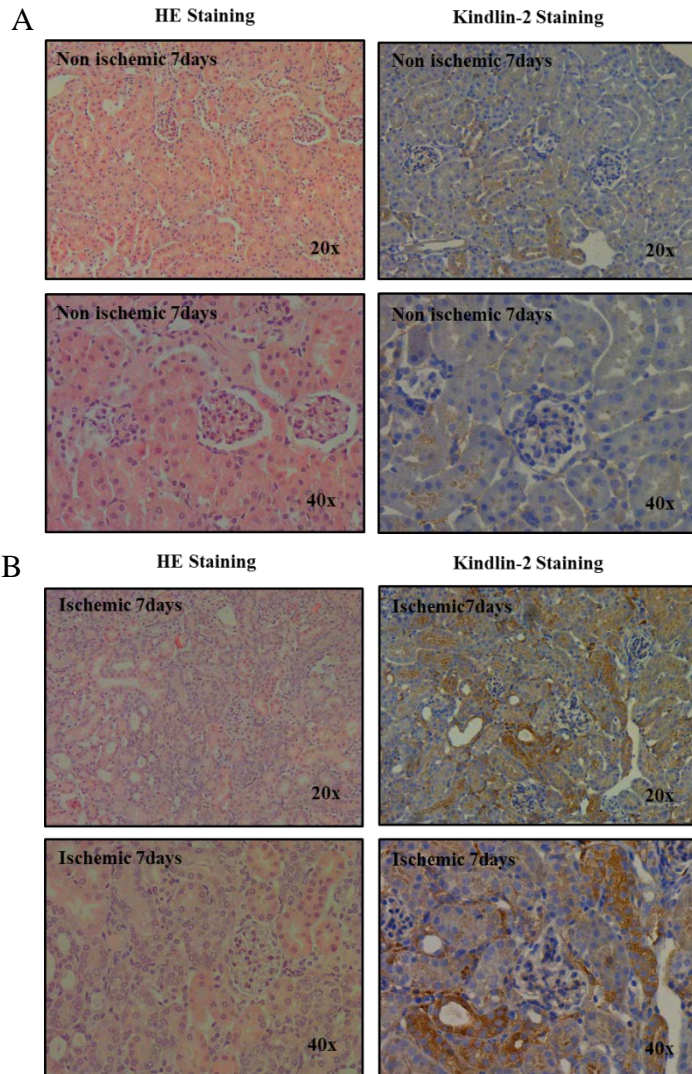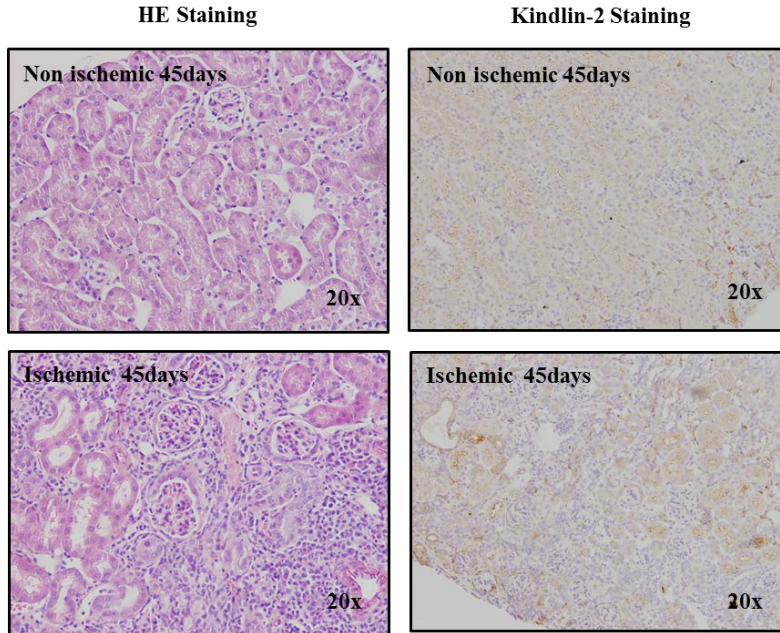
Figure 11: Kindlin-2 staining Ischemia/reperfusion influence on Kindlin-2 expression after 7days post-ischemia. Representative microphotographs of stained cortical sections after 7days post-ischemia of both Kindlin-2 and HE. Group A represents non-ischemic contralateral tissue, B represents ischemic tissue.

HE Staining   Kindlin-2 Staining

Non ischemic 45days   Non ischemic 45days

20x   20x

Ischemic 45days   Ischemic 45days

20x   20x

Figure 12: Kindlin-2 staining. Ischemia/reperfusion influence on Kindlin-2 expression after 45-days post-ischemia. Representative microphotographs of stained cortical sections after 45 days post-ischemia of both Kindlin-2 and HE, of non-ischemic contralateral and ischemic tissues.

Kindlin-2 immunostained areas were quantified using Image J software (Open Source Java Image Processing). Results showed that Kindlin-2 expression was significantly higher after 48 hours of follow-up in ischemic kidney as compared to the contralateral non-ischemic control only in the high salt drinking water group, while it was significantly higher 7 days and 45 days of follow-up in ischemic kidneys as compared to the contralateral non-ischemic controls, in both normal drinking water and high salt groups. Furthermore, Kindlin-2 expression was significantly reduced in the contralateral non-ischemic control of animals receiving high salt drinking water when compared to the contralateral non-ischemic control of the normal drinking water group (Figure 13).
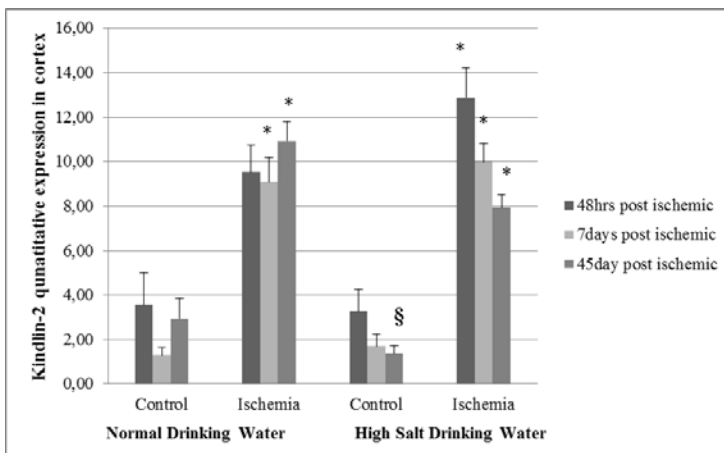
Figure 13: Kindlin-2 expression in ischemic tissue from all the study groups. Ischemia have significantly increased Kindlin-2 cortical expressions in the ischemic kidneys after 48 hrs, 7 days and 45 days post ischemia, in both normal and high salt drinking water groups. In 7 days post ischemia, high salt has significantly increased Kindlin-2 cortical expression in contralateral control kidney compared to the normal drinking water group. Data are expressed as mean±SEM. *p≤0.05 ischemic vs. contralateral control kidney, §p≤0.05 normal drinking water group vs. high salt group.

5.1.3.3.   α-SMA Immunostaining

In the ischemic tissue, α-SMA staining was also detected in the wall of peritubular capillaries, in the basement membrane of the Bowman´s capsule and in the cytoplasm of the cells composing the juxtaglomerular glomerular apparatus. In addition to this, α-SMA staining was also detected in the cortical interstitium surrounding the tubules; in addition, overexpressed staining was found in the endothelium of the peritubular cortical capillaries. Also, some weak staining was detected in tubular epithelial cells, as shown in Figures 14 to 16.
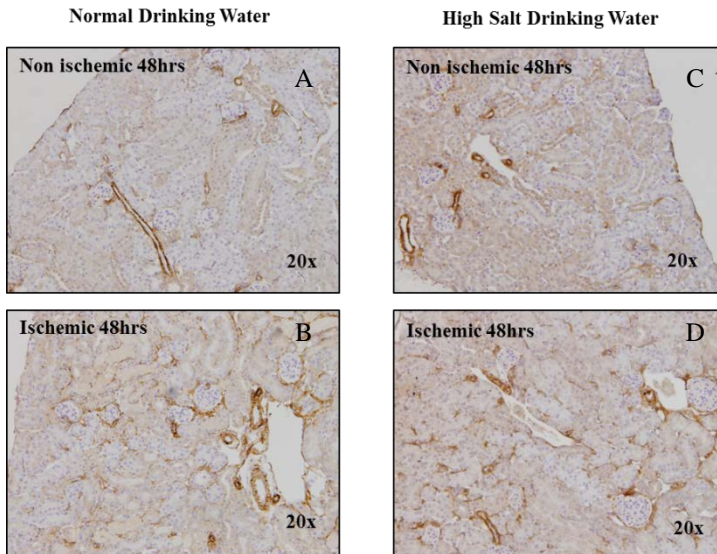
Figure 14: α-SMA staining. Ischemia/reperfusion influence on α-SMA expression in 48-hrs post-ischemic group. Representative microphotographs of cortical α-SMA immunostaining in 48-hrs post-ischemic groups. Panel A: contralateral control normal-water, B: ischemic kidney normal-water, C: contralateral control high-salt water, D: ischemic high-salt.
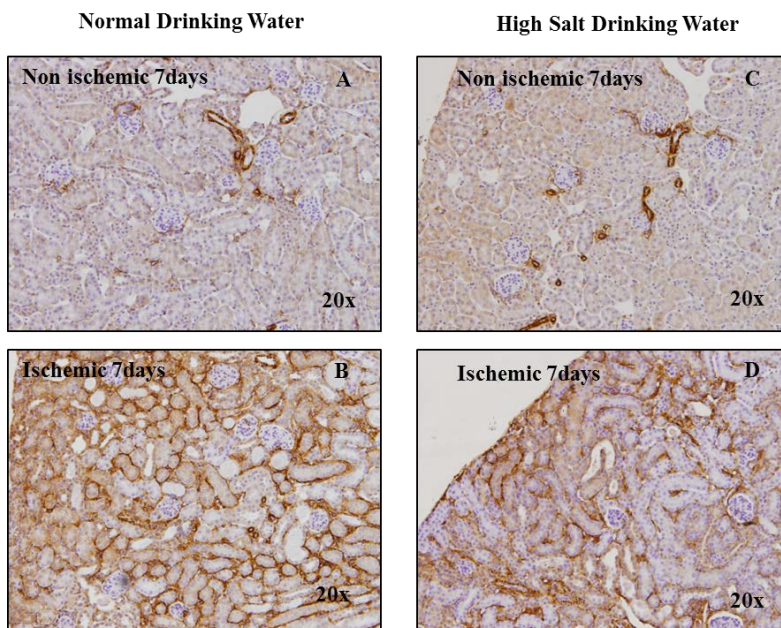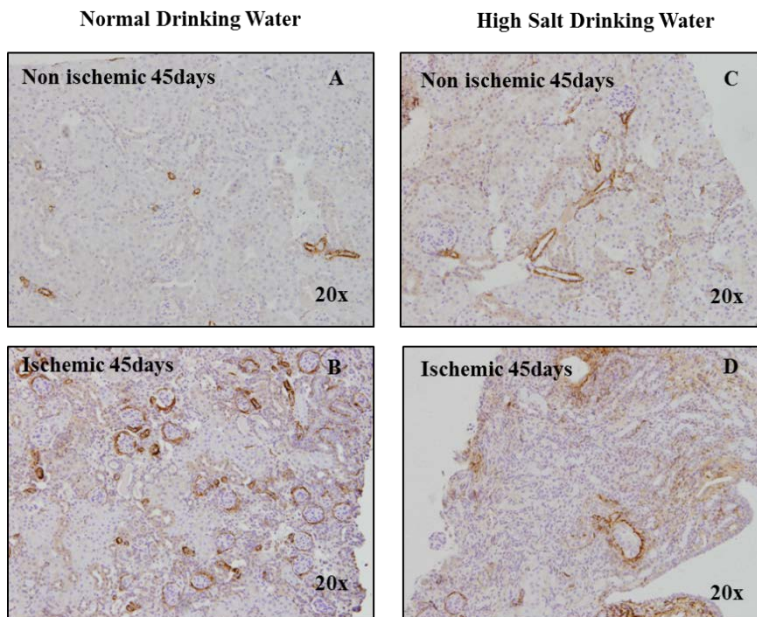
Normal Drinking Water   **High Salt Drinking Water**

Figure 15: α-SMA staining (10X). Ischemia/reperfusion influence on α-SMA expression in 7-days post-ischemic group. Representative microphotographs of cortical α-SMA immunostaining in 7-days post-ischemic groups. Panel A: contralateral control normal-water, B: ischemic kidney normal-water, C: contralateral control high-salt water, D: ischemic high-salt.

Figure 16: α-SMA staining (10X). Ischemia/reperfusion influence on α-SMA expression in 45-days post-ischemic group. Representative microphotographs of cortical α-SMA immunostaining in 45-days post-ischemic groups. Panel A: contralateral control normal-water, B: ischemic kidney normal-water, C: contralateral control high-salt water, D: ischemic high-salt.

α-SMA immunostaining expression was also quantified using Image J software (Open Source Java Image Processing). Results have demonstrated that α-SMA expression was significantly higher after 48 hours, 7 days and 45 days of follow-up in the ischemic kidneys as compared to the contralateral non-ischemic controls, in both normal-water and high-salt groups. In addition, after 7 days of follow-up, α-SMA intensity was significantly lower in the contralateral control kidney of high-salt group when compared to contralateral control kidney of normal drinking water group, as well as it was significantly lower in the ischemic

kidney of high-salt group when compared to the ischemic normal-water group after 48hrs follow-up, as shown in Figure 17.
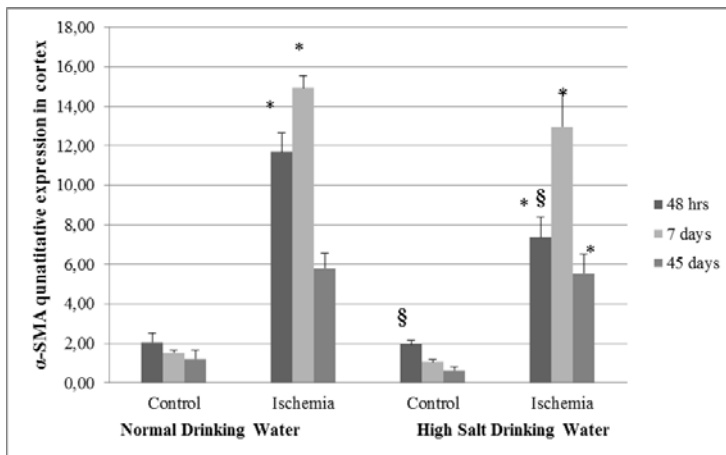

Figure 17: α-SMA expression in ischemic tissue from all the study groups. Ischemia have significantly increased α-SMA cortical expressions in the ischemic kidneys after 48 hrs, 7 days and 45 days post ischemia, in both normal and high salt drinking water groups. α-SMA is highest expressed in ischemic tissue 7 days post-ischemia. Data are expressed as mean±SEM. *p≤0.05 ischemic vs. contralateral control kidney, §p≤0.05 normal drinking water group vs. high salt group.

As general overview, Kindlin-2 cortical protein expression correlates with α-SMA in all ischemic tissues.

5.1.3.4.   Kindlin-2 in Human Renal Biopsies

Kindlin-2 expression was examined in renal biopsies from kidney transplanted patients. Two groups of transplanted patients were analyzed. One group with histological changes compatible with acute tubular necrosis (ATN) was used as ATN group, and one group not showing these changes was used as control group. In control biopsies, Kindlin-2

immunostaining was detected in the cytoplasm of tubular epithelial cells, and also in the cytoplasm of the endothelium peritubular capillaries and of the glomerular capillaries, and moreover in the cytoplasm of the podocytes (Figure 18-A, B, C)). In the samples with changes compatible with ATN (Figure 18-D, E, F), Kindlin-2 immunostaining was also detected in the smooth muscle cells of arteries, as shown in Figures 12 and 13. Percentages of stained cross-sections tubules using 40X microscopic fields in both ATN and control samples were quantified (Figure 19). An average of 63% of tubules showed Kindlin-2 staining in ATN samples, whereas only an average of 22% of tubules were stained in control samples, as shown in Figure 20.
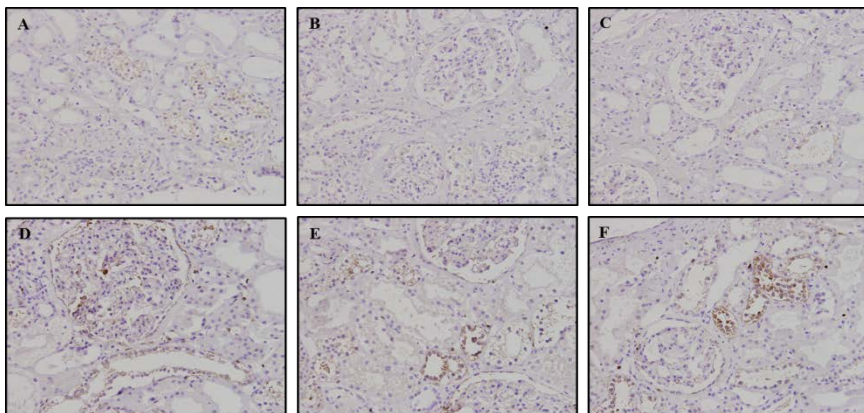

Figure 18: Kindlin-2 expression in Human Biopsies. Representative photomicrographs of Kindlin-2 staining from human biopsies. Original magnification x20. Kindlin-2 staining in control group in Panels A, B and C, and in ATN group in Panels D, E and F.
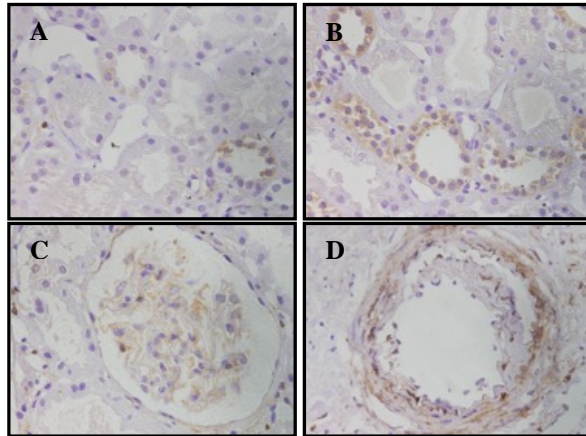
Figure 19: Kindlin-2 expression in Human Biopsies. Representative photomicrographs of Kindlin-2 staining from human biopsies. Original magnification x40. Tubular staining in Panel A of control sample. Panel B tubular staining in ATN patient. Panel C is staining in podocytes and in glomerular endothelium, and Panel D smooth muscle cell staining in artery in ATN sample.
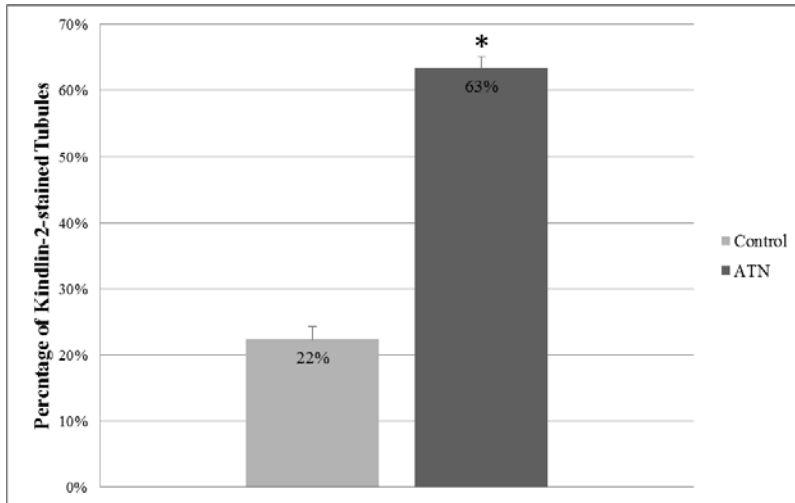

Figure 20: Kindlin-2 expression in Human Biopsies. Percentage of tubules stained in biopsies of ATN patients and non-necrotic control. Data are expressed as mean±SEM. *$p \leq 0.05$ ATN vs. control.

5.1.4. Quantitative Gene Expression Analysis

Gene expression analyses were performed as mentioned earlier by real time PCR in all study groups for different genes. After 48 hours post ischemia, renal Kindlin-2 gene expression in ischemic kidneys was similar in both groups; normal drinking water and high-salt drinking water. Similar profile was found after 7 days of ischemia.

However, after 45 days of follow-up after ischemia, Kindlin-2 gene expression was significantly increased in left ischemic kidneys as compared to the contralateral control kidneys in animals receiving normal drinking water. Kindlin-2 gene expression in animals drinking high-salt water was not significantly changed when comparing left ischemic kidney with contralateral control kidney. High salt drinking water had no influence in Kindlin-2 gene expression (Figure21).
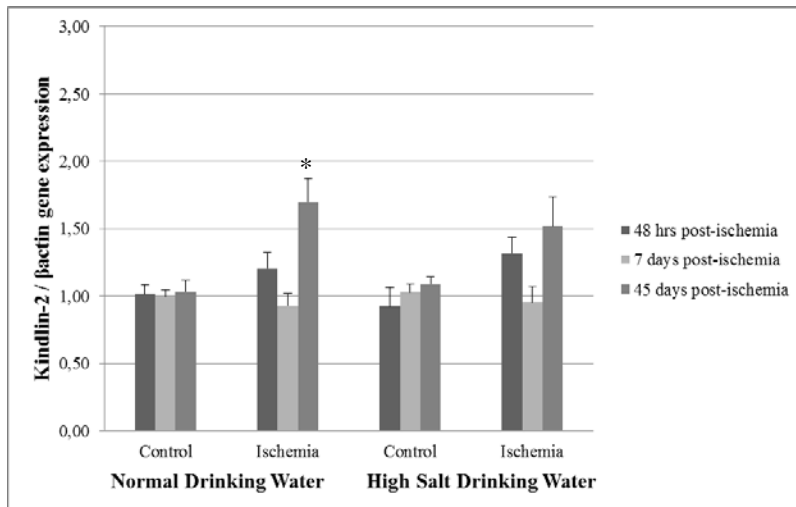

Figure 21: Kindlin2 Gene Expression. Kindlin-2 mRNA level was significantly increased in ischemic kidney at 45 days post-ischemia, but no changes were detected after 48 hrs and 7 days post-ischemia. Data are expressed as mean±SEM. *p≤0.05 ischemic vs. contralateral control kidney.

TGFβ1 gene expression was also analyzed. After 48 hours post ischemia TGF-β1 gene expression was found to be decreased in ischemic kidneys as compared to the control kidneys in animals drinking normal water. However, this decrease was not significant when kidneys from animals drinking high-salt water were studied.

In the 7 days post ischemia TGF-β1 gene expression was significantly increased in the ischemic kidney as compared to the contralateral control kidney in both groups of normal drinking water and high salt. Interestingly high-salt drinking water induced an increase of TGF-β1 gene expression in ischemic kidney significantly different from the ischemic kidney on normal drinking water group.

After 45 days of follow-up TGF-β1 gene expression levels were again significantly decreased in ischemic kidney as compared to contralateral control kidney. This decrease was observed in both groups of study, drinking normal water and high-salt water groups. (Figure22).
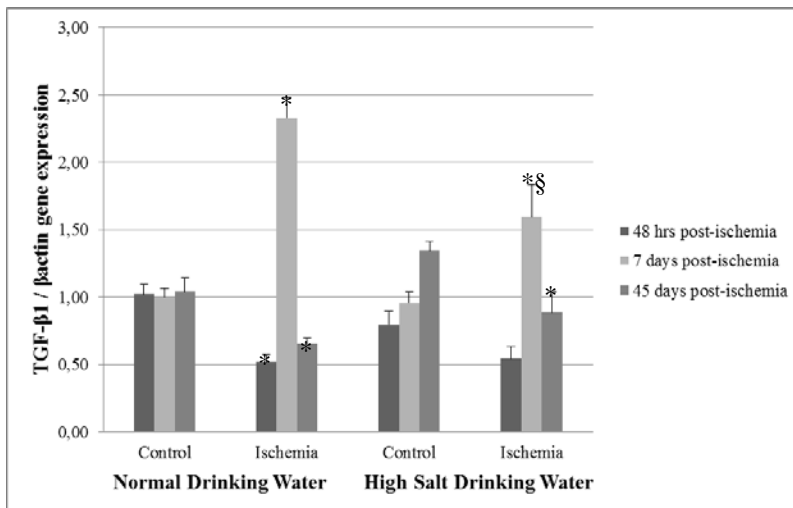

Figure 22: TGFβ1 Gene Expression. TGF-β1 mRNA expression levels were increased after 7 days following ischemia, while decreased 48 hrs and 45 days post-ischemia in normal drinking water groups. Data are expressed as mean±SEM. *p≤0.05

ischemic vs. contralateral normal kidney, §p≤0.05 normal drinking
water vs. high salt group.

On the other hand, neither ischemia nor high-salt groups had any
significant influence in CTGF gene expression in any of studied groups;
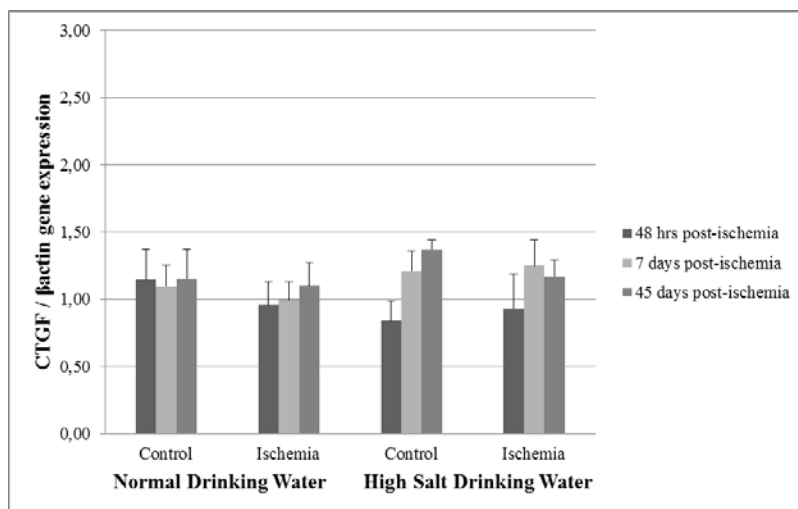48-hr, 7-day or 45-day, as shown in Figure 23.

Figure 23: CTGF Gene Expression. CTGF mRNA expression
levels were not changed in any of the post-ischemic groups. Data
are expressed as mean±SEM. *p≤0.05 ischemic vs. contralateral,
§p≤0.05 normal drinking water vs. high salt drinking water.

Pro-fibrotic genes related to the TGFβ signaling pathway such as Collagen
type 1 and Collagen type 4 were also analyzed. After 48 hours of
ischemia, Collagen type 1 expression was found to be significantly
decreased in ischemic kidneys as compared to contralateral control kidney
in animals drinking normal water in both groups; normal drinking water
and high-salt.

In the 7 days post ischemic kidneys, COL-1 was significantly increased as
compared to the contralateral kidneys in both normal drinking water and

high-salt groups. However, again an opposite profile was observed after 45 days of ischemia; COL-1 was also significantly decreased in ischemic kidney when compared to the contralateral control kidney in both, normal drinking water and high-salt drinking water groups. Interestingly, high salt has significantly increased COL-1 gene expression in the contralateral control kidney as compared to the contralateral control kidney of normal drinking water group, as shown in Figure 24.
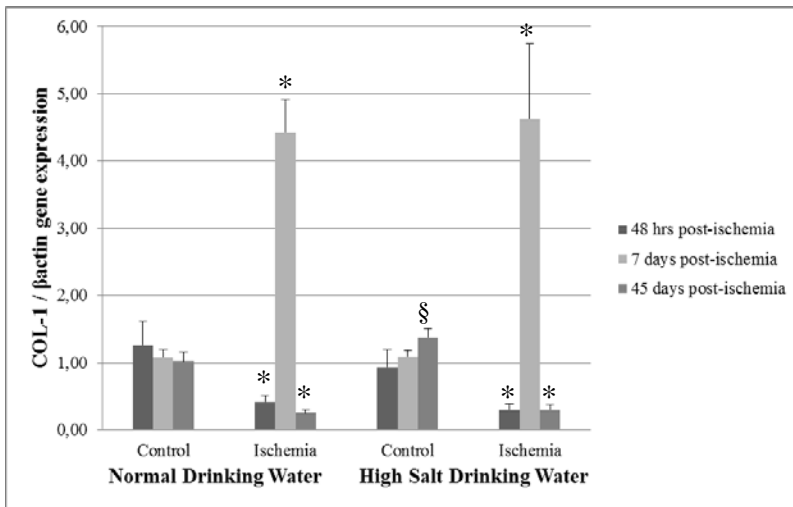

Figure 24: Collagen-1 Gene Expression. Collagen-1 mRNA levels were significantly increased 7 days post ischemia in both, normal drinking water high salt groups. While 48 hrs and 45 days post ischemia COL-1 was significantly decreased in ischemic kidney of only normal drinking water group. Data are expressed as mean±SEM. *$p \leq 0.05$ ischemic vs. contralateral control kidney, §$p \leq 0.05$ normal drinking water vs. high salt drinking water group.

Collagen type 4 was not significantly influenced in the ischemic kidney after 48 hrs post-ischemia in neither normal drinking water nor high salt groups. 7 days post-ischemia COL-4 was significantly increased in ischemic kidney as compared to the contralateral control kidney in both normal drinking water and high-salt groups. On the other hand, 45 days

post-ischemia the gene expression in ischemic kidney was similar to its expression in the contralateral control in both normal drinking water and high-salt groups, as shown in Figure 25.
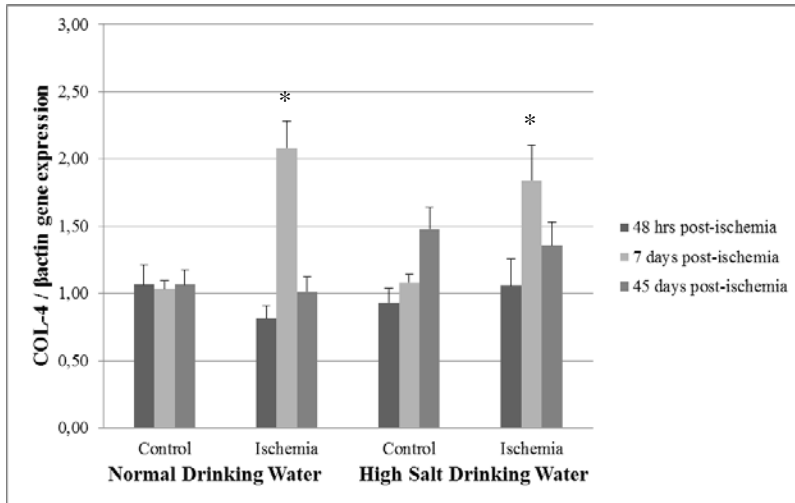

Figure 25: Collagen-4 Gene Expression. Collagen type 4 mRNA levels significantly increased in ischemia kidney in 7 days post-ischemia when compared to the contralateral normal kidney on the normal and high-salt drinking water groups. Data are expressed as mean±SEM. *p≤0.05 ischemic vs. contralateral control kidney, §p≤0.05 normal drinking water vs. high salt group.

α-SMA gene expression levels were significantly decreased in 48-hr post-ischemic groups in the normal drinking water group, but not in the high-salt group.

In the 7-days post-ischemic group α-SMA was significantly increased in ischemic kidney comparing to contralateral control kidney of normal drinking water group. On the other hand, after 45 days of ischemic significant decrease was also detected in the ischemic kidney when compared to the contralateral control kidney of the normal drinking water group, but not significant in the high salt group, as shown in Figure 26.
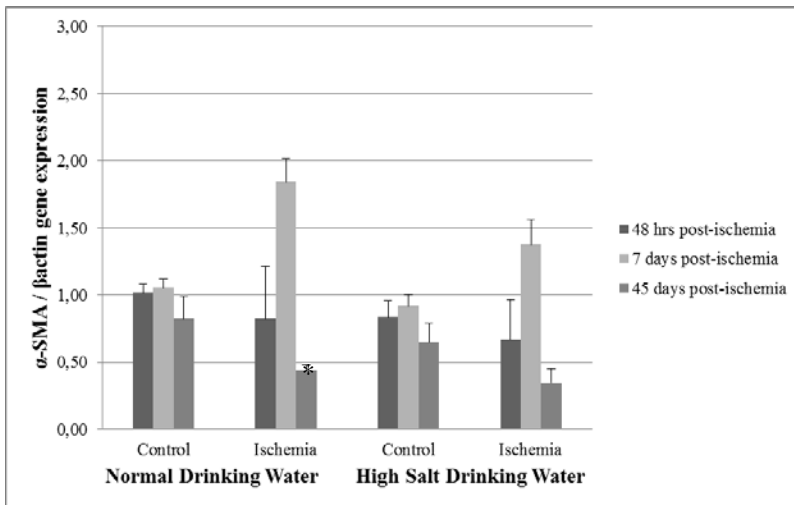
*

112

*

Figure 26: α-SMA Gene Expression. α-SMA significantly changed in the ischemic kidney compared to the contralateral control kidney 48 hrs, 7 days and 45 days post ischemic, only in the normal drinking water groups. Data are expressed as mean±SEM. *p≤0.05 ischemic vs. contralateral control kidney.

Fibronectin-1 gene expression (FN-1) was significantly decreased in 48 hours post-ischemia of both; normal drinking water and high salt groups. In the 7 days post-ischemia FN-1 expression was significantly increased in ischemic kidney as compared to the corresponding contralateral control kidneys of both normal drinking water and high-salt groups. In the other hand, in 45 days post-ischemia FN-1 was significantly decreased in ischemic kidneys of normal drinking water, as shown in Figure 27.
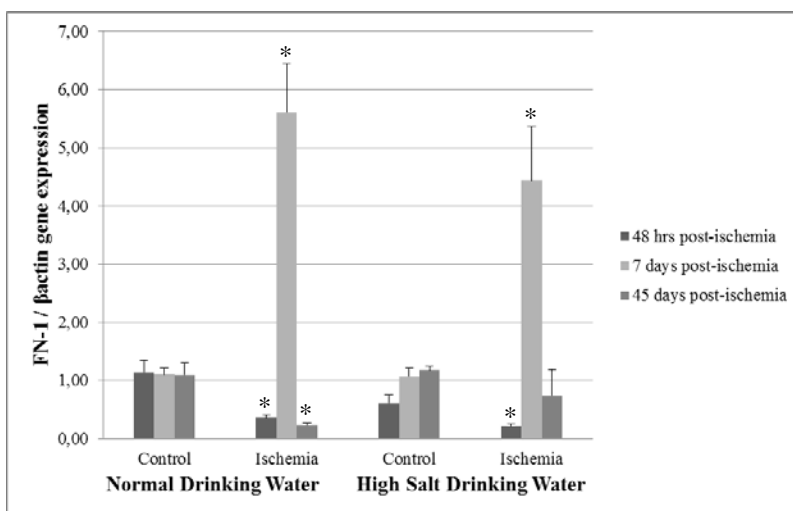
Figure 27: Fibronectin Gene Expression. Fibronectin-1 mRNA expression levels were significantly decreased in ischemic kidneys after 48hrs and 45 days post-ischemia in both normal drinking water (NW) and high salt (HS) groups. In 7 days post-ischemia FN-1 was significantly increased in ischemic kidneys of normal drinking water and high-salt groups. Data are expressed as mean±SEM. *$p \leq 0.05$ ischemic vs. contralateral control normal kidney, §$p \leq 0.05$ normal drinking water vs. high salt drinking water.

In all ischemic tissues, Kindlin-2 gene expression correlates in encounter pattern with COL-1 and FN-1, while TGF-b correlates similarly with COL-1, COL-4, a-SMA and FN-1. However, COL-1 gene expression correlates proportionally with COL-4, while both COL-4 and a-SMA correlate proportionally with FN-1 gene expression.

5.1.5. Kindlin-2 Protein Analysis

Kindlin-2 protein levels were analyzed in samples extracted from the renal cortex of tissue obtained after 48 hrs, 7 days and 45 days post-ischemia; both normal and high-salt drinking water groups.

Although some trends of increase were observed in Kindlin-2 protein expression level in ischemic kidneys, yet it was not statistically significant and high variability were found between samples of same study groups. Interestingly significant decrease of Kindlin-2 protein expression was detected in high-salt ischemic groups compared to the corresponding contralateral control in 45 days post-ischemia (Figure 28).
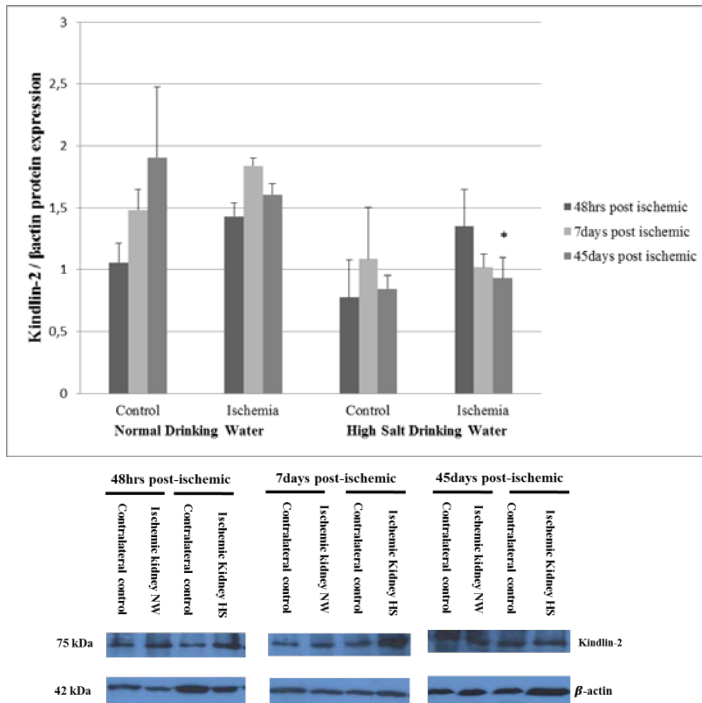

Figure 28: Kindlin-2 protein expression in animal study groups. Representative Immunoblot and densitometries of renal cortical Kindlin-2 protein expression normalized to βactin. Analysis has been performed using ImageJ software. Bands intensities were calculated and normalized to βactin. Data are

expressed as mean±SEM. *p≤0.05 ischemic vs. contralateral control kidney

5.2. *In-vitro* MODEL

5.2.1. Roexygenation Incubation Periods Setting Up

In the first set of experiments performed we were trying to optimize our experimental conditions to obtain the model mimicking the ischemic lesion to induce Kindlin-2 expression. Experiments were done using mouse tubular cells (MTC) as mentioned in the material and methods where hypoxia incubation followed by reoxygenation periods was performed to induce injury. Therefore, the effect of several hypoxia/reoxygenation periods inducing Kindlin-2 and TGF-β1 was tested on both gene and protein level. The time points tested included two main hypoxic incubation periods; 24 hours and 48 hours, where both are followed by different reoxygenetaion periods.

First, we tested the effect of hypoxia incubation in Kindlin-2 gene expression after 24 hours of incubation at 1% of oxygen. By performing real time PCR, hypoxia had no significant influence on Kindlin-2 expression; neither significant change was detected in cells incubated for 24 hours in hypoxia followed by 1 hour of reoxygenation (Figure 29). Furthermore, high variability between samples was detected which therefore the results obtained from this testing condition was inconclusive.
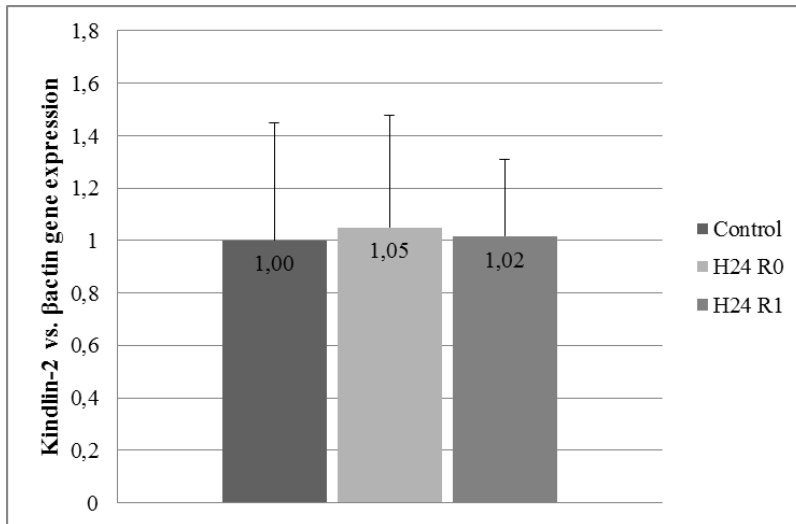
Figure 29: mRNA levels were assessed for Kindlin-2. Values were normalized to βactin gene expression. Data are expressed as mean±SEM. Kindlin2 gene expression was not influenced after 24hrs of hypoxia neither when followed by 1hr of reoxygenation as compared to the control group.

In order to test how the longer time of hypoxia could influence the targeted genes in MTCs we expanded the hypoxia incubation into 48hrs. Kindlin-2 gene expression was not significantly modified by 48hrs of hypoxic incubation followed by 1hr of reoxygenation (Figure 30). However, TGF-β1 gene expression was significantly decreased (Figure 31).

Figure 30: Kindlin-2 mRNA level was not influenced after 48 hours of hypoxia followed by 1 hour of reoxygenation. Values were normalized to β-actin gene expression. Data are expressed as mean±SEM.

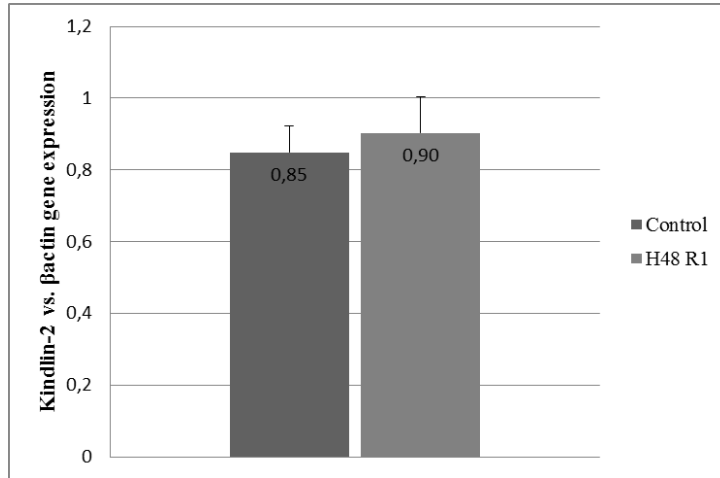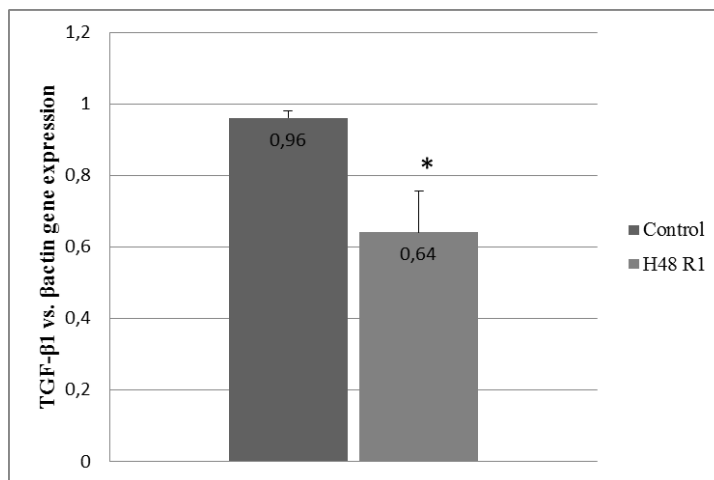**Figure 31:** TGF-β1 mRNA level was significantly decreased after 48 hours of hypoxia followed by 1 hour of reoxygenation compared to the control. Values were normalized to β-actin gene

expression. Data are expressed as mean±SEM. *p≤ H48hrs and R
1hr vs control.

In association to the gene expression analysis; TGF-β protein expression
was also tested. Total protein extracted from MTCs as mentioned in
material and methods were analyzed by Western Blot and two bands of
TGF-β were detected in our samples ranging from 45kDa and 65kDa, thus
we analyzed both specific bands of this range; <50kDa and >50kDa. 48hrs
of hypoxia followed by 1h of reoxygenation did not influence a significant
change on the TGF-β protein expression (Figure 32).

Figure 32: Densitometry analysis of TGF-β protein expression in cultured
MTCs. Cells was cultured under hypoxia for 48hrs followed by 1hr of
reoxygenation. The two panels representing the two ranged specific bands
of TGF-β; Panel A for bands <50kDa and Panel B for bands >50kDa.
Analysis has been performed using ImageJ software. Bands intensities were
calculated and normalized to β-actin.

Next, we wanted to explore the effect of several reoxygenation periods following the hypoxic incubation on Kindlin-2 gene expression and also on TGF-β1 gene expression. A trend of change in Kindlin-2 gene expression was detected under the influence of 48hrs hypoxic incubation, as well as change on the gene expression was observed in association to 1hr and 4hrs reoxygenation periods followed the hypoxia (Figure 33). TGF-β1 trend of change was reversed than the one detected in Kindlin-2 gene expression (Figure 34).
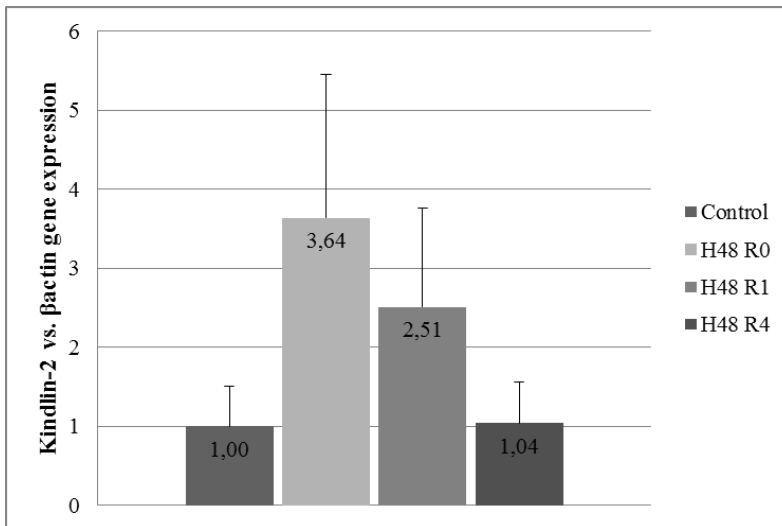
Figure 33: mRNA levels were assessed for Kindlin-2. Values were normalized to β-actin gene expression. Data are expressed as mean±SEM. Kindlin-2 gene expression after 48 hours of hypoxia and followed by 1 hour and 4 hours of reoxygeneation not significantly induced.
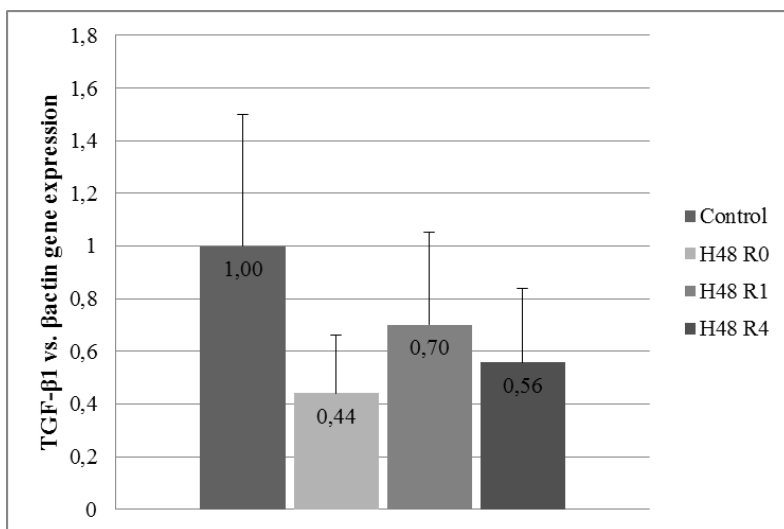
Figure 34: mRNA levels were assessed for TGF-β1 gene expression. Data are expressed as mean±SEM. TGF-β gene expression after 48 hours of hypoxia and followed by 1 and 4 hours of reoxygenation.

We followed several testing conditions in order to analyze TGF-β protein expression induced by 48hrs of hypoxia and when followed by several reoxygenation periods extending from 30mins to 12hrs as shown in Figure 35. Although no significant change could have been detected we were able to demonstrate that the longer reoxygenation periods had no influence on the protein expression, and shorter reoxygenation periods associated with 48hrs of hypoxia were sufficient to observe a trend of change. Furthermore, we decided to repeat testing 24hrs of hypoxia without reoxygenation, in addition to 30mins and 1hr of reoxygenation to analyze 24hrs hypoxia influenced TGF-β protein expression, graphs representing the protein expression on the tested conditions are shown in Figure 36, TGF-β protein expression was not significantly changed neither by 24hrs of 48hrs of hypoxia, nerveless when the hypoxic incubation been followed by several reoxygenation periods.

121

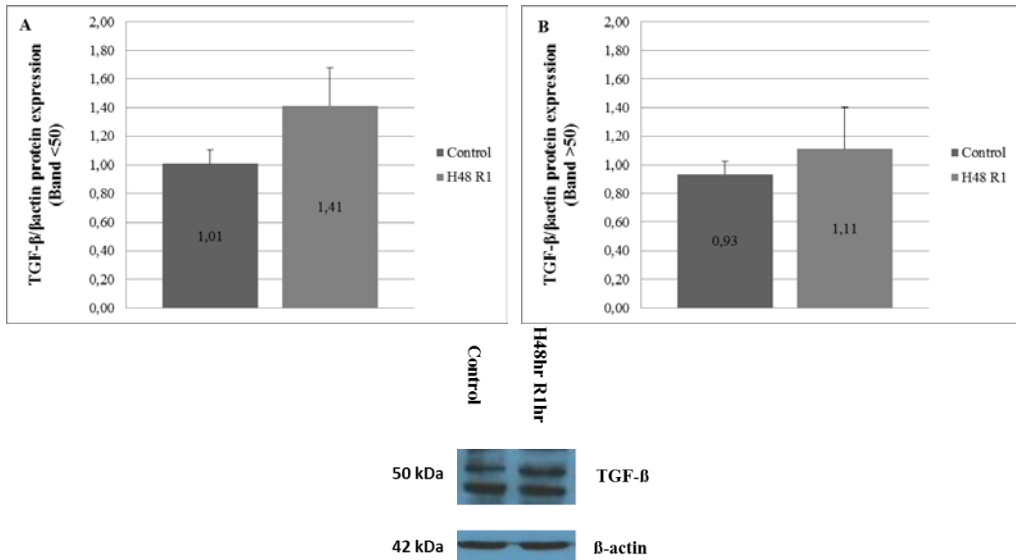**Figure 35:** Densitometry analysis of TGF-β protein expression in cultured MTCs. Cells were cultured under hypoxia for 48hrs with no reoxygenation, and followed by 30mins, 1hr, 2hr, 4hr, 6hr and 12hr of reoxygenation. The two panels representing the two ranged specific bands of TGF-β; Panel A for bands <50kDa and Panel B for bands >50kDa. Analysis has been performed using ImageJ software. Bands intensities were calculated and normalized to β-actin.
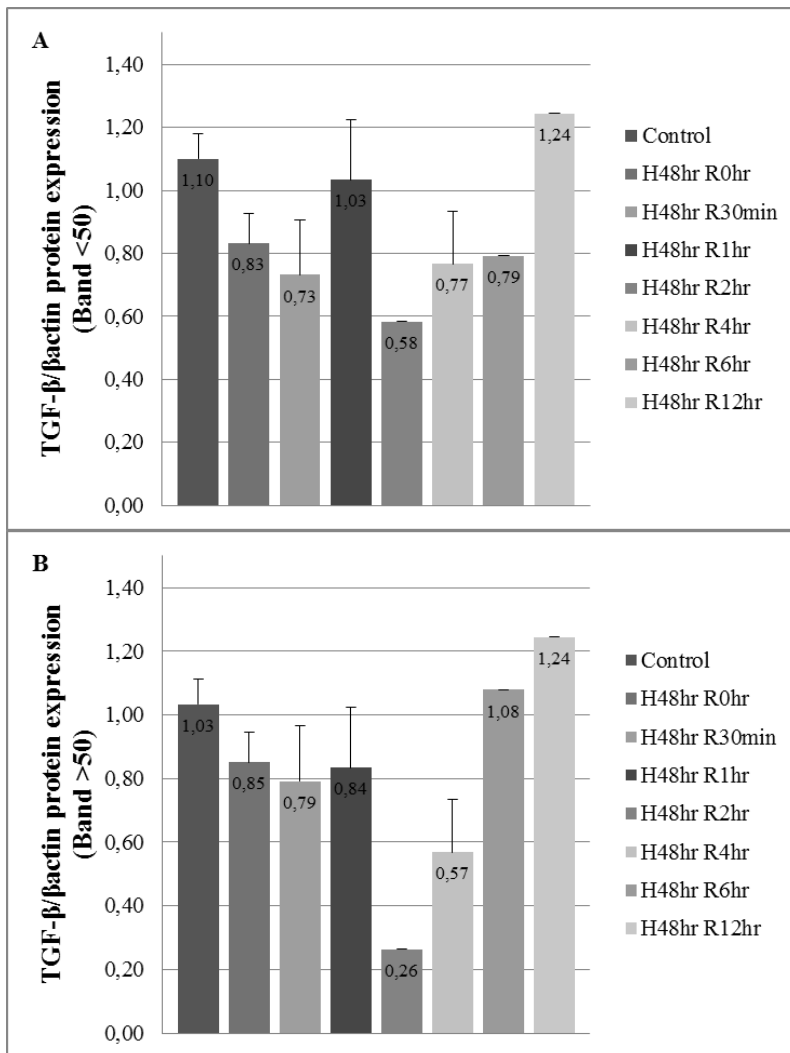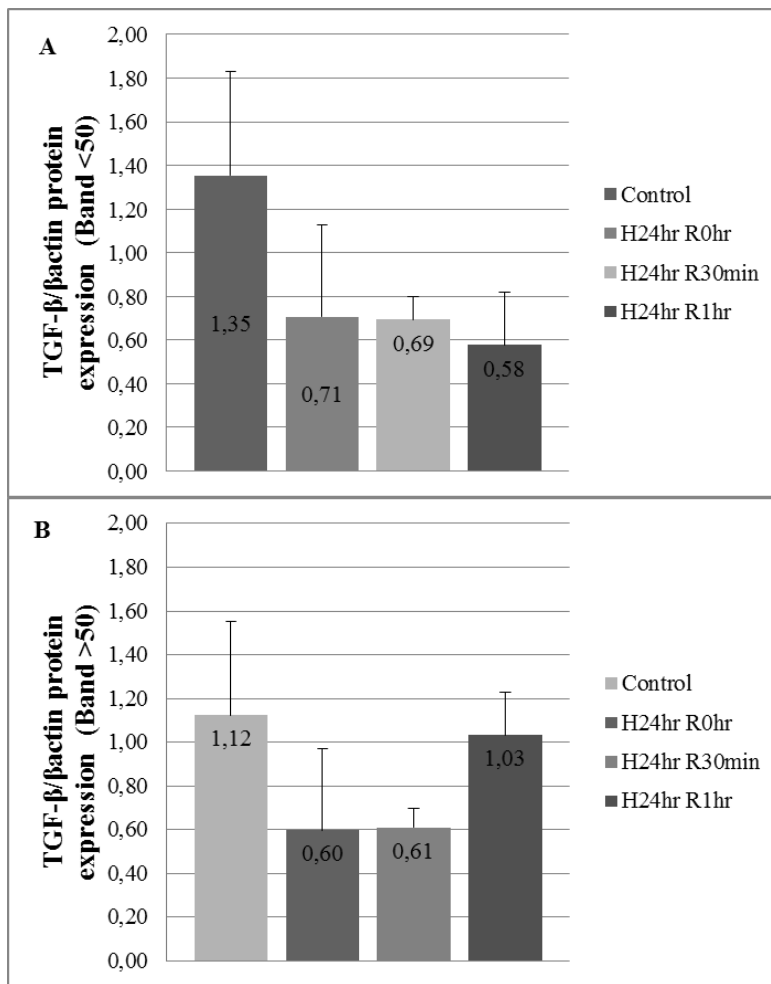
Figure 36: Densitometry analysis of TGF-β protein expression in cultured MTCs. Cells were cultured under hypoxia for 48hrs with no reoxygenation, and followed by 30mins and 1hr of reoxygenation. The two panels representing the two ranged specific bands of TGF-β; Panel A for bands <50kDa and Panel B for bands >50kDa. Analysis has been performed using ImageJ

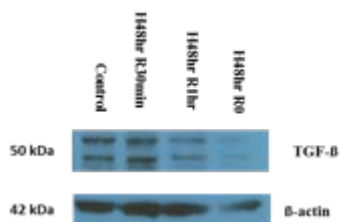software. Bands intensities were calculated and normalized to β-actin.

5.2.2. Experimental Conditions of MTCs Cultured Cells

Based on the results obtained from the optimizing conditions our definitive experimental conditions have been set for both 24 and 48hrs of hypoxia and followed up by short reoxygenation periods of 15mins and 3hrs. Tracing the changes of Kindlin-2 and TGF-ß in the testing conditions we found that the suggested incubation periods are sufficient to test the effect of hypoxia in the cultured cells, were significant changes of gene expression could have been detected, in addition, limiting down the variabilities between samples.

5.2.2.1. Genes Expression:

For the optimized experimental conditions, multiple gene expressions were analyzed in order to obtain an overview of the genetic profile of some molecules related to TGFβ/Smad signaling pathway such as CTGF, α-SMA, Fibronectin-1, Collagen-1 and Collagen-4 that are involved in enhancing cell proliferation and extracellular matrix production in EMT and fibrotic processes.

Below are graphs of quantitative real-time PCR from cells incubated under the proposed experimental conditions that are 24 or 48 hours of hypoxia followed by 15minutes or 3hours of reoxygenation. In two different sets of experiments where MTCs were incubated for either 24 or 48hrs of hypoxia, then both followed by 15mins and 3hrs of reoxygenation, Kindlin-2 gene expression was not significantly modified (Figure 37).

Figure 37: Kindlin-2 Gene Expression. mRNA levels were assessed for Kindlin-2. Values were normalized to βactin gene expression. Data are expressed as mean±SEM. No significant changes of Kindln-2 gene expression were detected after 24/48hrs of hypoxia followed by 15mins and 3hrs of reoxygenation.

TGF-β1 gene expression was not significantly induced by 24hrs of hypoxia followed by 15mins or 3hrs of reoxygenation, while it was significantly decreased after 48hrs of hypoxia followed by both 15mins and 3hrs of reoxygenation (Figure 38).

Figure 38: TGFβ Gene Expression. mRNA levels were assessed for TGFβ. Values were normalized to βactin gene expression. Data are expressed as mean±SEM. In 48hrs hypoxia group TGF-β1 gene expression was significantly decreased when followed by 15mins and also 3hrs of reoxygenation compared to control. * p≤0.05 vs. control.

On the other hand, CTGF was neither significantly induced by the 24hrs hypoxic incubation followed by the two periods of reoxygenation; 15mins and 3hrs, but it was significantly decreased by 48hrs hypoxic incubation when followed by 15mins reoxygenation, while the 3hrs reoxygenation following the 48hrs hypoxia have significantly increased CTGF compared to control (Figure 39).
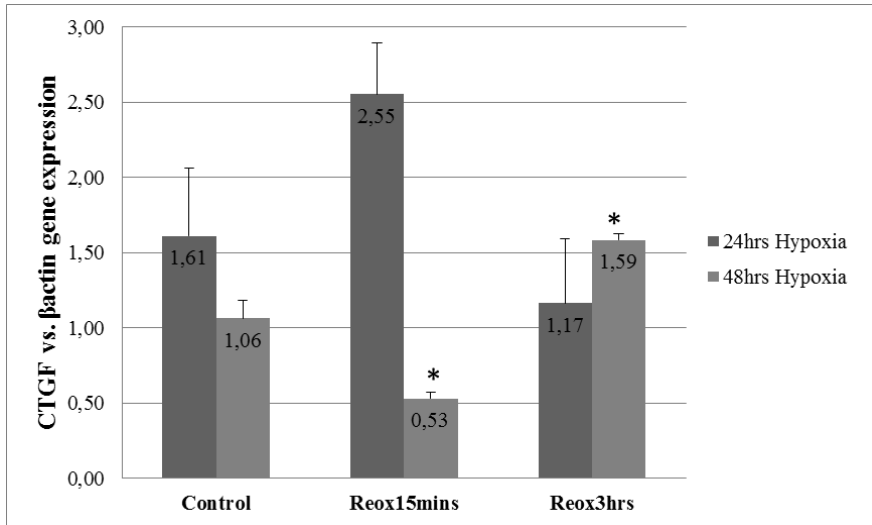
Figure 39: CTGF Gene Expression. mRNA levels were assessed for CTGF. Values were normalized to βactin gene expression. Data are expressed as mean±SEM. In 48hrs hypoxia group CTGF gene expression was significantly decreased following 15mins of reoxygenation, while it significantly increased after 3hrs of reoxygenation, compared to control. * p≤0.05 vs. control

Assessing the pro-fibrotic and pro-inflammatory genes, we found that 24hrs of hypoxia followed by 15mins of reoxygenation induced significantly increase of α-SMA gene expression. Furthermore, it was significantly increased with 3hrs of reoxygenation after 48hrs of hypoxia (Figure 40).
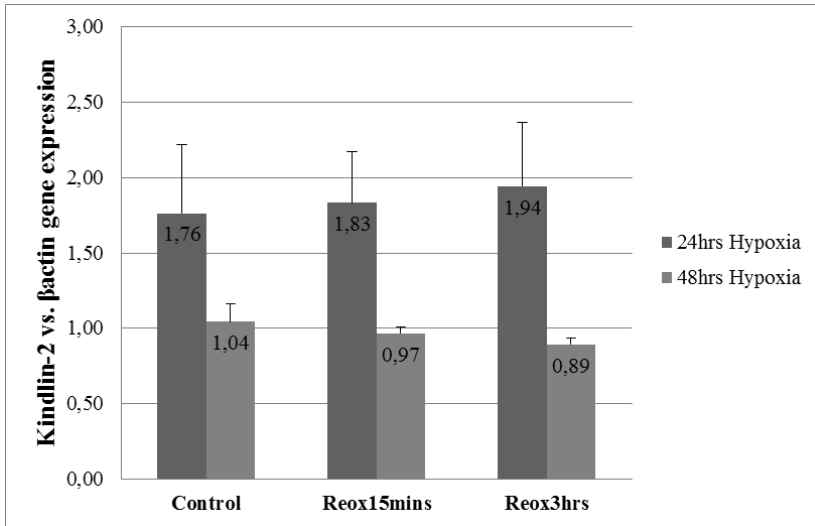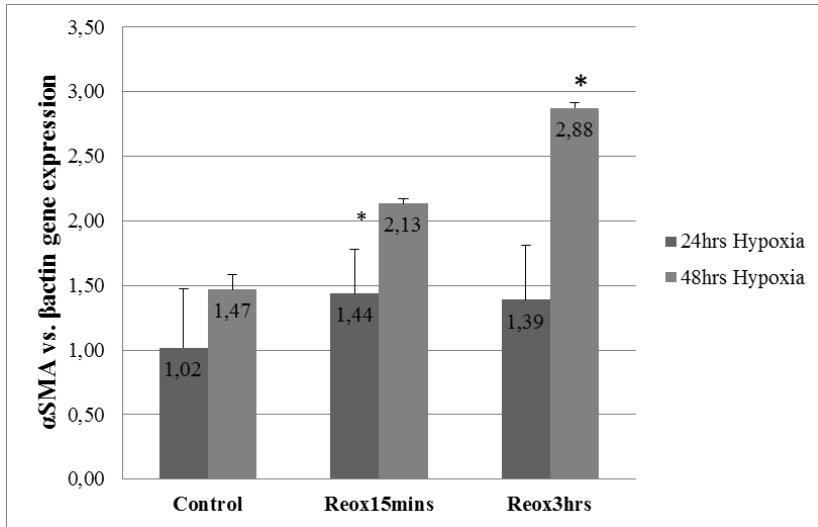
Figure 40: α-SMA Gene Expression. mRNA levels were assessed for α-SMA. Values were normalized to βactin gene expression. Data are expressed as mean±SEM. 24hrs hypoxia followed up with 15mins reoxygenation have significantly increased α-SMA gene expression, as well as it was significantly increased after 48hrs of hypoxia followed by 3hrs of reoxygenation, compared to control. *p≤0.05 experimental condition vs. control.

On the other hand, FN-1 gene expression was significantly increased only with 48hrs of hypoxia incubation followed by 15mins reoxygenation, as shown in Figure 41.
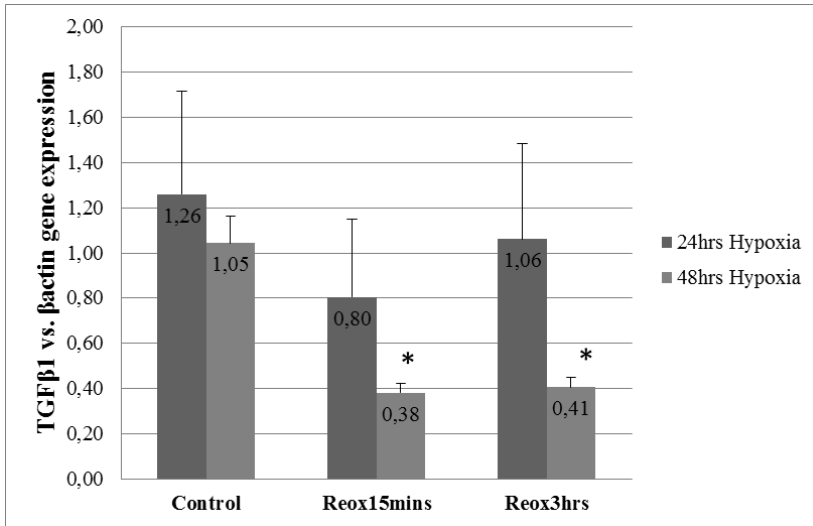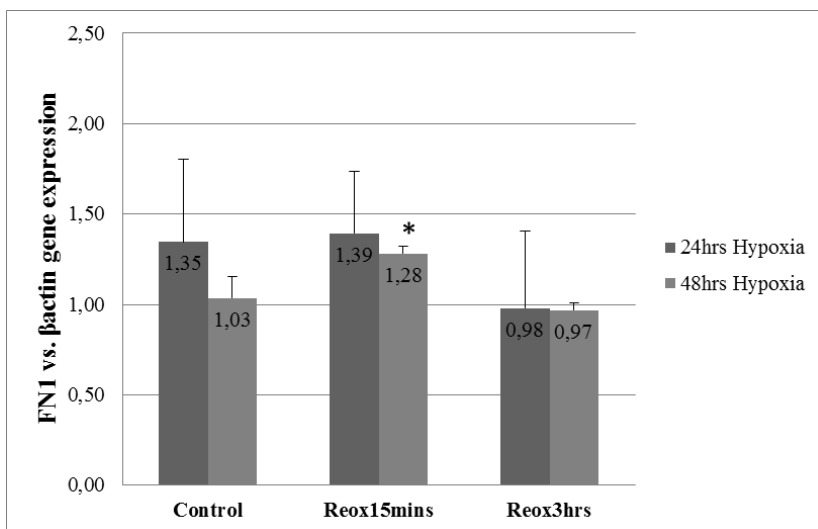
Figure 41: Fibronectin **Gene Expression**. mRNA levels were assessed for FN-1. Values were normalized to βactin gene expression. Data are expressed as mean±SEM. 48hrs of hypoxia followed by 15mins of reoxygenation have significantly increased FN-1 gene expression. * p≤0.05 vs. control.

Furthermore, 24hrs of hypoxia followed by 15mins reoxygenation have not significant influence Collagen type 1 when compared to the control, neither after 3hrs of reoxygenation. In the other hand, 48hrs of hypoxia followed by 3hrs of reoxygenation have significantly increased collagen-1 gene expression as compared to the control, but not significant change was detected after 15mins of reoxygenation (Figure 42).
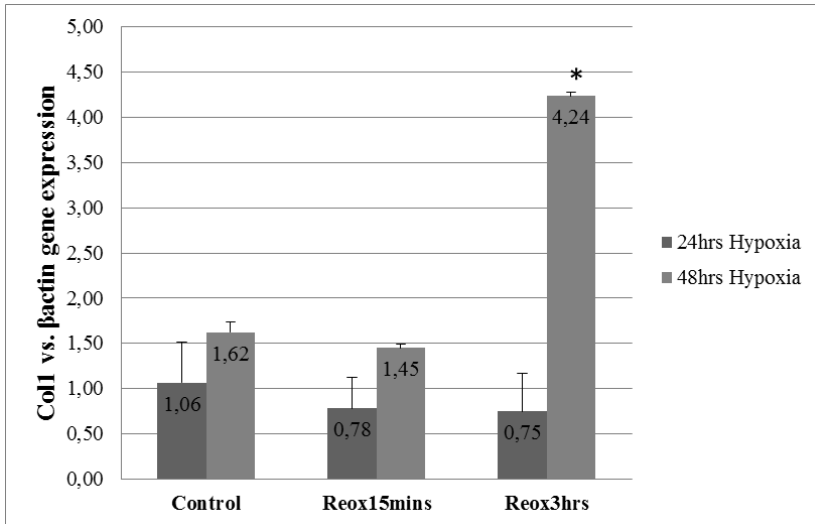
Figure 42: Collagen-1 Gene Expression. COL-1 mRNA levels were significantly increased when hypoxic incubated for 48hrs and followed by 3hrs of reoxygenation compared to the control. Values were normalized to βactin gene expression. Data are expressed as mean±SEM. * p≤0.05 vs. control

Collagen type 4 gene expression was also analyzed in both sets of experiments; 48hrs of hypoxia and 24hrs of hypoxia, no significant induction was detected in the 24hrs of hypoxia followed by 15mins neither 3hrs. In the other hand, a significant decreased was detected by the influence of 48hrs of hypoxia followed by 15mins of reoxygenation as shown in Figure 43.
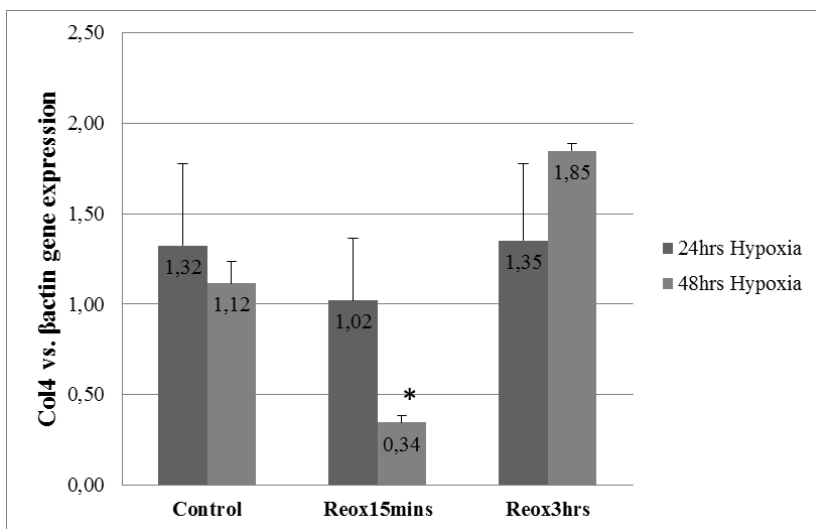
Figure 43: Collgen-4 Gene Expression. COL-5 mRNA levels were significantly decreased in 48hrs of hypoxia followed by 15mins of reoxygenation when compared to control. Values were normalized to βactin gene expression. Data are expressed as mean±SEM. * p≤0.05 vs. control.

5.2.2.2. Kindlin-2 Protein Expression

Protein levels for the same experiments were analyzed by Western Blot techniques. We analyzed Kindlin-2 protein expression in total protein extracts following the optimized conditions of western blot protocol as explained in the material and methods. As mentioned in the commercial datasheet of the antibody, Kindlin-2 band is weight 62kDa.

Kindlin-2 protein expression was also tested from the total protein extracts of the cultured cells. The protein expression was not significantly induced under the influence of the experimental conditions as shown in Figure 44.
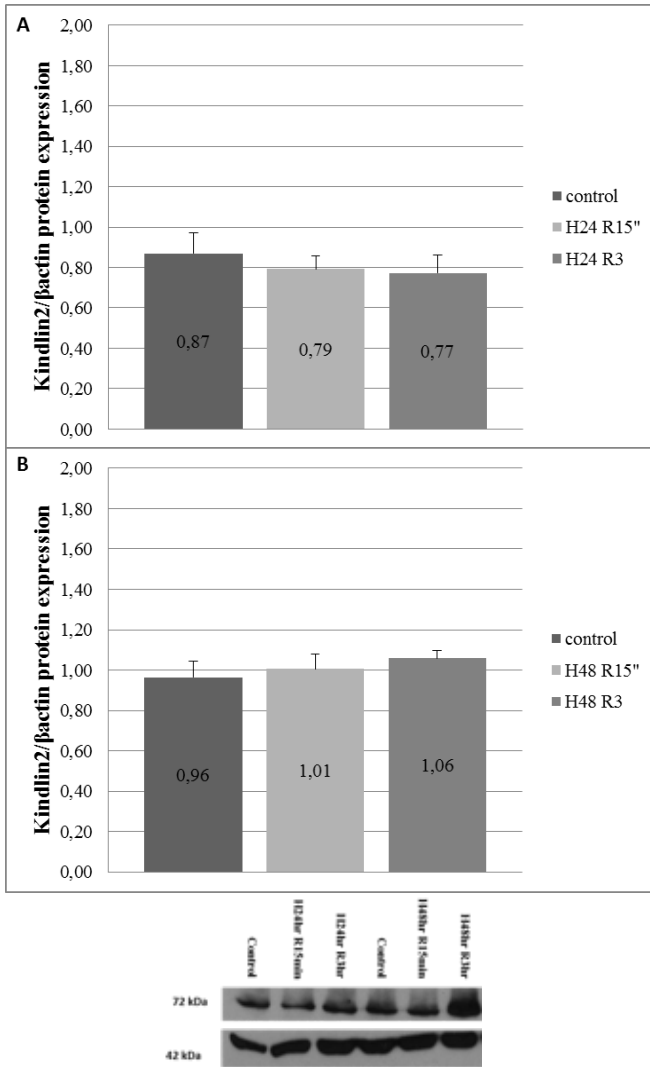
Figure 44: Densitometry analysis of Kindlin-2 protein expression in cultured cells. Analysis has been performed using ImageJ software. Bands intensities were calculated and normalized to βactin. Protein expression obtained from at least 5 experiments from each condition. Panel A for group of experiments of 24hrs of hypoxia and followed by 15mins and 1hr of reoxygenation, Panel B for group of experiments of 48hrs of hypoxia followed by 15mins and 1hr of reoxygenation.

5.2.2.3. Kindlin-2 Expression and Localization in MTCs

Kindlin-2 immunofluorescence staining have been located in the cytoplasm of the cultured tubular epithelial cells, furthermore as shown in Figures 45, 46, Kindlin-2 immunofluorescence staining is altered under the influence of the experimental conditions in association with morphological changes. In control cells Kindlin-2 staining is limited srounding of the nucleus, while in cells cultured under hypoxic conditions Kindlin-2 protein staining is seen extended wider in the cytoplasm more intense. Furthermore, differences in the protein intensity has been observed between cells incubated 24hrs under hypoxia and 48hrs, where in the 48hrs of hypoxia Kindlin-2 immunofluorescence is more intesnse.
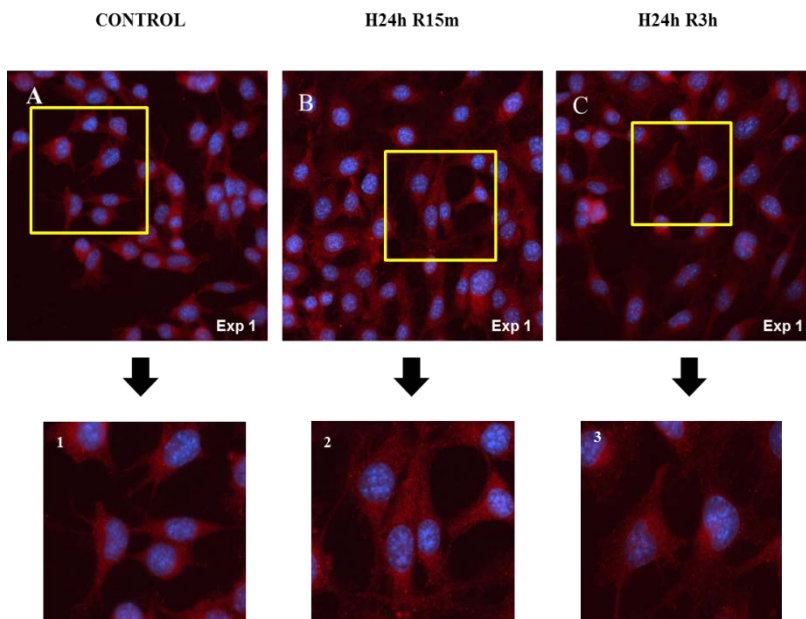
Figure 45: Immunofluorescence staining of Cultured TECs. Represents microphotographs of Kindlin-2 immunofluorescense staining of: (A) control TECs, (1) zoomed in of representative control cells (B) TECs incubated 24 hrs under hypoxia and followed by 15mins reoxygenation, (2) zoomed in of representative cells of the same captured area. (C) TECs incubated

24 hrs under hypoxia and followed by 3hrs reoxygenation, (3) zoomed in of representative cells of the same captured area
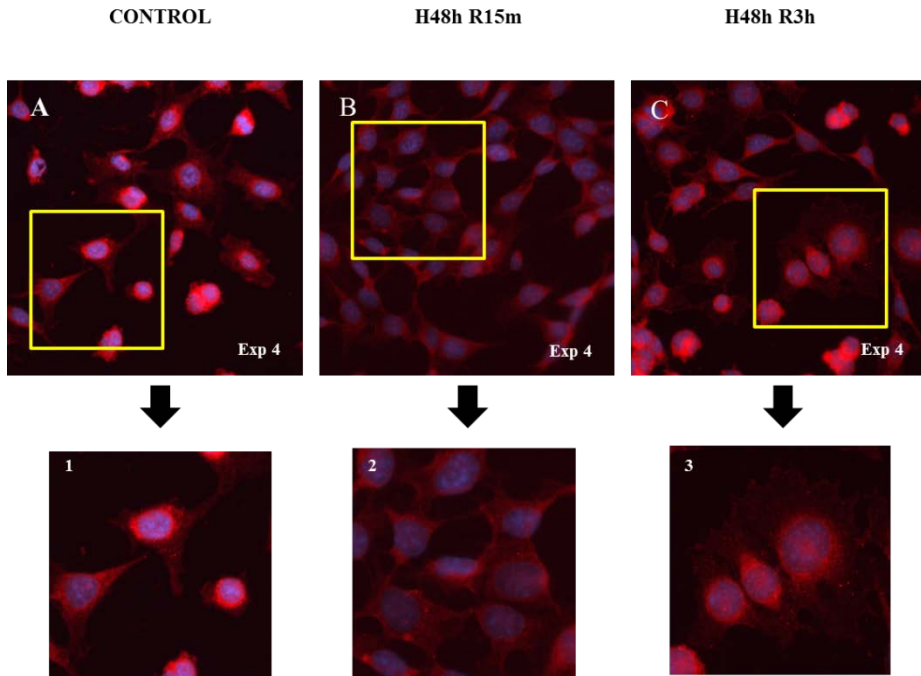
Figure 46: Immunofluorescence staining of Cultured TECs. Represents microphotographs of Kindlin-2 immunofluorescense staining of: (A) control TECs, (1) zoomed in of representative control cells (B) TECs incubated 48 hrs under hypoxia and followed by 15mins reoxygenation, (2) zoomed in of representative cells of the same captured area. (C) TECs incubated 48 hrs under hypoxia and followed by 3hrs reoxygenation, (3) zoomed in of representative cells of the same captured area.

DISCUSSION

6.   DISCUSSION

6.1.   Ischemia/Reperfusion Induced Injury in Mice

Ischemic injury affects the renal function and the progression of tubular injury, and several fibrotic markers have been studied in the injured renal tissue. Interestingly, immunohistochemical analysis of Kindlin-2 expression in our model showed definite Kindlin-2 staining in focal pattern. This suggest that the inconclusive Kindlin-2 expression seen at mRNA and protein levels might have been influenced by this focal expression which was not controlled while extracting RNA and protein from the cortical cut of the tissue. Most importantly, we have observed induction of Kindlin-2 staining in cortex of all ischemic tissues and this was in correlation with increased α-SMA staining, the increased α-SMA was highest in the 7days post-ischemic group and least increased in the 45days post-ischemic group. Data suggests that 7days post-ischemic group represents a tubulointerstitial fibrotic model induced by ischemia/reperfusion injury. This was assisted by the significant increased pro-fibrotic markers at the mRNA level, inducing fibrotic response in the cortical interstitium, and also increased expression of the myofibrotic marker; α-SMA. This further induced the accumulation of FN-1, COL-1 and COL-4 in progression of fibrotic process. In addition, as mentioned, Kindlin-2 expression was intense in the immunohistochemistry staining. Yet the induction of Kindlin-2 mRNA expression in the ischemic tissue was not conclusively associated with the increased TGF-β1 mRNA expression in the different post-ischemic periods. Thus, a definitive correlation of Kindlin-2 and TGF-β1 induced by ischemia/reperfusion is required in further investigation in addition to analyzing several markers including TGF-β signaling pathway as Smads. Finally, we demonstrated that 30 minutes ischemia can initiate progression of renal damage characterized by severe tubular injury, tubular atrophy, interstitial

Discussion

inflammation and renal fibrosis. Also, it was shown that the course of unilateral ischemic renal injury is not simply detected by early ischemic/post ischemic events, rather the ischemic insult initially trigger injury which progress for longer post-ischemic periods, as shown in the results of the cortical Kindlin-2 expression correlation with the myofibroblast activation marker; α-SMA. As shown in the results early 7 days post ischemia Kindlin-2 induction is associating with induced α-SMA, detecting the activation of myofibroblast in the process of tubular injury. However, in longer term as 45 days post ischemia, this correlation is not detected, contrarily α-SMA protein expression was lower in the ischemic tissue of 45 days post ischemia than in 7 days post ischemia, suggesting that the progression of injury have turned in different approach. Although mRNA levels of several genes; pro-fibrotic and inflammatory were measured significantly decreased, we hypothesize that it is not relative decrement rather due to the focal genes expression of different degrees of damaged areas in the tissue. Thus, further protein expression of fibrogenesis markers as COL-4 is essential.

On the other hand, we have assessed the presence and severity of cortical fibrosis by analyzing the gene expression level of different pro-fibrotic markers such as TGF-β1 and CTGF as indicators of fibrotic response, αSMA as marker of myofibroblast; highly specialized cells with the ability to secrete ECM components and remodel tissue due to their contractile properties, and also, Fibronectin, Collagen 1 and Collagen 4 as ECM components that are accumulated in fibrotic process. Kindlin-2 expression has been analyzed and relative expression to the previously mentioned markers to define the correlation of its expression in association with the processes raised with the ischemic/reperfusion injury. We found significant increased Kindlin-2 cortical gene expression 45 days post-ischemia in the normal drinking water group. This significant

increased expression of Kindlin-2 was associated with significant decreased TGF-β1, COL-1, α-SMA and FN-1 cortical genes expressions. A similar genes expression patterns was detected after 48 hours post-ischemic of TGF-β1, COL-1, α-SMA and FN-1, without significant induction of Kindlin-2 gene expression in the normal drinking water group. While in the high-salt group 48 hours and 45 days post ischemia, an opposite pattern of the genes expressions was detected 7 day post ischemia as TGF-β1 was significantly increased and this was correlated with highly significant increase of Col1, Col-4 and FN-1 mRNA levels, again in the normal drinking water group, while no induction of Kindlin-2 gene expression was detected. This suggests that ischemic/reperfusion induction of the TGF-β signaling pathway could be detected on time course basis post injury, were 7 days of reperfusion following the 30-mins of ischemia resulted in activation of pro-fibrotic TGF-β1 and myofibroblasts in the high expression of α-SMA, in addition to the accumulation of the ECM components COL-1, COL-4 and FN-1.

Although this data was not conclusive to obtain a definitive pattern of Kindlin-2 mRNA expression, yet the immunohistochemically of Kindlin-2 staining was significant and we were able to locate the expression of Kindlin-2 in the proximal tubular epithelial cells associated with morphological features consistent with acute tubular injury, consisting in focal detachment of tubular epithelial cells, loss of the epithelial apical brush border, which in literature is characterized as evidence of activation of the phenotype transitions and EMT-II, also it has been well demonstrated in previous studies that proximal tubular epithelial cells undergo EMT-II involving matrix-producing fibroblasts and contribute to the pathogenesis of renal fibrosis (63).

However, in all ischemic tissues proportional correlation between TGF-b mRNA expression was detected with COL-1, COL-4, α-SMA and FN-1, meanwhile Kindlin-2 mRNA expression correlates with decreased COL-1

Discussion

and FN-1 mRNA expression.. In addition, it has been demonstrated previously that Kidnlin-2 activates TGF-β receptor and is required for the TGF-β signaling pathway (87), and that the damaged TECs transdifferentiate into mesenchymal fibroblasts or undergo apoptosis, in finally lead to the progression of tubulointerstitial fibrosis (80). Thus, our results suggest morphological alteration of EMT induced by ischemia/reperfusion injury in the renal tubular epithelial cells and associated with altered expression of α-SMA indicating the loss of the epithelial marker. In addition, we have demonstrated alteration of focal Kindlin-2 expression which cooperate the involvement of Kindlin-2 in the EMT, yet further investigation is needed to link the expression of Kindlin-2 with epithelial markers and TGFβ signaling pathway.

Many studies have studied renal fibrosis using UUO model and it has been demonstrated that UUO model is a well characterized TIF model. Furthermore, the role of Kindlin-2 in the pathogenesis of renal TIF have been recently demonstrated by Wei and colleagues in male ICR mice, where fibrosis was induced by UUO and then mice where treated with Kindlin-2 siRNA, results confirmed remarkable upregulation of Kindlin-2 in renal tissue of UUO mice, predominantly detected in TECs. In addition, it has been shown that Kindlin-2 induction is associated with TGF-β1, p-Smad3 overexpression in the ligated kidney tissue. And also, Kindlin-2 knocking down have decreased the expression of Col-1, α-SMA and Snail at both mRNA and protein level, attenuated TIF(109). Also, depletion of Kindlin-2 in UUO have decreased the activation of ERK1/2 and Akt which are activated in the UUO model, this decreased activation further reduced fibroblast activation and EMC production (102). Both mentioned studies have demonstrated the role of Kindlin-2 in TIF induced by UUO and the findings suggest the role of Kindlin-2 in the progression of renal fibrosis by multiple signalling pathways, by far TGF-β/Smad and Ras signalling pathways. In these regards, further analysis of our model

demonstrating the association of Kindlin-2 expression to TGF-β signaling and furthermore definitive markers of EMT is needed.

6.2.   Role of Contralateral Kidney During Ischemic Injury

We aimed to induce injury developing fibrosis using UIRI without nephrectomy, allowing us to test the progression of injury in the ischemic tissue while maintaining the contralateral kidney, this provide us a control tissue maintaining the kidney function while influenced by the same cellular processes induced by the ischemic injury. Our results suggest that although assessing functional recovery was not possible without harvesting tissue yet remarkable difference in cortical gene expression was observed between ischemic kidneys vs. contralateral kidney. In addition, almost stable equal genes expressions were found in the contralateral cortical tissue of the different post-ischemia following up time periods. And also, histological sections of the contralateral kidney did not show any signs of changes, neither immunostaining of α-SMA were relative to the positive staining that was injury-induced in the ischemic tissue. Our results are demonstrating that the contralateral kidney retains normal histology and cortical genes expression suggesting that the ischemic tissue did not cause any obvious damage on the contralateral kidney. These results are also found in different studies of UIRI on rats subjected to 30 minutes of ischemia and followed post-ischemia periods extended to 3 weeks (110), and to 5-6 weeks (111), where in both studies the contralateral non ischemic kidneys were similar to the normal kidney of sham group, not showing any histological signs related to injury or damage. In models of AKI, UIRI without nephrectomy allows longer ischemia insults to be performed inducing range of histopathological renal injury more closely to the nephropathy in patients. Thus, it is a very robust model for induction of long term tubulointerstitial fibrosis. Le Celf et al in a recent study using UIRI without nephrectomy

demonstrated that time of ischemia determines the degree of long term fibrotic outcomes; where in twelve weeks after UIRI a significant increase in fibrotic related gene expression was detected in renal cortex of ischemic tissue (COL-1 and TGF-β). The genes expressions were also temperature dependent as higher expression with higher body temperature during ischemia (112). On the other hand, BIRI although is widely used model of AKI in mice yet it has its limitation, among them that with longer ischemia times to develop consistent tubular injury, mortality rate increase within the first 3days after injury due to severe renal insufficiency (105). Thus, in UIRI mice can survive much longer periods of ischemia and tend to develop more severe post-injury fibrosis, and results of Natalia I. Skrypnyk et al study on UIRI developed model where nephrectomy of contralateral kidney was performed 9 days after ischemia clumping, indicated that with the same periods of ischemia, UIRI mice develop more severe fibrosis than BIRI or UIRI with nephrectomy(105).

6.3.   Effect of High Salt Drinking Water in Renal Tissue

We have demonstrated that high salt drinking water (0.3% NaCl) trigger changes in mRNA expression of pro-fibrotic markers where significant decrease TGF-β1 mRNA level in the cortex of the ischemic tissue 7 days post-ischemia when comparing the high-salt group with the normal water group was detected in our model. And also in COL-1 mRNA detecting ECM accumulation in cortex which was significantly increased in the contralateral control kidney of the high-salt group when compared to the normal water group. On the other hand, significant decreased Kindlin-2 cortex staining was detected in the contralateral high-salt group tissue when compared to the contralateral of normal-water group in 7 days post-ischemia.

Furthermore, high salt induced changes in Kindlin-2 staining in the ischemic kidney as it was significantly increased in 7 days ischemic high

salt ischemic kidney vs. the ischemic normal-water group. A definitive correlation of high salt treatment and ischemic injury inductions should be analyzed, as seen in our results genes expressions have been altered under the influence of high salt in the ischemic tissue, as considerations of high salt histological alteration in the tubular cells should be taken into account.

The effect of dietary high salt in the progression of hypertension and inducing kidney injury has been established in different models. High salt dietary induced kidney injury have been shown in association to increased oxidative stress in rat model for 8-weeks study (113). Furthermore, the high salt sensitivity has been linked to the renal Angiotensin-Converting Enzyme inducing renal injury in mice (114). Our results might add link of the high salt induction of proximal tubular kidney injury in correlation with TGFβ signalling pathway.

6.4. Ischemia and High Salt Influence on Renal Mass

Our results have demonstrated that ischemia/reperfusion injury significantly reduce the ratio of renal weight/body weight in long term, as detected 45 days post-ischemia regardless of the high salt drinking water treatment. While 7 days post-ischemia the ratio of renal weight/body weight was significantly reduced under the influence of both ischemic injury and high salt drinking water treatment. On the other hand, ischemia/reperfusion injury had no influence on the ratio of renal weight/body weight in short term, as seen in the analysis performed 48 hours post-ischemia. In accordance, Nathalie Le Clef and colleagues have reported that UIRI causes ischemia and in time-dependent manner reduce the renal mass, as longer ischemia times induce severe reduction in renal mass (108).

Discussion

6.5. Kindlin-2 Expression in Human Biopsies

We analyzed Kindlin-2 staining in biopsies obtained from renal transplanted patients developed ATN, and these allowed us to locate Kindlin-2 expression in the cytoplasm of tubular epithelial cells, cytoplasm of endothelium peritubular capillaries, cytoplasm of glomerular capillaries and cytoplasm of podocytes. Furthermore, these expression increases in association with the progression of ATN, Kindlin-2 was as also detected in normal renal biopsies in similar localization yet in lower number of tubular cells.

Kindlin-2 expression have been studied in a different study by Wei and his colleagues, in human fibrotic kidney of biopsies obtained from patients with chronic renal tubulointerstitial fibrosis; IgA nephropathy, membranous nephropathy, membranoproliferative nephritis, chronic tubulointerstitial nephropathy and crescentic GN (109). Kindlin-2 expression has been found to be significantly induced in association with TGF-β1 and p-Smad3. Vongwiwatana et al have explored the emergence of EMT markers in human kidney transplant at the time of renal allograft dysfunction, and the results demonstrated that TECs contribute to the fibrogenesis during late deterioration in kidney transplants through the EMT process (80).

6.6. Hypoxia/Reoxygenation Effect on Cultured MTCs

In this work, we induced injury on cultured MTCs by hypoxia incubation and further followed by reoxygenation period allowing us to track the influences of the signaling pathway induced by the hypoxia/reoxygenation incubation. In our experimental conditions of hypoxia/reoxygenation periods we have detected lowering of TGF- β1 expression and these decrements have been statistically induced by 48hrs of hypoxia when followed by 15mins reoxygenation and also 3hrs, at mRNA level. Even

though Kindlin-2 have been described to be induced in time and dose dependent manner of TGF-ß1 influence, in our system of hypoxia followed by reoxygenation incubation no influence was detected on Kindlin-2 mRNA expression although this experimental incubation periods have significantly decreased TGF-β1 mRNA levels (48hrs hypoxia followed by 15mins and 3hrs reoxygenation). In the other hands, we have detected high exposed bands of TGF-β when analyzing the supernatant collected from the medium of the cultured cells by western blot, findings in relative with the results mentioned of the study of L. Young Ki and colleagues.

A study by Hrikkinrn in the modulation of TGF-β1 signaling by hypoxia, proposed that in hypoxic conditions, Smad3 could inhibit the downstream TGF-β1/Smads signaling pathway by upregulating the TGF-β1 inhibitor protein (Smad7), an effect that could affect our system, where TGF-β1 showed decreased expression, suggesting that shortened hypoxia incubation periods might demonstrate and help to track the increased TGF-β1 expressions and its correlation with Kindlin-2 expression which could assist in analyzing the involved mechanism of Kindlin-2 in TGF-β signaling. In consideration of the role of hypoxia stimulating TGF-β1 production (115,116) and in addition to the results of Manotham and colleagues work demonstrating an important role of hypoxia in tubular EMT as a critical step in renal fibrosis and progression of kidney disease (117), we expand the analysis of more genes which their role in renal fibrosis have been previously studies and determined. CTGF act as both pro-fibrotic marker and downstream mediator of TGFβ, in a study where data suggested that TGF-β1 is mediator to increase CTGF mRNA expression by hypoxia in renal tubular epithelial cells, it was suggested that TGF-β1 is not the primary mediator of the hypoxia induced CTGF expression in renal TECs. Moreover, it was found that TGF-β1 signaling was not required for hypoxia induction of CTGF promotor activity in the

Discussion

renal tubular epithelial cells, thus hypoxia regulates CTGF expression through TGF-β1 independent pathway(118). In our system, we detected significant increase in CTGF mRNA expression in 48hrs hypoxia treated cells followed by 3hrs of reoxygenation, in contrast of TGF-β1 mRNA expression in the same cells where it was significantly decreased. The CTGF hypoxia/reoxygenation induced expression was also accompanied with increased α-SMA and Col-1 mRNA expression. Our data support finding in a study of hypoxia cultured renal proximal tubular epithelial cells (RPTEC), were 48hrs hypoxia although failed to reach statistical significance yet it has increased transcript levels of several mesenchymal genes such as vimentin, smooth muscle actin/ACTA2 collagen 1A2. More data of that study have indicated that hypoxia promotes a mesenchymal and migratory phenotype in renal epithelial cells associated with increased matrix metalloproteinase 2 (MMP2) expression (115).

Although in our experimental model Kindlin-2 expression was not significantly altered at the time points of H/R applied, yet we could detect Kindlin-2 in our cell model and located in the cytosol, and altered under the influence of H/R incubation comparing to the control cells. Furthermore, our results suggest that Kindlin-2 is required for the elevated expression of TGF-β1, finding that has been reflected by not detecting significant alteration in Kindlin-2 at both protein and mRNA levels when TGF-β1 levels are significantly decreased.

These results demonstrate that in cultured MTCs, hypoxia/reoxygenation induce changes in genes expressions which is conditioned by the incubation periods proposed, as seen in our data the different hypoxia and reoxygenation incubations periods have altered genes expressions differently. Perhaps, suggesting that long hypoxia incubation raises the possible inhibition of the activated TGF-β, were in the experimental conditions the gene expression detected significant decrease. In addition, apparent effect of hypoxia been detected in the genes expression and trace

of changes when followed by longer reoxygenation periods, suggesting a possible affect not only of hypoxia but also of the reoxygenation periods as detected by significant increased TGF-β1, CTGF, Col-1 and α-SMA gene expressions in the longer reoxygenation periods followed after 48hrs of hypoxia when compared to the shorted reoxygenation periods from the same hypoxia incubation period. Suggesting mesenchymal phenotype changes in our system of hypoxia/reoxygenation incubated mouse tubular epithelial cells.

The role of TGF ß/Smad signaling in renal fibrosis have been widely studied in renal tissue. Furthermore, studies have demonstrated that the activation of TGF-ß1 in tubular epithelium is sufficient to cause tubular injury and it has been found upregulated in kidney disease correlating to the degree of fibrosis (74,84–86,119). In addition, high expression of Kindlin-2 has been localized in the cytosol of cultured human kidney tubular epithelial cells. Results showed that TGF-ß1 transfected cells showed high expression of Kindlin-2, and that Kindlin-2 increased expression was dose and time dependent manner of TGF-ß1 induction (102,109,120). Furthermore, it has been demonstrated that Kindlin-2 have a critical role mediating EMT; which has been detected by the induced EMT by Kindlin-2 overexpression in HKCs as detected by loss of E-cadherin expression, and upregulation of α-SMA and fibronectin. Furthermore, Kindlin-2 have significantly activated ERK1/2 and Akt mediated by Ras activation in HKCs, in addition, inhibitors of ERK1/2 and Akt have significantly suppressed Kindlin-2 induced EMT (102).

In the other hand, Hypoxia has been also shown to have a role in tubulointerstitial fibrosis; it increases ECM synthesis in renal tubular epithelial cells, induces EMT and regulates the expression of several growth factors. Results published of different group have indicated that TGF-β1 was 91% increased after 4hrs of hypoxia as compared to the control. Also after 24hrs hypoxia, the expression increased by 161%, this

Discussion

increased expression was detected in MTC serum free medium cultured cells under hypoxia. However, this study was performed without any period of reoxygenation as performed in our work (118).

Realizing the increasing prevalence of both acute and chronic kidney disease worldwide and given the complex pathophysiology and the high risk involved complications; not only improving care and outcomes of kidney disease is required, but also an effective intervention and therapeutic treatments for all the major pathophysiological components (19,29,121,122)

CONCLUSIONS

7.   CONCLUSIONS

1.   Kindlin-2 expression is influenced by the progression of acute kidney injury in a model of mouse unilateral renal ischemia.

2.   Kindlin-2 gene expression correlates with COL-1 and FN-1 expression-

3.   Kindlin-2 cortical expression is detected early after injury in correlation with α-SMA expression. In long term this correlation is lost although Kindlin-2 expression is high.

4.   We have seen in our model that inducing the renal unilateral injury is sufficient to induce tubular morphological changes consistent with the progression of the fibrotic process, in the same time providing a contralateral control slightly influenced by the same cellular processes while maintaining the normal histological structure.

5.   High salt induces TGF-β and fibrotic markers.

6.   High salt in association with the ischemic injury reduces the renal mass at 7 days and 45 days post ischemia, but not early at 48 hours.

7.   Kindlin-2 is localized in biopsies of renal transplanted patients and the expression increase in association with the presence of acute tubular necrosis.

.

LIMITATIONS AND FUTURE PRESPECTIVES

8. LIMITATIONS AND FUTURE PERSPECTIVES

8.1. Limitations

In the in vivo studies, we have demonstrated that UIRI induce acute tubular injury and alter gene expressions mediating the activation of epithelial to mesenchymal transition. However, we were not able to detect significant induction of neither Kindlin-2 mRNA level nor protein level. In the same time, Kindlin-2 showed focal staining in the cortical area, which explains the non-significant induction of Kindlin-2 mRNA or protein from the extracted ischemic tissue.

Although morphological changed have been detected assessing phenotype changes in the tubular epithelial cells, and the induction of genes expressions relating to the activation of epithelial to mesenchymal transition in correlation to the following up time after injury. Yet further analysis of EMT markers in the protein level would give us complete analysis of the cellular alterations induced by the ischemic injury in correlation with the induction of Kidnlin-2 expression, with consideration of the structural alteration in the long term period post injury.

In our in vitro studies, the long hypoxia incubation periods induced might have raised the possibilities of the inhibition of the targeted TGF-β signaling pathway, we have not analysed the activation of the pathway. Our approach testing TGF-ß from the cultured medium collected has revealed the presence and induction of TGF-ß by the ischemia/reperfusion incubation. Thus, analysing Smads to detected the state of the signalling pathway, in addition to epithelial (E-cadherin) and mesenchymal (Snail-1) markers could have assist to clarify the status and activation of the signalling pathway, but maintaining the experimental process performed on MTCs have showed many technical points that affected the growing of the cultured cells, mainly balancing between maintaining stable confluent

monolayer and applying long periods of experimental conditions have been difficult to standardize in the different number of experiments.

8.2.   Future Perspectives

In this thesis Kindlin-2 expression has been proposed as possible early indicator of the TGF-β signalling activation and enrolled in the progression and severity of tubular injury. Furthermore, the experimental studies in ischemic model have revealed possible correlation of Kindlin-2 with the morphological changes detected in the histological analysis of the ischemic tissue. Given the detected association of Kindlin-2 with the progression of fibrotic process, future studies should be designed:

- To deepen analyse the cellular pathway activated in ischemic tissue and related biomarkers.

- To correlate the relation between Kindlin-2 expression with the activated signalling pathways.

- To study the effect of Kindlin-2 depletion in the experimental model, investigating the possible amelioration of the tubular injury.

BIBLIOGRAPHY

9. BIBLIOGRAPHY

1. Brenner BM, Levine SA. the Kidney. 1120-21 p.

2. Bertram JF, Soosaipillai MC, Ricardo SD, Ryan GB. Total numbers of glomeruli and individual glomerular cell types in the normal rat kidney. Cell Tissue Res [Internet]. 1992 Oct [cited 2017 Jul 4];270(1):37–45. Available from: http://www.ncbi.nlm.nih.gov/pubmed/1423523

3. Nyengaard JR. The quantitative development of glomerular capillaries in rats with special reference to unbiased stereological estimates of their number and sizes. Microvasc Res [Internet]. 1993 May [cited 2017 Jul 4];45(3):243–61. Available from: http://linkinghub.elsevier.com/retrieve/pii/S0026286283710228

4. Baines AD, de Rouffignac C. Functional heterogeneity of nephrons. II. Filtration rates, intraluminal flow velocities and fractional water reabsorption. Pflugers Arch [Internet]. 1969 [cited 2017 Jul 4];308(3):260–76. Available from: http://www.ncbi.nlm.nih.gov/pubmed/5813954

5. Samuel T, Hoy WE, Douglas-Denton R, Hughson MD, Bertram JF. Determinants of glomerular volume in different cortical zones of the human kidney. J Am Soc Nephrol [Internet]. 2005 Oct 24 [cited 2017 Jul 4];16(10):3102–9. Available from: http://www.jasn.org/cgi/doi/10.1681/ASN.2005010123

6. Guyton AC, Hall JE (John E. Textbook of medical physiology. Elsevier Saunders; 2006. 1116 p.

7. Maton A. Human biology and health. Prentice Hall; 1993. 256 p.

8. Lin S-L, Kisseleva T, Brenner DA, Duffield JS. Pericytes and perivascular fibroblasts are the primary source of collagen-producing cells in obstructive fibrosis of the kidney. Am J Pathol [Internet]. American Society for Investigative Pathology; 2008

Bibliography

Dec [cited 2017 Apr 17];173(6):1617–27. Available from: http://www.ncbi.nlm.nih.gov/pubmed/19008372

9.   Jarad G, Miner JH. Update on the glomerular filtration barrier. Curr Opin Nephrol Hypertens [Internet]. NIH Public Access; 2009 May [cited 2017 Jul 11];18(3):226–32. Available from: http://www.ncbi.nlm.nih.gov/pubmed/19374010

10.   Tisher CC, Bulger RE, Trump BF. Human renal ultrastructure. I. Proximal tubule of healthy individuals. Lab Invest [Internet]. 1966 Aug [cited 2017 Jul 4];15(8):1357–94. Available from: http://www.ncbi.nlm.nih.gov/pubmed/5920363

11.   Maunsbach AB. Observations on the segmentation of the proximal tubule in the rat kidney. Comparison of results from phase contrast, fluorescence and electron microscopy. J Ultrastruct Res [Internet]. 1966 Oct [cited 2017 Jul 4];16(3):239–58. Available from: http://www.ncbi.nlm.nih.gov/pubmed/5333381

12.   Boor P, Floege J. The renal (myo-)fibroblast: A heterogeneous group of cells [Internet]. Nephrology Dialysis Transplantation. Oxford University Press; 2012 [cited 2017 Apr 6]. p. 3027–36. Available from: https://academic.oup.com/ndt/article-lookup/doi/10.1093/ndt/gfs296

13.   Fox CS, Larson MG, Leip EP, Culleton B, Wilson PWF, Levy D. Predictors of New-Onset Kidney Disease in a Community-Based Population. JAMA [Internet]. 2004 Feb 18 [cited 2017 Jul 5];291(7):844. Available from: http://www.ncbi.nlm.nih.gov/pubmed/14970063

14.   Haroun MK, Jaar BG, Hoffman SC, Comstock GW, Klag MJ, Coresh J. Risk factors for chronic kidney disease: a prospective study of 23,534 men and women in Washington County, Maryland. J Am Soc Nephrol [Internet]. 2003 Nov [cited 2017 Jul 5];14(11):2934–41. Available from:

http://www.ncbi.nlm.nih.gov/pubmed/14569104

15. Basile D, Anderson M, Sutton T. Pathophysiology of Acute Kidney Injury. Compr Physiol [Internet]. 2012 [cited 2017 Apr 26];2(2):1303–53. Available from: https://www.ncbi.nlm.nih.gov/pmc/articles/PMC3919808/pdf/nih ms545925.pdf

16. Haase M, Mertens PR. Biomarkers: more than just markers! Nephrol Dial Transplant [Internet]. 2015;30(1):33–8. Available from: http://ndt.oxfordjournals.org/cgi/doi/10.1093/ndt/gfu085

17. Chawla LS, Eggers PW, Star RA, Kimmel PL. Acute Kidney Injury and Chronic Kidney Disease as Interconnected Syndromes. N Engl J Med [Internet]. Massachusetts Medical Society; 2014 Jul 3 [cited 2017 Jun 7];371(1):58–66. Available from: http://www.nejm.org/doi/10.1056/NEJMra1214243

18. Cho MH. Renal fibrosis. Korean J Pediatr [Internet]. Korean Pediatric Society; 2010 Jul [cited 2017 Apr 6];53(7):735–40. Available from: http://www.ncbi.nlm.nih.gov/pubmed/21189948

19. Kellum J a, Lameire N, Aspelin P, Barsoum RS, Burdmann E a, Goldstein SL, et al. KDIGO Clinical Practice Guideline for Acute Kidney Injury. Kidney Int Suppl [Internet]. 2012 [cited 2017 Mar 9];2(1):1–138. Available from: http://www.kidney-international.org

20. Levin A, Stevens PE. Summary of KDIGO 2012 CKD Guideline: behind the scenes, need for guidance, and a framework for moving forward. Kidney Int [Internet]. 2013 [cited 2017 Jul 5];85:49–61. Available from: http://search.proquest.com/docview/1472021728?accountid=14708

21. Chou Y-H, Huang T-M, Chu T-S. Novel insights into acute kidney injury?chronic kidney disease continuum and the role of renin?angiotensin system. J Formos Med Assoc [Internet]. 2017

Jun 11 [cited 2017 Jul 5]; Available from: http://www.ncbi.nlm.nih.gov/pubmed/28615146

22.   Patschan D, Müller GA. Acute kidney injury. J Inj Violence Res [Internet]. 2015;7(1):19–26. Available from: http://www.jivresearch.org

23.   Cerdá J, Lameire N, Eggers P, Pannu N, Uchino S, Wang H, et al. Epidemiology of Acute Kidney Injury. Clin J Am Soc Nephrol [Internet]. 2008 [cited 2017 May 25];3:881–6. Available from: http://cjasn.asnjournals.org/content/3/3/881.full.pdf

24.   Sutton TA. Alteration of microvascular permeability in acute kidney injury. [cited 2017 Apr 16]; Available from: https://www.ncbi.nlm.nih.gov/pmc/articles/PMC2680138/pdf/nihms103951.pdf

25.   Louis K, Hertig A. Kevin Louis, Alexandre Hertig. 2015;4(3):367–73.

26.   Mehta RL, Cerdá J, Burdmann EA, Tonelli M, García-García G, Jha V, et al. International Society of Nephrology's 0by25 initiative for acute kidney injury (zero preventable deaths by 2025): A human rights case for nephrology. Lancet [Internet]. 2015 [cited 2017 May 18];385(9987):2616–43. Available from: http://www.sciencedirect.com/science/article/pii/S014067361560126X

27.   Sancho-Martínez SM, López-Novoa JM, López-Hernández FJ. Pathophysiological role of different tubular epithelial cell death modes in acute kidney injury. Clin Kidney J [Internet]. 2015;8(5):548–59. Available from: http://ckj.oxfordjournals.org/content/8/5/548.abstract

28.   Jefferies JL, Devarajan P. Early detection of acute kidney injury after pediatric cardiac surgery. Prog Pediatr Cardiol [Internet]. Elsevier Ireland Ltd; 2016;41:9–16. Available from:

http://dx.doi.org/10.1016/j.ppedcard.2016.01.011

29.   Tögel F, Westenfelder C. Recent advances in the understanding of acute kidney injury. F1000Prime Rep [Internet]. Faculty of 1000 Ltd; 2014 [cited 2017 May 4];6(September):83. Available from: http://www.ncbi.nlm.nih.gov/pubmed/25343040

30.   Hesketh EE, Czopek A, Clay M, Borthwick G, Ferenbach D, Kluth D, et al. Renal ischaemia reperfusion injury: a mouse model of injury and regeneration. J Vis Exp [Internet]. MyJoVE Corporation; 2014 Jun 7 [cited 2017 Mar 8];15(88):e51816. Available from: http://www.ncbi.nlm.nih.gov/pubmed/24961244

31.   Kinsey GR, Huang L, Vergis AL, Li L, Okusa MD. Regulatory T cells contribute to the protective effect of ischemic preconditioning in the kidney. Kidney Int [Internet]. NIH Public Access; 2010 May [cited 2017 Apr 16];77(9):771–80. Available from: http://www.ncbi.nlm.nih.gov/pubmed/20164824

32.   Lee HT, Emala CW. Protective effects of renal ischemic preconditioning and adenosine pretreatment: role of A1 and A3receptors. Am J Physiol - Ren Physiol [Internet]. 2000 [cited 2017 Apr 16];278(3). Available from: http://ajprenal.physiology.org/content/278/3/F380.long

33.   Park KM, Chen A, Bonventre J V. Prevention of Kidney Ischemia/Reperfusion-induced Functional Injury and JNK, p38, and MAPK Kinase Activation by Remote Ischemic Pretreatment. J Biol Chem. 2001;

34.   Shimizu M, Saxena P, Konstantinov IE, Cherepanov V, Cheung MMH, Wearden P, et al. Remote Ischemic Preconditioning Decreases Adhesion and Selectively Modifies Functional Responses of Human Neutrophils. J Surg Res [Internet]. BioMed Central; 2010 Jan [cited 2017 Apr 16];158(1):155–61. Available from:

Bibliography

http://linkinghub.elsevier.com/retrieve/pii/S0022480408005374

35.   Devarajan P. Update on mechanisms of ischemic acute kidney injury. J Am Soc Nephrol [Internet]. 2006 Jun [cited 2015 May 13];17(6):1503–20.   Available   from: http://www.ncbi.nlm.nih.gov/pubmed/16707563

36.   Bonventre J, Yang L. Cellular pathophysiology of ischemic acute kidney injury. J Clin Invest. 2011;121(11):4210–21.

37.   Klausner JM, Paterson IS, Goldman G, Kobzik L, Rodzen C, Lawrence R, et al. Postischemic renal injury is mediated by neutrophils and leukotrienes. Am J Physiol [Internet]. 1989 May [cited 2017 Jul 17];256(5 Pt 2):F794-802. Available from: http://www.ncbi.nlm.nih.gov/pubmed/2541628

38.   Hellberg PO, Källskog OT, Ojteg G, Wolgast M. Peritubular capillary permeability and intravascular RBC aggregation after ischemia: effects of neutrophils. Am J Physiol [Internet]. 1990 Apr [cited 2017 Jul 17];258(4 Pt 2):F1018-25. Available from: http://www.ncbi.nlm.nih.gov/pubmed/2330969

39.   Paller MS. Effect of neutrophil depletion on ischemic renal injury in the rat. J Lab Clin Med [Internet]. 1989 Mar [cited 2017 Jul 17];113(3):379–86.   Available   from: http://www.ncbi.nlm.nih.gov/pubmed/2926243

40.   Thornton MA, Winn R, Alpers CE, Zager RA. An evaluation of the neutrophil as a mediator of in vivo renal ischemic-reperfusion injury. Am J Pathol [Internet]. 1989 Sep [cited 2017 Jul 17];135(3):509–15.   Available   from: http://www.ncbi.nlm.nih.gov/pubmed/2782382

41.   Kelly KJ, Williams WW, Colvin RB, Meehan SM, Springer TA, Gutierrez-Ramos JC, et al. Intercellular Adhesion Molecule-1– deficient Mice Are Protected against Ischemic Renal Injury. J Clin Invest [Internet]. American Society for Clinical Investigation;

1996 Feb 15 [cited 2017 Apr 4];97(4):1056–63. Available from: https://www.ncbi.nlm.nih.gov/pmc/articles/PMC507153/pdf/97105 6.pdf

42.   Ko GJ, Boo CS, Jo SK, Cho WY, Kim HK. Macrophages contribute to the development of renal fibrosis following ischaemia/reperfusion-induced acute kidney injury. Nephrol Dial Transplant [Internet]. Oxford University Press; 2008 Oct 15 [cited 2017 Apr 4];23(3):842–52. Available from: https://academic.oup.com/ndt/article-lookup/doi/10.1093/ndt/gfm694

43.   Kellum JA, Chawla LS. Cell-cycle arrest and acute kidney injury: the light and the dark sides. Nephrol Dial Transplant [Internet]. 2015;(June 2015):1–7. Available from: http://ndt.oxfordjournals.org/cgi/doi/10.1093/ndt/gfv130%5Cnhttp: //www.ncbi.nlm.nih.gov/pubmed/26044835

44.   Yoshida M, Honma S. Regeneration of injured renal tubules. J Pharmacol Sci [Internet]. 2014;124(2):117–22. Available from: http://www.ncbi.nlm.nih.gov/pubmed/24463777

45.   Sanders PW. Effect of salt intake on progression of chronic kidney disease. Curr Opin Nephrol Hypertens [Internet]. 2006 Jan [cited 2017 May 5];15(1):54–60. Available from: http://www.ncbi.nlm.nih.gov/pubmed/16340667

46.   Pletinck A, Consoli C, Van Landschoot M, Steppan S, Topley N, Passlick-Deetjen J, et al. Salt intake induces epithelial-to-mesenchymal transition of the peritoneal membrane in rats. Nephrol Dial Transplant [Internet]. Oxford University Press; 2010 May 1 [cited 2017 May 4];25(5):1688–96. Available from: https://academic.oup.com/ndt/article-lookup/doi/10.1093/ndt/gfq036

47.   Xie JX, Li X, Xie Z. Regulation of renal function and structure by

Bibliography

the signaling Na/K-ATPase [Internet]. IUBMB Life. NIH Public Access; 2013 [cited 2017 Sep 3]. p. 991–8. Available from: http://www.ncbi.nlm.nih.gov/pubmed/24323927

48.   Yan Y, Shapiro JI. The physiological and clinical importance of sodium potassium ATPase in cardiovascular diseases. Curr Opin Pharmacol [Internet]. 2016 [cited 2017 Sep 2];27:43–9. Available from: http://dx.doi.org/10.1016/j.coph.2016.01.009

49.   Xie JX, Li X, Xie ZJ. Regulation of Renal Function and Structure by the Signaling Na/K-ATPase. IUBMB Life [Internet]. Tian and Xie Blanco and Wallace; 2013 [cited 2017 Sep 3];65(12):991–8. Available   from: http://onlinelibrary.wiley.com/store/10.1002/iub.1229/asset/iub122 9.pdf?v=1&t=j752xpv9&s=054aaa71463e99eac894cefbb7f0ff352 7e7d426

50.   Ying WZ, Sanders PW. Dietary salt modulates renal production of transforming growth factor-beta in rats. Am J Physiol [Internet]. 1998 [cited 2017 May 5];274(4 Pt 2):F635-41. Available from: http://ajprenal.physiology.org/content/274/4/F635.long

51.   Zeisberg M, Neilson EG. Mechanisms of tubulointerstitial fibrosis. J Am Soc Nephrol. 2010;21:1819–34.

52.   Dagher PC, Herget-Rosenthal S, Ruehm SG, Jo S-K, Star RA, Agarwal R, et al. Newly developed techniques to study and diagnose acute renal failure. J Am Soc Nephrol [Internet]. American Society of Nephrology; 2003 Aug [cited 2017 Apr 16];14(8):2188–98.   Available   from: http://www.ncbi.nlm.nih.gov/pubmed/12874475

53.   Just A. Mechanisms of renal blood flow autoregulation: dynamics and contributions. Am J Physiol - Regul Integr Comp Physiol [Internet]. 2006 [cited 2017 Apr 16];292(1). Available from: http://ajpregu.physiology.org/content/292/1/R1.long

54.   Kalogeris   T,   Baines   CP,   Krenz   M,   Korthuis   RJ.
       Ischemia/Reperfusion. Compr Physiol [Internet]. Hoboken, NJ,
       USA: John Wiley & Sons, Inc.; 2016 Dec 6 [cited 2017 Mar
       8];7(January):113–70.   Available   from:
       http://doi.wiley.com/10.1002/cphy.c160006

55.   Munshi R, Hsu C, Himmelfarb J. Advances in understanding
       ischemic acute kidney injury. BMC Med [Internet]. BioMed
       Central; 2011 Feb 2 [cited 2017 Apr 16];9:11. Available from:
       http://www.ncbi.nlm.nih.gov/pubmed/21288330

56.   Sanz a B, Sanchez-Nino MD, Martin-Cleary C, Ortiz a, Ramos a
       M. Progress in the development of animal models of acute kidney
       injury and its impact on drug discovery. Expert Opin Drug Discov
       [Internet].   2013;8:879–95.   Available   from:
       http://www.ncbi.nlm.nih.gov/entrez/query.fcgi?cmd=Retrieve&db
       =PubMed&dopt=Citation&list_uids=23627598

57.   T Janssen WM, Beekhuis H, Bruin R DE, De Jong PE, Zeeuw D
       DE, de Bruin R, et al. Noninvasive measurement of intrarenal
       blood flow distribution: kinetic model of renal 1231-hippuran
       handling.   [cited   2017   Apr   16];   Available   from:
       http://ajprenal.physiology.org/content/ajprenal/269/4/F571.full.pdf

58.   Legrand M, Mik EG, Johannes T, Payen D, Ince C. Renal hypoxia
       and dysoxia after reperfusion of the ischemic kidney. Mol Med
       [Internet]. The Feinstein Institute for Medical Research; 2008
       [cited   2017   Apr   16];14(7–8):502–16.   Available   from:
       http://www.ncbi.nlm.nih.gov/pubmed/18488066

59.   Mackensen-Haen S, Bohle A, Christensen J, Wehrmann M,
       Kendziorra H, Kokot F. The consequences for renal function of
       widening of the interstitium and changes in the tubular epithelium
       of the renal cortex and outer medulla in various renal diseases.
       Clin Nephrol [Internet]. 1992 Feb [cited 2017 Apr 4];37(2):70–7.

Bibliography

Available from: http://www.ncbi.nlm.nih.gov/pubmed/1551253

60. Bechtel W, McGoohan S, Zeisberg EM, Müller GA, Kalbacher H, Salant DJ, et al. Methylation determines fibroblast activation and fibrogenesis in the kidney. Nat Med [Internet]. Nature Publishing Group; 2010 May [cited 2017 Apr 17];16(5):544–50. Available from: http://www.nature.com/doifinder/10.1038/nm.2135

61. Jiang YS, Jiang T, Huang B, Chen PS, Ouyang J. Epithelial-mesenchymal transition of renal tubules: divergent processes of repairing in acute or chronic injury? Med Hypotheses [Internet]. Elsevier Ltd; 2013 Jul [cited 2015 Apr 22];81(1):73–5. Available from: http://www.ncbi.nlm.nih.gov/pubmed/23601763

62. Kalluri R, Weinberg R a. Review series The basics of epithelial-mesenchymal transition. J Clin Invest. 2009;119(6):1420–8.

63. Carew RM, Wang B, Kantharidis P. The role of EMT in renal fibrosis. Cell Tissue Res [Internet]. 2012 Jan [cited 2015 Apr 7];347(1):103–16. Available from: http://www.ncbi.nlm.nih.gov/pubmed/21845400

64. Yeh Y-C, Wei W-C, Wang Y-K, Lin S-C, Sung J-M, Tang M-J. Transforming growth factor-{beta}1 induces Smad3-dependent {beta}1 integrin gene expression in epithelial-to-mesenchymal transition during chronic tubulointerstitial fibrosis. Am J Pathol [Internet]. American Society for Investigative Pathology; 2010;177(4):1743–54. Available from: http://dx.doi.org/10.2353/ajpath.2010.091183

65. Iwano M, Plieth D, Danoff TM, Xue C, Okada H, Neilson EG. Evidence that fibroblasts derive from epithelium during tissue fibrosis. J Clin Invest [Internet]. American Society for Clinical Investigation; 2002 Aug [cited 2017 Apr 16];110(3):341–50. Available from: http://www.ncbi.nlm.nih.gov/pubmed/12163453

66. Kalluri R, Neilson EG. Epithelial-mesenchymal transition and its

Bibliography

implications for fibrosis. J Clin Invest [Internet]. American Society for Clinical Investigation; 2003 Dec [cited 2017 Apr 16];112(12):1776–84. Available from: http://www.ncbi.nlm.nih.gov/pubmed/14679171

67. Liu Y. Epithelial to mesenchymal transition in renal fibrogenesis: pathologic significance, molecular mechanism, and therapeutic intervention. J Am Soc Nephrol [Internet]. American Society of Nephrology; 2004 Jan [cited 2017 Apr 16];15(1):1–12. Available from: http://www.ncbi.nlm.nih.gov/pubmed/14694152

68. Strutz F. Pathogenesis of tubulointerstitial fibrosis in chronic allograft dysfunction. Clin Transplant. 2009;23(SUPPL.21):26–32.

69. Zavadil J, Böttinger EP. TGF-β and epithelial-to-mesenchymal transitions. Oncogene [Internet]. Nature Publishing Group; 2005 Aug 29 [cited 2017 Apr 16];24(37):5764–74. Available from: http://www.nature.com/doifinder/10.1038/sj.onc.1208927

70. Zeisberg M, Neilson EG. Biomarkers for epithelial-mesenchymal transitions. J Clin Invest [Internet]. American Society for Clinical Investigation; 2009 Jun [cited 2017 Apr 16];119(6):1429–37. Available from: http://www.ncbi.nlm.nih.gov/pubmed/19487819

71. Liu Y. New insights into epithelial-mesenchymal transition in kidney fibrosis. J Am Soc Nephrol [Internet]. NIH Public Access; 2010 Feb [cited 2017 Apr 16];21(2):212–22. Available from: http://www.ncbi.nlm.nih.gov/pubmed/20019167

72. Picard N, Baum O, Vogetseder A, Kaissling B, Le Hir M. Origin of renal myofibroblasts in the model of unilateral ureter obstruction in the rat. Histochem Cell Biol [Internet]. Springer; 2008 Jul [cited 2017 Apr 17];130(1):141–55. Available from: http://www.ncbi.nlm.nih.gov/pubmed/18449560

73. Vitalone MJ, O'Connell PJ, Jimenez-Vera E, Yuksel A, Wavamunno M, Fung CL-S, et al. Epithelial-to-mesenchymal

transition in early transplant tubulointerstitial damage. J Am Soc Nephrol [Internet]. American Society of Nephrology; 2008 Aug [cited 2017 Apr 17];19(8):1571–83. Available from: http://www.ncbi.nlm.nih.gov/pubmed/18480317

74.   Liu Y. Renal fibrosis: New insights into the pathogenesis and therapeutics. Kidney Int [Internet]. 2006 Jan [cited 2017 Apr 17];69(2):213–7. Available from: http://www.ncbi.nlm.nih.gov/pubmed/16408108

75.   Strutz F, Neilson EG. New insights into mechanisms of fibrosis in immune renal injury. Springer Semin Immunopathol [Internet]. 2003 May 1 [cited 2017 Apr 17];24(4):459–76. Available from: http://www.ncbi.nlm.nih.gov/pubmed/12778339

76.   Yang J, Liu Y. Dissection of key events in tubular epithelial to myofibroblast transition and its implications in renal interstitial fibrosis. Am J Pathol [Internet]. American Society for Investigative Pathology; 2001 Oct [cited 2017 Apr 17];159(4):1465–75. Available from: http://www.ncbi.nlm.nih.gov/pubmed/11583974

77.   Grande MT, Sánchez-Laorden B, López-Blau C, De Frutos CA, Boutet A, Arévalo M, et al. Snail1-induced partial epithelial-to-mesenchymal transition drives renal fibrosis in mice and can be targeted to reverse established disease. Nat Med [Internet]. 2015 Aug 3 [cited 2017 Jul 23];21(9):989–97. Available from: http://www.ncbi.nlm.nih.gov/pubmed/26236989

78.   El-Zoghby ZM, Stegall MD, Lager DJ, Kremers WK, Amer H, Gloor JM, et al. Identifying specific causes of kidney allograft loss. Am J Transplant. 2009;9(3):527–35.

79.   Riella L V., Djamali A, Pascual J. Chronic allograft injury: Mechanisms and potential treatment targets. Transplant Rev [Internet]. Elsevier Inc.; 2017;31(1):1–9. Available from:

http://dx.doi.org/10.1016/j.trre.2016.10.005

80. Vongwiwatana A, Tasanarong A, Rayner DC, Melk A, Halloran PF. Epithelial to mesenchymal transition during late deterioration of human kidney transplants: The role of tubular cells in fibrogenesis. Am J Transplant. 2005;5(6):1367–74.

81. Hertig A, Verine J, Mougenot B, Jouanneau C, Ouali N, Sebe P, et al. Risk factors for early epithelial to mesenchymal transition in renal grafts. Am J Transplant. 2006;6(12):2937–46.

82. Boor P, Floege J. Renal Allograft Fibrosis: Biology and Therapeutic Targets. Am J Transplant [Internet]. 2015 Feb 17 [cited 2015 Mar 12];863–86. Available from: http://www.ncbi.nlm.nih.gov/pubmed/25691290

83. Duffield JS. Cellular and molecular mechanisms in kidney fibrosis [Internet]. Journal of Clinical Investigation. American Society for Clinical Investigation; 2014 [cited 2017 Apr 6]. p. 2299–306. Available from: http://www.ncbi.nlm.nih.gov/pubmed/24892703

84. Gentle ME, Shi S, Daehn I, Zhang T, Qi H, Yu L, et al. Epithelial cell TGFβ signaling induces acute tubular injury and interstitial inflammation. J Am Soc Nephrol [Internet]. 2013;24:787–99. Available from: http://www.pubmedcentral.nih.gov/articlerender.fcgi?artid=3636798&tool=pmcentrez&rendertype=abstract

85. Böttinger EP, Bitzer M. TGF-beta signaling in renal disease. J Am Soc Nephrol. 2002;13:2600–10.

86. Meng X-MM, Tang PMK, Li J, Lan HY, Nikolic-Paterson D, Condliffe S, et al. TGF-??/Smad signaling in renal fibrosis. Front Physiol [Internet]. Frontiers; 2015 Mar 19 [cited 2017 Jul 31];6(MAR):82. Available from: http://www.frontiersin.org/Renal_and_Epithelial_Physiology/10.3389/fphys.2015.00082/abstract

Bibliography

87.   Wei X, Xia Y, Li F, Tang Y, Nie J, Liu Y, et al. Kindlin-2 Mediates Activation of TGF- /Smad Signaling and Renal Fibrosis. J Am Soc Nephrol [Internet]. 2013 Sep 1 [cited 2017 Mar 7];24(9):1387–98.   Available   from: http://www.jasn.org/cgi/doi/10.1681/ASN.2012101041

88.   Yamamoto T, Noble NA, Cohen AH, Nast CC, Hishida A, Gold LI, et al. Expression of transforming growth factor-beta isoforms in human glomerular diseases. Kidney Int [Internet]. 1996 Feb [cited   2017   Aug   1];49(2):461–9.   Available   from: http://www.ncbi.nlm.nih.gov/pubmed/8821830

89.   Furuta C, Miyamoto T, Takagi T, Noguchi Y, Kaneko J, Itoh S, et al. Transforming growth factor-?? signaling enhancement by long-term exposure to hypoxia in a tumor microenvironment composed of Lewis lung carcinoma cells. Cancer Sci [Internet]. 2015 Nov [cited   2017   Mar   7];106(11):1524–33.   Available   from: http://doi.wiley.com/10.1111/cas.12773

90.   Koli K, Saharinen J, Hyytiäinen M, Penttinen C, Keski-Oja J. Latency, activation, and binding proteins of TGF-β. Microscopy Research and Technique. 2001. p. 354–62.

91.   Meng XM, Tang PMK, Li J, Lan HY. TGF-??/Smad signaling in renal fibrosis. Frontiers in Physiology. 2015.

92.   Moon J-A, Kim H-T, Cho I-S, Sheen YY, Kim D-K. IN-1130, a novel transforming growth factor-beta type I receptor kinase (ALK5) inhibitor, suppresses renal fibrosis in obstructive nephropathy. Kidney Int [Internet]. 2006 Oct [cited 2017 Aug 1];70(7):1234–43.   Available   from: http://linkinghub.elsevier.com/retrieve/pii/S0085253815521340

93.   Petersen M, Thorikay M, Deckers M, van Dinther M, Grygielko ET, Gellibert F, et al. Oral administration of GW788388, an inhibitor of TGF-beta type I and II receptor kinases, decreases

renal fibrosis. Kidney Int [Internet]. 2008 Mar [cited 2017 Aug 1];73(6):705–15. Available from: http://linkinghub.elsevier.com/retrieve/pii/S0085253815530615

94. Larjava H, Plow EF, Wu C. Kindlins: essential regulators of integrin signalling and cell-matrix adhesion. EMBO Rep [Internet]. European Molecular Biology Organization; 2008 Dec [cited 2017 Jul 21];9(November):1203–8. Available from: http://www.ncbi.nlm.nih.gov/pubmed/18997731

95. Malinin NL, Plow EF, Byzova T V. Kindlins in FERM adhesion [Internet]. Blood American Society of Hematology; May 20, 2010 p. 4011–7. Available from: http://www.ncbi.nlm.nih.gov/pubmed/20228270

96. Montanez E, Ussar S, Schifferer M, Bosl M, Zent R, Moser M, et al. Kindlin-2 controls bidirectional signaling of integrins. Genes Dev [Internet]. 2008 May 15 [cited 2017 Jul 22];22(10):1325–30. Available from: http://www.genesdev.org/cgi/doi/10.1101/gad.469408

97. Mory A, Feigelson SW, Yarali N, Kilic SS, Bayhan GI, Gershoni-Baruch R, et al. Kindlin-3: a new gene involved in the pathogenesis of LAD-III. Blood [Internet]. 2008 Sep 15 [cited 2017 Jul 22];112(6):2591. Available from: http://www.bloodjournal.org/cgi/doi/10.1182/blood-2008-06-163162

98. Bledzka K, Bialkowska K, Sossey-Alaoui K, Vaynberg J, Pluskota E, Qin J, et al. Kindlin-2 directly binds actin and regulates integrin outside-in signaling. J Cell Biol [Internet]. The Rockefeller University Press; 2016 Apr 11 [cited 2017 Jul 21];213(1):97–108. Available from: http://www.ncbi.nlm.nih.gov/pubmed/27044892

99. Dowling JJ, Gibbs E, Russell M, Goldman D, Minarcik J, Golden JA, et al. Kindlin-2 Is an Essential Component of Intercalated

Discs and Is Required for Vertebrate Cardiac Structure and Function. Circ Res [Internet]. 2008 Feb 29 [cited 2017 Jul 22];102(4):423–31. Available from: http://www.ncbi.nlm.nih.gov/pubmed/18174465

100. Rognoni E, Ruppert R, Fässler R. The kindlin family: functions, signaling properties and implications for human disease. J Cell Sci [Internet]. 2016 Jan 1 [cited 2016 Jun 21];129(1):17–27. Available from: http://jcs.biologists.org/content/129/1/17

101. Hirschberg R. Kindlin-2 : A New Player in Renal Fibrogenesis Ultrasonic Stimulation of the Cholinergic Anti-In fl ammatory Pathway for Renal Protection. 2013;1339–40.

102. Wei X, Wang X, Xia Y, Tang Y, Li F, Fang W, et al. Kindlin-2 regulates renal tubular cell plasticity by activation of Ras and its downstream signaling. Am J Physiol Renal Physiol [Internet]. 2014 Jan 15 [cited 2017 Mar 7];306(46):F271-8. Available from: http://www.ncbi.nlm.nih.gov/pubmed/24226523

103. Sun Y, Guo C, Ma P, Lai Y, Yang F, Cai J, et al. Kindlin-2 Association with Rho GDP-Dissociation Inhibitor α Suppresses Rac1 Activation and Podocyte Injury. J Am Soc Nephrol [Internet]. 2017 Aug 3 [cited 2017 Sep 9];ASN.2016091021. Available from: http://www.ncbi.nlm.nih.gov/pubmed/28775002

104. Meves A, Stremmel C, Gottschalk K, Fässler R. The Kindlin protein family: new members to the club of focal adhesion proteins. Trends Cell Biol [Internet]. 2009 Oct [cited 2017 Jul 22];19(10):504–13. Available from: http://linkinghub.elsevier.com/retrieve/pii/S0962892409001524

105. Skrypnyk NI, Harris RC, de Caestecker MP. Ischemia-reperfusion model of acute kidney injury and post injury fibrosis in mice. J Vis Exp [Internet]. 2013 Aug 9 [cited 2017 Mar 8];(78):6–11. Available from: http://www.ncbi.nlm.nih.gov/pubmed/23963468

106. Ucero AC, Benito-Martin A, Izquierdo MC, Sanchez-Niño MD, Sanz AB, Ramos AM, et al. Unilateral ureteral obstruction: Beyond obstruction [Internet]. International Urology and Nephrology. 2014 [cited 2017 Mar 8]. p. 765–76. Available from: http://www.ncbi.nlm.nih.gov/pubmed/24072452

107. Chevalier RL, Forbes MS, Thornhill BA. Ureteral obstruction as a model of renal interstitial fibrosis and obstructive nephropathy. Kidney Int [Internet]. 2009 Jun [cited 2017 Mar 8];75(11):1145–52. Available from: http://www.ncbi.nlm.nih.gov/pubmed/19340094

108. Le Clef N, Verhulst A, D'Haese PC, Vervaet BA. Unilateral renal ischemia-reperfusion as a robust model for acute to chronic kidney injury in mice. PLoS One. 2016;11(3).

109. Wei X, Xia Y, Li F, Tang Y, Nie J, Liu Y, et al. Kindlin-2 mediates activation of TGF-β/Smad signaling and renal fibrosis. J Am Soc Nephrol [Internet]. 2013;24:1387–98. Available from: http://www.ncbi.nlm.nih.gov/pubmed/23723426

110. Zager RA, Johnson ACM, Becker K. Acute unilateral ischemic renal injury induces progressive renal inflammation, lipid accumulation, histone modification, and "end-stage" kidney disease. Am J Physiol - Ren Physiol [Internet]. 2011 [cited 2017 Aug 26];301(6). Available from: http://ajprenal.physiology.org/content/301/6/F1334

111. Basile DP, Leonard EC, Tonade D, Friedrich JL, Goenka S. Distinct effects on long-term function of injured and contralateral kidneys following unilateral renal ischemia-reperfusion. Am J Physiol - Ren Physiol [Internet]. 2012 [cited 2017 Aug 26];302(5). Available from: http://ajprenal.physiology.org/content/302/5/F625

112. Le Clef N, Verhulst A, D'Haese PC, Vervaet BA. Unilateral renal ischemia-reperfusion as a robust model for acute to chronic kidney

injury in mice. Chatziantoniou C, editor. PLoS One [Internet]. Public Library of Science; 2016 Mar 23 [cited 2017 Mar 8];11(3):e0152153. Available from: http://www.ncbi.nlm.nih.gov/pubmed/27007127

113. Leibowitz A, Volkov A, Voloshin K, Shemesh C, Barshack I, Grossman E. Melatonin prevents kidney injury in a high salt diet-induced hypertension model by decreasing oxidative stress. J Pineal Res [Internet]. 2016 Jan [cited 2017 May 4];60(1):48–54. Available from: http://www.ncbi.nlm.nih.gov/pubmed/26465239

114. Giani JF, Bernstein KE, Janjulia T, Han J, Toblli JE, Shen XZ, et al. Salt Sensitivity in Response to Renal Injury Requires Renal Angiotensin-Converting Enzyme. Hypertension [Internet]. 2015 [cited 2017 May 4];66(3):534–42. Available from: http://hyper.ahajournals.org/content/66/3/534

115. Zell S, Schmitt R, Witting S, Kreipe HH, Hussein K, Becker JU. Hypoxia Induces Mesenchymal Gene Expression in Renal Tubular Epithelial Cells: An in vitro Model of Kidney Transplant Fibrosis. Nephron Extra [Internet]. 2013;3(1):50–8. Available from: http://www.karger.com?doi=10.1159/000351046

116. Kroening S, Neubauer E, Wessel J, Wiesener M, Goppelt-Struebe M. Hypoxia interferes with connective tissue growth factor (CTGF) gene expression in human proximal tubular cell lines. Nephrol Dial Transplant. 2009;24(11):3319–25.

117. Manotham K, Tanaka T, Matsumoto M, Ohse T, Inagi R, Miyata T, et al. Transdifferentiation of cultured tubular cells induced by hypoxia. Kidney Int [Internet]. 2004 [cited 2017 Apr 7];65(3):871–80. Available from: http://www.sciencedirect.com/science/article/pii/S0085253815497790

118. Lee YK, Kim E-J, Lee JE, Noh JW, Kim Y-G. Hypoxia induces

connective tissue growth factor mRNA expression. J Korean Med Sci [Internet]. 2009 Jan [cited 2017 Apr 17];24 Suppl(Suppl 1):S176-82. Available from: http://www.ncbi.nlm.nih.gov/pubmed/19194549

119. Zavadil J, Böttinger EP. TGF-beta and epithelial-to-mesenchymal transitions. Oncogene. 2005;24:5764–74.

120. Hirschberg R. Kindlin-2: a new player in renal fibrogenesis. J Am Soc Nephrol [Internet]. American Society of Nephrology; 2013 Sep [cited 2017 Jul 21];24(9):1339–40. Available from: http://www.ncbi.nlm.nih.gov/entrez/query.fcgi?cmd=Retrieve&db=PubMed&dopt=Citation&list_uids=23847279

121. Gueler F, Shushakova N, Mengel M, Hueper K, Chen R, Liu X, et al. A Novel Therapy to Attenuate Acute Kidney Injury and Ischemic Allograft Damage after Allogenic Kidney Transplantation in Mice. 2015;

122. Mårtensson J, Martling C-R, Bell M. Novel biomarkers of acute kidney injury and failure: clinical applicability. Br J Anaesth [Internet]. Oxford University Press; 2012 Dec 1 [cited 2017 Apr 5];109(6):843–50. Available from: https://academic.oup.com/bja/article-lookup/doi/10.1093/bja/aes357

Bibliography